

**JAERI-Conf
2004-015**



JP0550055



**PROCEEDINGS OF THE SYMPOSIUM ON
NITRIDE FUEL CYCLE TECHNOLOGY
JULY 28, 2004, JAERI, TOKAI, JAPAN**

December 2004

(Ed.) Research Group for Actinides Science

**日本原子力研究所
Japan Atomic Energy Research Institute**

本レポートは、日本原子力研究所が不定期に公刊している研究報告書です。
入手の問合わせは、日本原子力研究所研究情報部研究情報課（〒319-1195 茨城県那珂郡東海村）あて、お申し越してください。なお、このほかに財団法人原子力弘済会資料センター（〒319-1195 茨城県那珂郡東海村日本原子力研究所内）で複写による実費頒布をおこなっております。

This report is issued irregularly.

Inquiries about availability of the reports should be addressed to Research Information Division, Department of Intellectual Resources, Japan Atomic Energy Research Institute, Tokai-mura, Naka-gun, Ibaraki-ken 319-1195, Japan.

© Japan Atomic Energy Research Institute, 2004

編集兼発行 日本原子力研究所

Proceedings of the Symposium on Nitride Fuel Cycle Technology
July 28, 2004, JAERI, Tokai, Japan

(Ed.) Research Group for Actinides Science

Department of Materials Science
Tokai Research Establishment
Japan Atomic Energy Research Institute
Tokai-mura, Naka-gun, Ibaraki-ken

(Received October 15, 2004)

This report is the Proceedings of the Symposium of Nitride Fuel Cycle Technology, which was held on July 28, 2004, at the Tokai Research Establishment of the Japan Atomic Energy Research Institute .

The purpose of this symposium is to exchange information and views on nitride fuel cycle technology among researchers from foreign and domestic organizations, and to discuss the recent and future research activities. The topics discussed in the symposium are Present State of the Technology Development in the World and Japan, Fabrication Technology, Property Measurement and Pyrochemical Process. The intensive discussion was made among 53 participants.

This report consists of 2 papers as invited presentations and 12 papers as contributed papers.

Keywords: Nitride Fuel, Fuel Cycle, Fabrication, Property, Measurement, Pyrochemical Process

窒化物燃料サイクル技術シンポジウム論文集
2004 年 7 月 28 日、東海研究所、東海村

日本原子力研究所東海研究所物質科学研究部
(編) アクチノイド科学研究グループ

(2004 年 10 月 15 日 受理)

この報告書は、2004 年 7 月 28 日に日本原子力研究所東海研究所で開催された「窒化物燃料サイクル技術」シンポジウムの論文集である。

このシンポジウムの目的は、国内外の専門家間で窒化物燃料サイクル技術に関する情報及び意見を交換し、この研究分野での現状、将来の研究について議論することにある。シンポジウムで発表・討論されたトピックスは、国内外における技術開発の現状、調製技術、物性測定及び乾式再処理プロセスである。シンポジウムには 53 名の参加者があり、活発な討論が行われた。

この報告書は招待講演としての 2 論文、一般講演の 12 論文を取りまとめたものである。

Contents

1. Session A: Present State of the Technology Development in the World	
1.1 Investigations of Nitride Fuels for Fast Reactors in Russia	1
L.M. ZABUDKO, V.M. POPLAVSKY	
1.2 Research and Development of Nitride Fuel Cycle Technology in Europe	15
J. WALLENIOUS	
2. Session B: Present State of the Technology Development in Japan	
2.1 Research and Development of Nitride Fuel Cycle Technology in Japan	25
K. MINATO, Y. ARAI, M. AKABORI, M. UNO, Y. TAMAKI, K. ITO	
3. Session B-1: Fabrication Technology	
3.1 Fabrication of Minor Actinide Nitrides	33
M. TAKANO, A. ITOH, M. AKABORI, Y. ARAI, K. MINATO	
3.2 Fabrication of Lanthanide Nitride Pellets and Simulated Burnup Fuels	41
K. YAMASAKI, Y. TAMAKI, M. TAKANO, M. AKABORI, K. MINATO, Y. ARAI	
4. Session B-2: Property Measurements	
4.1 Properties of Minor Actinide Nitrides	49
M. TAKANO, A. ITOH, M. AKABORI, Y. ARAI, K. MINATO	
4.2 Properties of Simulated Burnup Fuels	59
M. UNO, K. KUROSAKI, S. YAMANAKA, K. MINATO	
4.3 Compressive Creep of Simulated Burnup Fuel	67
N. FUKUDA, Y. KOSAKA, K. ITO, K. MINATO	
4.4 Molecular Dynamics Studies of Actinide Nitrides	75
K. KUROSAKI, M. UNO, S. YAMANAKA, K. MINATO	
4.5 New Technique for Property Measurement of Small Sized Specimen	83
H. FUJII, Y. KOSAKA, K. ITO, K. MINATO	
5. Session B-3: Pyrochemical Process	
5.1 Pyrochemical Reprocessing of Nitride Fuel	91
Y. NAKAZONO, T. IWAI, Y. ARAI	
5.2 Renitridation of Recovered Pu in Liquid Cd	97
T. IWAI, Y. NAKAZONO, Y. ARAI	
5.3 Experiments of Pyrochemical Process with Americium	105
H. HAYASHI, K. MINATO	
5.4 Influence of N-15 Enrichment on Neutronics, Costs and C-14 Production in Nitride Fuel Cycle Scenarios	111
J. WALLENIOUS, Y. ARAI, K. MINATO	
Appendix	
A.1 Program	121
A.2 List of Participants	123
A.3 Viewgraphs	127

目 次

1. セッション A : 世界における技術開発の現状	
1.1 ロシアにおける高速炉用窒化物燃料の研究	1
L.M. ZABUDKO、V.M. POPLAVSKY	
1.2 欧州における窒化物燃料サイクル技術の研究開発	15
Janne WALLENIOUS	
2. セッション B : 日本における技術開発の現状	
2.1 日本における窒化物燃料サイクル技術の研究開発	25
湊 和生、荒井康夫、赤堀光雄、宇埜正美、田巻喜久、伊藤邦博	
3. セッション B-1 : 調製技術	
3.1 マイナーアクチノイド窒化物の調製	33
高野公秀、伊藤昭憲、赤堀光雄、荒井康夫、湊 和生	
3.2 希土類窒化物ペレット及び模擬照射済み燃料の調製	41
山崎和彦、田巻喜久、高野公秀、赤堀光雄、湊 和生、荒井康夫	
4. セッション B-2 : 物性測定	
4.1 マイナーアクチノイド窒化物の物性	49
高野公秀、伊藤昭憲、赤堀光雄、荒井康夫、湊 和生	
4.2 模擬照射済み燃料の物性	59
宇埜正美、黒崎 健、山中伸介、湊 和生	
4.3 模擬照射済み燃料の圧縮クリープ	67
福田信幸、高阪裕二、伊藤邦博、湊 和生	
4.4 アクチノイド窒化物の分子動力学研究	75
黒崎 健、宇埜正美、山中伸介、湊 和生	
4.5 微小試料物性測定のための新技術	83
藤井 創、高阪裕二、伊藤邦博、湊 和生	
5. セッション B-3 : 乾式再処理プロセス	
5.1 窒化物燃料の乾式再処理	91
中園 祥央、岩井 孝、荒井康夫	
5.2 液体 Cd 回収 Pu の再窒化	97
岩井 孝、中園 祥央、荒井康夫	
5.3 Am を用いた乾式プロセス実験	105
林 博和、湊 和生	
5.4 N-15 濃縮度の核特性、経済性及び C-14 生成量への影響	111
Janne WALLENIOUS、荒井康夫、湊 和生	
付録	
A.1 プログラム	121
A.2 参加者リスト	123
A.3 講演 OHP 資料集	127

Preface

In order to develop future nuclear fuel cycles with reduction of environmental burden and efficient utilization of resources, technical developments of fuels containing minor actinide elements, new reprocessing etc., are indispensable. The nitride fuel cycle technology which combines the nitride fuel and the pyrochemical reprocessing has been proposed as one of innovative technologies.

On the basis of such a background, the Japan Atomic Energy Research Institute has carried out the study on the nuclear fuel cycle based on nitride fuel and pyrochemical re-processing in a five-year-program named *PROMINENT* within the framework of the Development of Innovative Nuclear Technology by the Ministry of Education, Culture, Sports, Science and Technology of Japan. In this program, component-technology development of four items of (1) fabrication of nitride fuels, (2) properties measurement and evaluation of nitride fuels, (3) pyrochemical reprocessing and renitriding of nitride fuels, and (4) irradiation behavior evaluation of nitride fuels, has been performed.

In this situation, it was honored of us that we held the Symposium on Nitride Fuel Cycle Technology at JAERI. The major objective of the symposium was planned to discuss above important issues up to date by gathering a number of researchers with each special research field. 53 participants were attended, and 15 presentations were made in five sessions. The symposium was also held under the auspices of Kita-Kanto Branch of Atomic Energy Society of Japan. We would like to thank everybody who was involved with the symposium.

Organizer of the Symposium

This is a blank page.

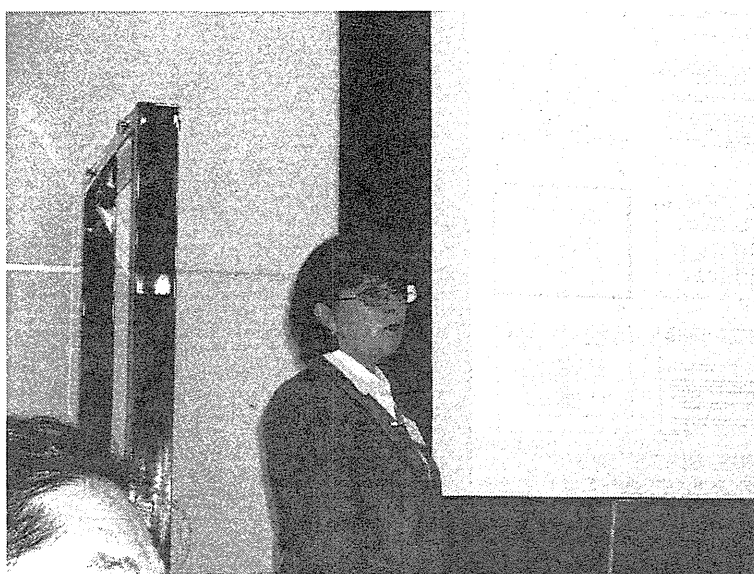


1. Session A: Present State of the Technology Development in the World

1.1 Investigations of Nitride Fuels for Fast Reactors in Russia

L.M. ZABUDKO, V.M. POPLAVSKY

Institute for Physics and Power Engineering, Obninsk, RUSSIA



This is a blank page.

Investigations of Nitride Fuels for Fast Reactors in Russia

L.M.ZABUDKO, V.M.POPLAVSKY

Institute for Physics and Power Engineering,
Obninsk, RUSSIA

Abstract

Nitride fuel allows to improve characteristics of fast power reactors in a part of physics, safety and economics. The researches of last years conducted at IPPE have shown that the following features could be achieved in an optimized fast reactor with sodium coolant and nitride fuel, what meets the modern requirements to advanced nuclear installations:

- zero reactivity excess per fuel burn-up ensuring any refueling interval;
- zero value of sodium void reactivity effect (SVRE) at sodium loss;
- possibility to use the special technology without separation of uranium, plutonium and minor actinides. The technology should improve fuel cycle economics and ensure proliferation resistance.

The core basic design of the BN-800 reactor and the design proposals for the advanced BN-1800 reactor core have been developed. In both designs the mixed nitride fuel is supposed to be used: UPuN for first loading, UPuN+MA for next loadings. One of problem of advanced reactor designs is the problem of reliable nitride pins. At realization of researches the shortage of data on nitrides properties, on irradiation behavior of nitrides is felt. The domestic experience on irradiation behavior of nitrides covers the followings:

- Two loadings of the BR-10 reactor with UN (660 fuel pins and 590 fuel pins). All fuel pins are helium-bonded. Maximum burn-up ~9 at%, maximum linear rating - 45 KW / m, maximum fuel temperature 1175 K, pellet density - 85-94 %.
- The BOR-60 reactor: 1) tens pins with UN, maximum burn-up more than 8 at%, maximum fuel temperature - 1775 K; 2) few pins with UPuN, maximum burn-up 4 at%, 8.95 at%, maximum fuel temperature - 2475 K, 1750 K, accordingly, pellet density - 85-86 %. All pins are helium-bonded. At the moment 4 helium-bonded pins with mixed nitrides with increased Pu content (45 % and 60 %) are irradiated in the BOR-60 reactor within the

frame of joint Russian-French experiment BORA-BORA. Planned maximum burn-up – 11 at%, maximum fuel temperature no more than 1775 K, pellet density - 85 %.

The results of the analysis of nitride irradiation in the BR-10 reactor are presented in the paper.

Besides the power generation reactors, using the nitrides as a fuel for actinides transmutation is under consideration today in many countries. The most attractive innovative fuel is uranium free fuel that avoids any additional actinides production.

The first stage of irradiation and post irradiation examinations of nitrides fuel pins (UPuN, PuN+ZrN) containing more than 40 % of plutonium have been accomplished. The fuel pins are irradiated in the BOR-60 reactor in the frame of BORA-BORA experiment. The basic results of the first stage of the program are discussed.

Short description is done on the ISTC Project which has been started on May 1, 2004: “MATINE – Study of minor actinides transmutation in nitrides: modeling and measurements of out-of-pile properties”.

1. Introduction

Nitride fuel allows to improve characteristics of fast power reactors in a part of physics, safety and economics. The researches of last years conducted at IPPE have shown that the following features could be achieved in a optimized fast reactor with sodium coolant and nitride fuel, what meets the modern requirements to advanced nuclear installations:

- zero reactivity excess per fuel burn-up ensuring any refueling interval;
- zero value of sodium void reactivity effect (SVRE) at sodium loss;
- possibility to use the special technology without separation of uranium, plutonium and minor actinides.

The technology should improve fuel cycle economics and ensure proliferation resistance.

The core basic design of the BN-800 reactor and the design proposals for the advanced BN-1800 reactor core have been developed. In both designs the mixed nitride fuel is supposed to be used: UPuN for first loading, UPuN+MA for next loadings. One of problem of advanced reactor designs is the problem of reliable nitride pins. At realization of researches the shortage of data on nitrides properties, on irradiation behavior of nitrides is felt. The domestic experience on irradiation behavior of nitrides covers the followings:

- Two loadings of the BR-10 reactor with UN (660 fuel pins and 590 fuel pins). All fuel pins are helium-bonded. Maximum burn-up ~9 at%, maximum linear rating - 45 KW/m, maximum fuel temperature 1175 K, pellet density - 85-94 %.
- The BOR-60 reactor: 1) tens pins with UN, maximum burn-up more than 8 at%, maximum fuel temperature - 1775K; 2) few pins with UPuN, maximum burn-up 4at %, 8.95at %, maximum fuel temperature - 2475K, 1750K, accordingly, pellet density - 85-86 %. All pins are helium-bonded. At the moment 4 helium-bonded pins with mixed nitrides with increased Pu content (45 % and 60 %) are irradiated in the BOR-60 reactor within the frame of joint Russian-French experiment BORA-BORA. Planned maximum burn-up – 11at%, maximum fuel temperature no more than 1775K, pellet density - 85 %.

2. Nitride fuel irradiation in BR-10 reactor

The first period (IV reactor loading) with nitride fuel the BR-10 reactor was operated since May, 1983 till August, 1989, the second period with nitride fuel (V reactor loading) the BR-10 reactor was in maintenance since 1990 on 2002.

The data on the operation conditions and pin design with nitride fuel of IV and V loadings are shown in Table 1. The nitride pellets of 90 % enrichment on uranium - 235 with the density not less than 95 % from theoretical one are used.

Eighteen years operation of the BR-10 reactor with UN fuel has shown its good performance. The maximum fuel burn-up in the first core loading was 8at%, in the second – 8.8at%. More than 99 % of fuel pins have reached the design value of burn-up (8at %) without failures.

The generalized data on operation results of two nitride loadings of BR-10 core are given in Table 2. It is seen that for the second core the number of fuel failures has increased, mainly, at burn-up values more than 8at%. 24 cases of fuel failures were detected in the second core. The analysis of results of calculation researchers of nitrides pins performance shows, that the most probable reason of fuel failure is fuel-cladding mechanical interaction (FCMI).

The PIEs of 6 fuel assemblies of IV reactor loading have been carried out. The results of the investigations of swelling and gas-release from nitrides after irradiation of fuel pins in the BR -10 reactor, in comparing the American data, are given in Fig.1, 2. It is necessary to mention however that there are no representative experimental data on swelling and gas release of nitride or carbide fuel with different type and value of the porosity today.

In 2002r the fuel assembly (FA) of V reactor loading was taken from among suspected on a leakage for fuel post-irradiation examination. FA AB811 № 60 was discharged from the reactor on April 24, 1999 at 8.4 at% together with other FAs with high burn-ups due to coolant activity increase caused by pins failures. At the PIE of AB811 № 60 basic attentions planned to be given to the searching

of leaked pins and location of an imperfection. Besides the dependence of fuel swelling on temperature and density should be studied. Currently the PIE is delayed due to lack of funding.

Table 1 Operation conditions and geometry of BR-10 pins with nitride fuel [1]

Parameter	IV loading	V loading
Reactor power, MW	8 MW	
Operating period, efpd.	882	970...1130
Pellet density, g/cm ³	12....13.4	
Max linear rating, KW/m	45.0	
Max burn-up, at%	8.0	8.8
Max neutron flux, n/cm ² c	$8.6 \cdot 10^{14}$	
Inlet coolant temperature, °C	325...350	
Max inlet/outlet temperature increase of coolant, °C	165	
Diameter*wall thickness of cladding, mm	8.4*0.4	
Fuel pellet diameter, mm	7.4	
Core height, mm	400	
Gas plenum height (top), mm	100	

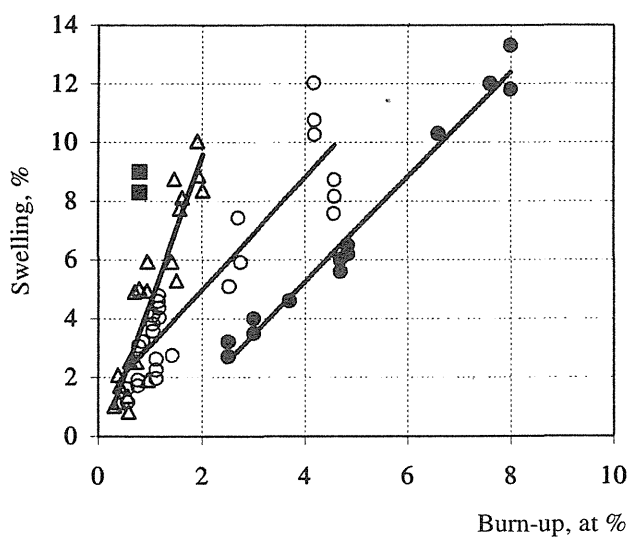


Fig.1 Swelling of nitride fuel

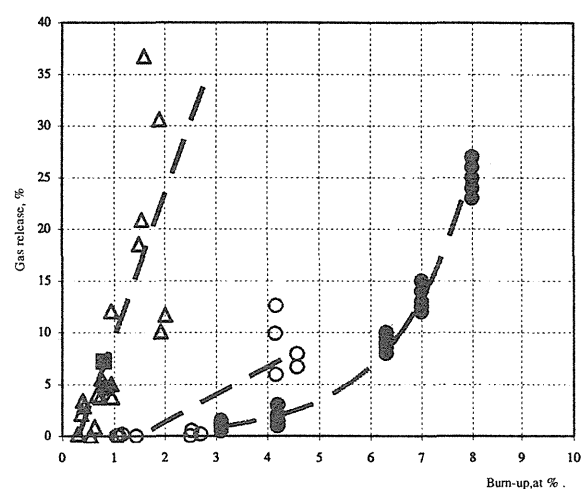


Fig.2 Gas release from nitride fuel

- △ UN, max fuel temperature 1675 K, density 93%, [2]
- UN, max fuel temperature 1460 K, density 95%, [2]
- UN, max fuel temperature 1173 K, density 85 – 94%, [3]
- UN, max fuel temperature 1953 K, density 87%, [2]

Table 2 Main results of operation of standard FAs of IV and V loadings of BR-10 reactor [1]

N	Parameter	IV loading	V loading
1	Methods of pin integrity monitoring.	1) gas leakage-6 times per day of sampling 2) permanent monitoring on delayed neutrons (DND)	
2	Number of failures (including of DN signal).	2 (0)	24 (1)
3	Max burn-up at the time of failure, at% (date of failure). For loading V only failure cases with max activity are shown.	1) 5.37at% (19.02.1987) 2) 7.1at% (18.11.1988)	1) 6.3 at% (1.02.1996) 2) 7.8at% (18.04.1997) - the reactor was shut down in order to exchange gas in the pumps gas plenums; full power increase; stop on June 1997. 3) ~8.8 at% (7.09.1999) – power decrease to 0; gas exchange; power increase; stop; discharge of FAs with max burn-up
4	Searching of leaked pins in the core.	“Pressing-out” of sodium from FA – no result	No checking
5	Washing of FA from sodium.	1) No washing after discharge. 2) The washing after 10 years of storage in the tight containers with argon-air (1999)	1) No washing after discharge up to April 1988. 2) Beginning on April 1998 obligatory checking of pins after discharge and washing
6	Results of damaged FAs searching by out-of-pile system (SODS-V system)	1) 33 spent FAs with max burn-up of 1.2at%-6.23at% are checked 2) 5 FAs (5.68at%-6.23at%) with gas leakage pins, 2 FAs (5.68 at%, 5.84 at%) with DN signal	1) 63 spent FAs with max burn-up of 6.95at% (1), 7.62at%(1), rest FAs with 8.25-8.79at% 2) 20 FAs with gas leakage pins: 1- 6.95at%, rest 8.25-8.78at%

3. BORA-BORA experiment

Within the framework of agreement between CEA (France) and Minatom (Russia) the experiment is under way on irradiation of different types of fuel with higher plutonium content in the BOR-60 reactor. Beginning on August, 2000 the fuel pins incorporated in two dismountable FAs (19 fuel pins) have been under irradiation in the BOR-60 core. The fuel compositions are as follows:

- 4 fuel pins with MOX pellets $\text{UPu}_{0.45}\text{O}_2$
- 4 fuel pins with vibropac MOX fuel $\text{UPu}_{0.45}\text{O}_2$
- 2 fuel pins with pelletized nitride fuel $\text{UPu}_{0.45}\text{N}$
- 2 fuel pins with pelletized nitride fuel $\text{UPu}_{0.6}\text{N}$
- 2 fuel pins with pelletized fuel composition 40%PuN + 60%ZrN
- 2 fuel pins with pelletized fuel composition 40%PuO₂ + 60%MgO

On November, 2002, two fuel assemblies were unloaded for intermediate post irradiation examinations at burn-ups within 5.4 - 11.3 at% depending on fuel type. The first phase of PIE (nondestructive examinations) has been completed.

3.1 Fuel fabrication

UPuN

The fuel was fabricated in VNIINM, Moscow. The nitrides $\text{UPu}_{0.45}\text{N}$ and $\text{UPu}_{0.6}\text{N}$ powder has been made of initial metals U and Pu, Figure 3. Two fuel pins with $\text{UPu}_{0.45}\text{N}$ and two fuel pins with $\text{UPu}_{0.6}\text{N}$ have been fabricated. Main parameters of fuel pellets are shown in Table 3.

Table 3 Fabrication parameters of BORA-BORA mixed nitrides [4]

Parameter	$\text{UPu}_{0.45}\text{N}$	$\text{UPu}_{0.6}\text{N}$
Density, g/cm^3	12.15 to 12.17	12.1 to 12.16
Content of Pu, wt%	45±0.2	60±0.2
Content of N, O, C, wt%	N 5.3, O < 0.15, C < 0.1	N 5.3 to 5.4, O < 0.15, C < 0.1
Diameter, mm	5.8 to 5.9	5.8 to 5.9
Height, mm	8.85 to 10.2	8.85 to 10.4
Non-uniformity of Pu distribution, %	±3.	±3.

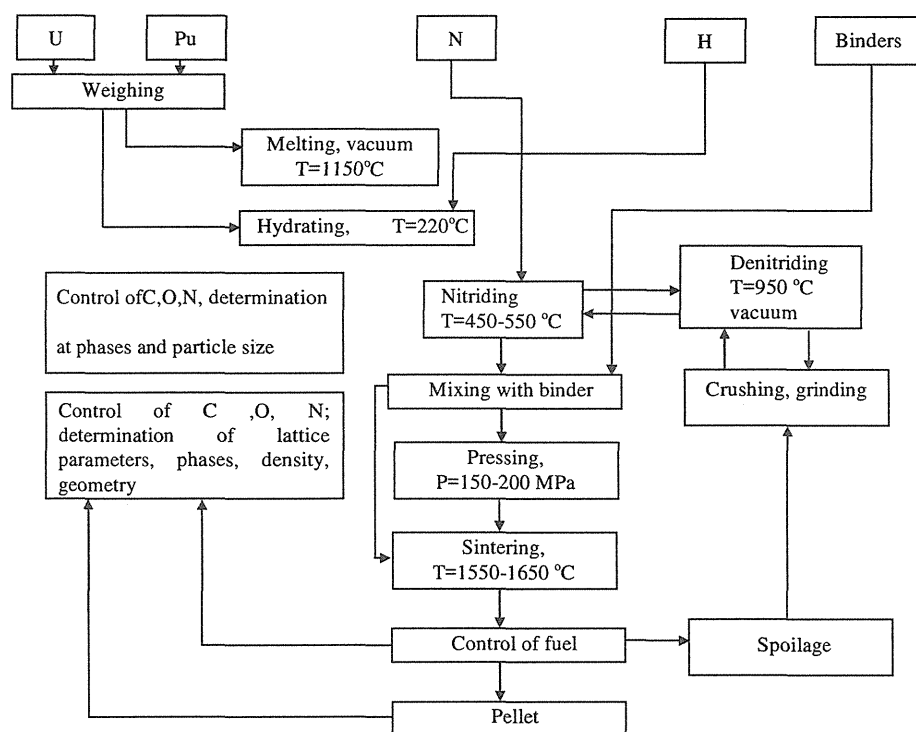


Fig.3 Method of nitride fuel fabrication from metals [4]

PuN+ZrN fuel

The fuel was fabricated in VNIINM, Moscow, from the following initial materials:

- zirconium nitride, obtained from high temperature nitriding (with nitrogen gas) of electrolytic powder of Zr;
- Pu nitride, obtained by hydrogenating the initial Pu metal and then nitriding;
- 40wt%PuN+ 60wt%ZrN inert matrix fuel, obtained by mixing the initial individual powders of Pu and Zr.

The solid solution obtained included two phases enriched by Pu and Zr. Two fuel pins with PuN+ZrN have been fabricated, with parameters as shown in the Table 4.

Table 4 Fabrication parameters of PuN+ZrN [4]

Parameter	Value
Density, g/cm ³	7.4 to 7.5
Content of Pu, wt%	37.5
Content of N, O, C, wt %	N 9.85 to 9.9, O 0.2, C 0.2
Pellet diameter, mm	5.8 to 5.9
Pellet height; mm	8.85 to 10.1
Non-uniformity of Pu distribution	±4 %

3.2 Irradiation in BOR-60 reactor

Parameters of the fuel pins irradiation were selected, taking into account calculated admissible fuel temperature. It was taken for $UPu_{0.6}N$ and $UPu_{0.45}N$ that the maximum calculated temperature should be less than 1800K.

MOX fuel pins and the ones containing the other fuels were loaded into different experimental FAs (VS-217E and VS-263E, correspondingly), which were irradiated in the 5th and 6th rows of the BOR-60 core. The experimental fuel pins were tested in the BOR-60 reactor from August 2000 till October 2002, over runs 71B – 75A for 514 efpd.

The neutronics parameters of the fuel pins under irradiation were calculated by using TRIGEX-CONSYST2-BNAB90 and SMC codes sets. The codes allow to take into account actual fuel isotope composition in the whole experimental FA and to estimate total and group densities of neutron fluxes, rates of fission and capture reactions, variations in isotope composition, damage dose in the fuel pins claddings. The irradiation history of fuels maximum linear rating is presented in Fig. 4 [5].

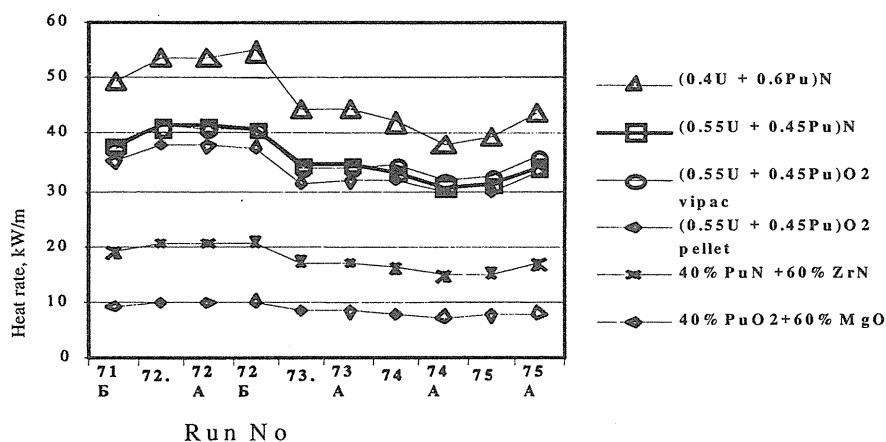


Fig.4 Maximum linear rating of BORA-BORA fuels under the first irradiation stage.

The other irradiation parameters are given in Table 5.

Table 5 Irradiation parameters of BORA-BORA nitrides

Parameter	Value
Maximum fuel burnup, at% :	
PuN +ZrN	11.3
UPu _{0.45} N	5.4
UPu _{0.6} N	7.0
Maximum damage dose , dpa	23.0
Maximum cladding temperature, °C	590

3.3 Post-irradiation examinations of fuels

The post-irradiation examinations are carried out by RIAR. The first phase of intermediate PIE (NDE methods) of the fuel pins has been accomplished – all fuel pins had visual inspection and leak testing by ^{95}Kr . More detailed NDE examinations were performed for six fuel pins with oxides and nitrides (each fuel composition was represented by one fuel pin) – diameter measurement, eddy-current flaw detection, gamma-scanning, analysis of the under-cladding gas.

Distributions of migrating Cs and poor-migrating Zr and Ru fission products (FPs), Fig.5, in the fuel pins with ZrN fuel correspond to neutron flux distribution under irradiation and show no axial migrations both of fuel and volatile FPs. In the fuel pins with fuel $\text{UPu}_{0.45}\text{N}$ a periodic decrease in the activity both of migrating and poor-migrating FPs is observed along the whole fuel pin core, its causes will be identified in the course of destructive examinations.

The fuel pins with mixed compositions $\text{UPu}_{0.45}\text{N}$ and $\text{UPu}_{0.6}\text{N}$ are characterized by release of volatile FPs (Cs) in the lower blanket. Apparently, Cs deposits on the pellets surface and in inter-pellets gaps. Periodic peaks of activity correspond with the height of individual pellets in the blanket.

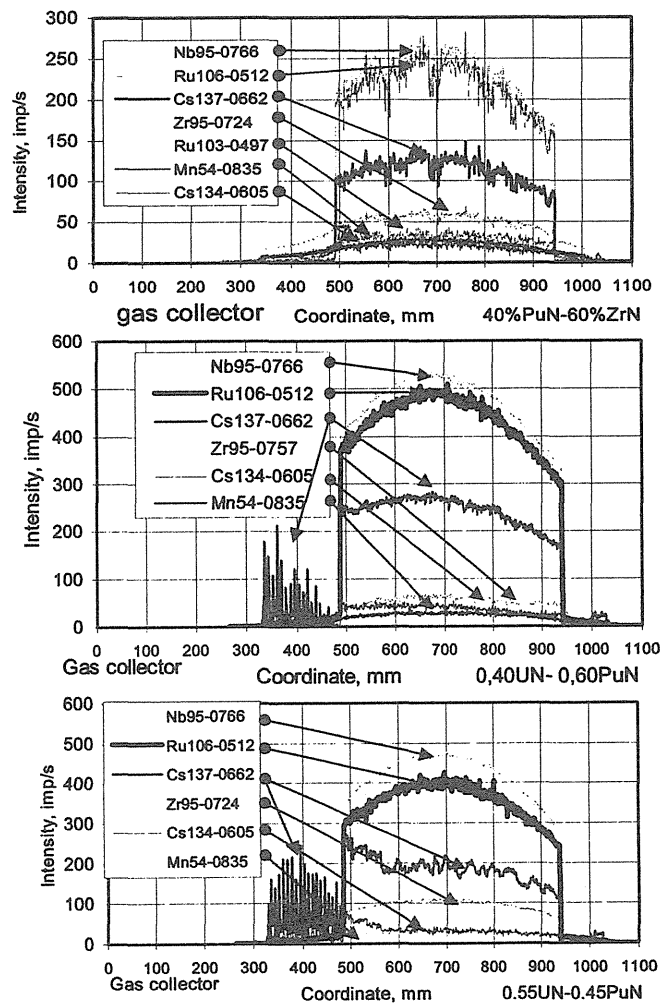


Fig.5 Axial FP distributions in nitrides [5].

Gas composition was identified for each fuel pin by mass-spectrometric method. Taking into consideration measurement error, in the pin with PuN+ZrN no gas release is observed. In the fuel pins with U_{0.45}N and U_{0.6}N a release of gaseous FPs (Kr, Xe) is registered.

Non-destructive examinations have shown:

- all fuel pins are found to be leak-tight after the first irradiation stage;
- in the PuN+ZrN fuel pins no axial migrations of fuel, volatile FP and gaseous FPs are registered.

The destructive examinations of fuel pins with all fuel types are planned, including ceramography, electron probe microanalysis (EPMA), analysis of the residual gases, fuel density, burn-up (Nd analysis by EPMA), X-ray structure analysis (O/M, lattice parameters, phases).

After leak-testing by ⁹⁵Kr and visual inspection ten fuel pins have been reassembled in VS-263 and reloaded in the BOR-60 core for the second irradiation stage in November, 2003. The plan is to continue irradiation up to a burn-up of 11at% for mixed nitrides fuel pins and up to a burn-up of about 20at% for PuN+ZrN fuel.

4. "MATINE Study of Minor Actinide Transmutation in Nitrides: modeling and measurements of out-of-pile properties" - ISTC Project

Neutron transmutation of long lived radioactive minor actinides (MA – neptunium, americium, curium) by the fission process, producing energy and simultaneously turning them into shorter lived nuclides, is being intensely analyzed and discussed as a possible solution of the problem of radwaste utilization. Accelerator Driven Systems (ADS) with the options to consider sodium, lead-bismuth or helium coolants with a solid fuel (based on sodium-cooled fast reactor technology) are under consideration. Uranium free fuels have been proposed to use for transmutation of americium and curium in ADS with fast neutron spectrum in Europe. Presently several fuel types of this kind are investigated in Japanese, EU and US research programs. The programs cover study of different fabrication techniques, out-of-pile properties, modeling, irradiation tests and post-irradiation examinations. Today there is no clear understanding on irradiation behavior of uranium free fuel and on in-reactor behavior of MA containing fuel. Hence the international collaboration in this field is very important.

Beginning on May, 1 2004 the ISTC Project has started. The objective of the Project is to carry out comprehensive modeling of the performance of (Pu,Am,Cm,Zr)N (with ZrN=60%, Pu/Am/Cm=40/50/10) fuel under irradiation in fast neutron spectrum of ADS, currently under development, up to high burn-up in order to compare relative performance of helium, sodium and lead-bismuth bonded pins. Two different fuel forms (pellet and vibropacked) should be compared also. Compilation of data from existing nitride fuel investigations in- and outside of Russia and measurements of thermo-physical properties of (Pu,Zr)N laboratory samples, such as creep rates, thermal conductivity and high temperature stability, will be done in order to perform data file on (Pu,Am,Cm,Zr)N properties. Besides, assessment of the feasibility of fabricating nitride fuels

containing up to 10 atomic percent of curium at RIAR site will be carried out by RIAR, in order to define the possibility of future collaborative work. The main result of the project is identification of uranium-free nitride fuel types that would perform well under irradiation to high burn-up in a fast neutron spectrum. The proposed work is well in line with CONFIRM and EUROTRANS Programs. The Project consists of four tasks.

In the first task compilation of literature data from existing nitride fuel investigations in – and outside of Russia will be done in addition with compilation of data on MA fuels irradiation behavior. The objective of this task is to perform input data for KONDOR and VIKOND codes. The second task will cover fabrication of (Pu,Zr)N samples and measurement of its thermal conductivity, creep rates and high temperature stability. The third task will involve modeling of the performance of (Pu,Am,Cm,Zr)N fuel under irradiation up to high burn-up in fast neutron spectrum. The fuel form would be either pellets or vibropacked granulates/microspheres. In the case of pellets, modeling is to be made for both helium, sodium and lead-bismuth bonded pins to compare their relative performance and to select the optimum fuel pin design. For vibropacked fuel modeling is to be made for helium-bonded pins only. The forth task will be devoted to technical – economical assessments of the feasibility of fabricating nitride fuels with fraction of ZrN inert matrix up to $60\pm 10\%$, containing up to 10 % of curium, at RIAR site.

The main result of the project is identification of uranium-free nitride fuel types that would perform well under irradiation to high burn-up in a fast neutron spectrum.

5. Conclusion

The core basic design of the BN-800 reactor and design proposals for the advanced BN-1800 reactor cores with mixed nitride have been developed in order to meet the requirements to nuclear installations of future generation: sustainability, proliferation resistance, waste management, safety, economics. Specific feature of proposed designs is the fuel cycle without separation of uranium, plutonium and minor actinides that leads to additions of up to 3w% of MA in nitride fuel. At realization of researches the shortage of data on nitrides properties, on specific features of nitride irradiation behavior is felt.

The analysis of theoretical and experimental data on nitride behavior and also calculated researches of nitride irradiation performance have allowed to define the additional experimental researches, required for the correct prediction of fuel elements performance of the advanced fast reactors. There are the followings.

1. Technological researches aiming the fabrication of UPuN pellets of necessary purity, porosity type, chemical content.
2. Out-of-pile study of UPuN properties:
 - Creep rate as a function of density, temperature, stress, chemical composition, technology;

- High temperature behavior.

3. Post-irradiation examinations (PIE) of already irradiated or currently irradiated fuel pins with the purpose to define reasons of pins failures, and also fuel swelling data and gas release in dependence on fuel chemical composition, magnitude and type of porosity, fuel-cladding corrosion interaction:

Besides the power generation reactors, using the nitrides as a fuel for actinides transmutation is currently under consideration in many countries. The most attractive innovative fuel is uranium free fuel that avoids any additional actinides production.

The first stage of irradiation and PIE of nitrides fuel pins (with and w/o U) containing ~40% of plutonium have been accomplished. The fuel pins have been irradiated in the BOR-60 reactor in the frame of BORA-BORA experiment. PIE results have shown that the fuel pins have admissible geometric changes; distributions of the main FPs along the fuel pin core length indicate, that the fuel column is stable, no axial fuel migration is observed and under-cladding gas content and composition are also within anticipated limits. The PIEs have shown that the fuel irradiation could be prolonged.

In addition to the results of irradiation behavior of (Pu,Zr)N, the MATINE program will give some thermo-physical properties of (Pu,Zr)N required for the fuel performance calculation. Besides the experimental fuel data the comparative modeling data of both pellet and vibropacked (Pu,Am,Cm,Zr)N fuel pins with different sublayers will help to define the best solution for fuel pin design of fast neutron ADS. KTH (Sweden) will prepare the input data on irradiation conditions and geometry of ADS core elements, necessary for fuel performance modeling.

References

1. L.Zabudko, A.Kamaev, L.Mamaev, A.Trufanov. Nitride fuel for advanced fast sodium reactors. Proc. of GLOBAL-2003, New Orleans, LA, USA, Nov. 16-20, 2003, p.1679
2. R.B.Matthews, K.M.Chidester, C.W.Hoth et al. Fabrication and testing of uranium nitride fuel for space power reactors. J.Nucl. Mat., 151 (1988), p.334.
3. S.I. Porollo, L.I. Moseev, B.S.Kirjanov et al. Investigation of irradiation characteristics of uranium - nitride fuel at burn-ups. Proceedings of the Conference «35 years to Sverdlovsk Nuclear Centre», Zarechniy, June 5-7, 2001, p. 38.
4. L.Zaboudko, I.Kurina, A.Maershin et al. "Status of CEA-MINATOM collaborative experiment BORA-BORA: fuels with high plutonium content" Proc. of GLOBAL-2001, Paris-FRANCE, 9-13 September 2001. , #292
5. .A.Maershin, V.A.Kisly, O.V.Shishalov et al Irradiation of oxide and nitride fuels and fuel with inert matrix with high plutonium content in BOR-60 reactor: status of Russia-French experiment BORA-BORA, ibid /1/, p.1989.



1.2 Research and Development of Nitride Fuel Cycle Technology in Europe

Janne WALLENIS

Department of Nuclear and Reactor Physics, Royal Institute of Technology (KTH),
AlbaNova University Centre, Sweden



This is a blank page.

Research and Development of Nitride Fuel Cycle Technology in Europe

Janne WALLENIS

Department of Nuclear and Reactor Physics, Royal Institute of Technology (KTH),
AlbaNova University Centre, S-106 91 Stockholm, Sweden
janne@neutron.kth.se

Abstract

Research and development on nitride fuels for minor actinide burning in accelerator driven systems is performed in Europe in context of the CONFIRM project. Dry and wet methods for fabrication of uranium free nitride fuels have been developed with the assistance of thermo-chemical modeling. Four (Pu,Zr) pins have been fabricated by PSI and will be irradiated in Studsvik at a rating of 40-50 kW/m. The thermal conductivity of (Pu,Zr)N has been measured and was found to be in agreement with earlier theoretical assessments. Safety modeling indicates that americium bearing nitride fuels, in spite of their relatively poor high temperature stability under atmospheric pressure, can survive power transients as long as the fuel cladding remains intact.

1. Introduction

Comparing with alternative fuels for fast reactor application, nitride fuel offers some potential advantages, such as a high power to melt and good solubility in nitric acid. The relative complexity of the fabrication process however makes nitride fuels less competitive in the context of commercial electricity production. Therefore, nitrides presently are under consideration in Europe for the purpose of minor actinide transmutation in accelerator driven systems (ADS) and gas cooled fast reactors (GCFR). These are systems where high performance of the fuel is required, whereas the cost penalty imposed by the selection of nitride fuel itself would be of relatively small significance. In the case of the GCFR, the addition of 2-3 percent minor actinides to standard (U,Pu)N is foreseen to have comparatively small impact on the fuel properties as well as performance in pile. The ADS fuel on the other hand would be uranium free, supported by an inert matrix and feature about 60% minor actinides^{1,2)} The practical experience of such fuels is fairly limited, although some progress has been made in recent years. Hence there is a need for basic research on nitride fuels for application in ADS, including development of fabrication processes, properties measurements and safety modeling. Further, irradiation testing under prototypic conditions is a mandatory step before large scale application can be considered. In Europe,

such work has been performed within the CONFIRM project. In what follows, the major results of the CONFIRM project and related activities will be reviewed.

2. Development of fabrication processes

Several fabrication paths have been under investigation. When handling americium, and especially curium, processes generating dust are to be avoided. One possible route is to use the Sol-Gel method for fabrication of micro-spheres followed by Direct Coagulation Casting of pellets. Initial attempts to implement this route at PSI for fabrication of (Pu,Zr)N did not provide pellets of sufficiently good quality for irradiation purposes. Hence it was decided to use traditional powder pressing methods for the main fabrication campaign. Mixing powders of plutonium oxide and zirconia with carbon black, carbo-thermic nitridation was performed by step-wise raising the temperature from 1500 to 1870 Kelvin. In the final step, nitrogen gas was exchanged for N₂-H₂ in order to remove residual carbon according to the reaction³⁾



Performing the de-carburization step in an atmosphere of Ar-H₂, as is customary during UN fabrication leads to formation of highly stable ZrC according to



which in the present context must be avoided. Since the use of inert gas in the standard process apparently is motivated by need for control of UN stoichiometry, it should be of no relevance for uranium free fuel fabrication.

After pressing and sintering in N₂ at T = 2020 K for seven hours, pellets with a golden color (see Figure 1) and oxygen impurity levels below 0.2 weight percent were obtained. The residual carbon concentration ranged from 0.6 to 1.1 weight percent. The density of the pellets could not be increased above 82 percent, indicating that higher densities obtained in earlier tests with impure materials could be due to oxygen acting as a sintering aid.

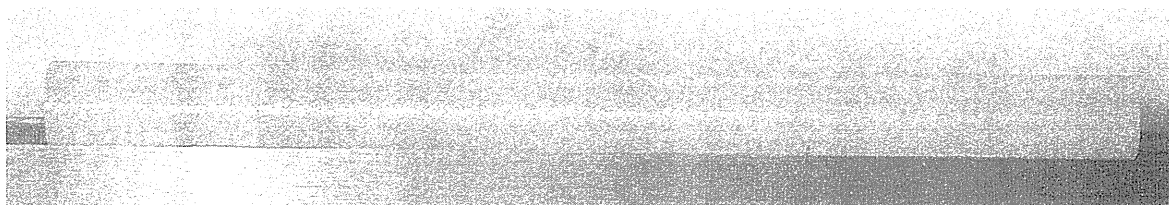


Fig.1: (Pu,Zr)N pellets fabricated by PSI using the powder pressing route.

During autumn 2003, four (Pu,Zr)N fuel pins were fabricated for irradiation testing in Studsvik. Two of the pins contained pellets with 30 percent molar fraction of plutonium, the two other 20 percent.

Meanwhile, measures to improve the wet fabrication route were pursued at ITU. By adding carbon directly to the aqueous sol gel solution, beads of zirconia with a homogeneous distribution of carbon could be obtained. Uranium nitrate was infiltrated into the porosity of the beads, which then were calcined. After carbo-thermic nitridation the beads were pressed into pellets and sintered. Using this so called “Carbon Integration Method”, the produced (U,Zr)N pellets were mechanically stable, having a density of 80% and a golden color indicating a low oxygen content.

3. Property measurements

Thermo-physical properties of ZrN and (Pu,Zr)N were measured at Cadarache. The thermal conductivity was obtained as the product of the experimentally measured thermal diffusivity, density, and heat capacity. The thermal diffusivity was measured by a laser flash technique over the range 700 – 2000 K. Drop calorimetry was used to obtain the heat capacity.

The pellets used for the measurement derived from an earlier stage of the fabrication tests at PSI, featuring 25 molar percent plutonium, oxygen impurities of about one weight percent and a density of 89% TD. The thermal conductivity of these pellets, normalized to 100% density, is shown in Figure 2.

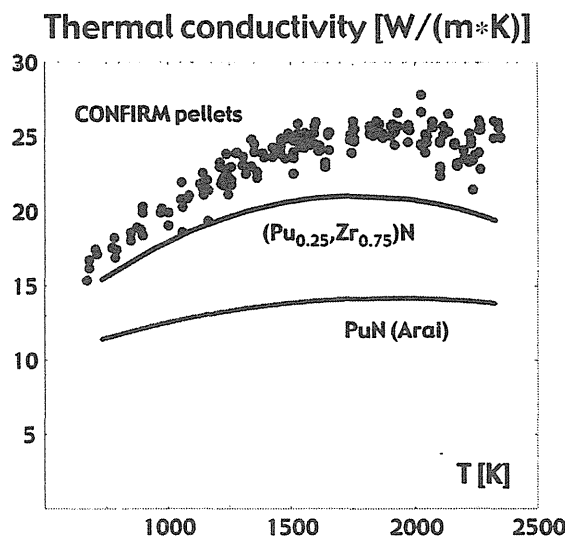


Fig.2: Thermal conductivity of $(\text{Pu}_{0.25},\text{Zr}_{0.75})\text{N}$, normalized to 100% TD. Blue dots represent measured data, black line the Harwell assessment.

It is seen that the normalized experimental data are systematically about 20% higher than the values of the Harwell recommendation⁴⁾ using the present data for thermal conductivity of ZrN and PuN data from Arai et al⁵⁾.

4. Safety and performance modeling

A major concern raised in connection with use of nitride fuels is the dissociation of actinide nitrides, which occurs at temperatures below the melting point.

UN is stabilized by forming a solid solution with ZrN. Solidus and liquidus temperatures of $(U_{0.2},Zr_{0.8})N$ have been measured in a high pressure test⁴⁾. Unfortunately a similar effect is not observed for $(Am,Zr)N$, where significant amounts of americium were vaporized during sintering tests in inert atmosphere⁶⁾. On the other hand, thermo-chemical modeling has indicated that sintering under nitrogen atmosphere should improve the stability of AmN ³⁾. Tests made by JAERI indeed showed that losses of Am while sintering $(Am,Zr)N$ at $T = 1800$ K in nitrogen were decreased by one order of magnitude, as compared to sintering in argon⁷⁾. Recent modeling efforts have further shown that the in-pile stability of $(Pu,Am,Zr)N$ should be considerably better than in glove-box environments⁸⁾. In a small, closed volume like a fuel pin, the equilibrium of the reaction



is shifted to the left, leading to a very low equilibrium pressure of Am in the gas phase. Figure 3 shows the calculated Am pressure in the bonding gas of a $(Pu_{0.2},Am_{0.3},Zr_{0.5})N$ pin with a plenum volume equal to 1.5 times the fuel stack volume. The pressure remains negligible up to at least 2400 K. As long as the fuel clad remains intact, there should thus not be any serious concern about pressure buildup due to dissociation of AmN .

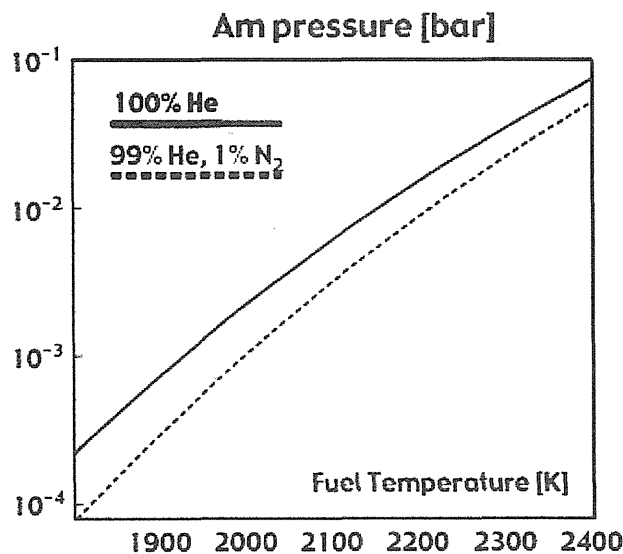


Fig. 3: Americium vapor pressure in a $(Pu_{0.2},Am_{0.3},Zr_{0.5})N$ fuel pin, as function of temperature.

Adding 1% N_2 to the bonding gas decreases Am pressure by a factor of two.

The neutronic performance of the fuel was assessed by doing Monte Carlo calculations for 800 MWth lead-bismuth cooled cores with different geometry, assuming an average linear rating of 36 kW/m¹). The fraction of plutonium in the fresh fuel was fixed to 40%, in order to minimize the reactivity swing over a large number of burn-up cycles²). The remainder of the fuel consists of americium and curium in proportions arising from a mixture of spent UOX and MOX fuel from LWRs (5/1). The inert matrix fraction was adjusted in order to achieve a k-eigenvalue of 0.97 and a radial power peaking factor less than 1.3. For the latter requirement to be fulfilled it was found sufficient to divide the core into three fuel zones with different inert matrix content.

In order to ensure sufficient cooling of the clad, transient calculations of unprotected loss of flow (ULOF) accidents were made. By “unprotected” accident, we here mean that the proton beam is not shut down. Assuming only natural circulation of lead-bismuth, it was shown that by increasing the distance between the pins up to $P/D = 1.75$ the hot spot temperature could be maintained below the rapid burst limit of austenitic steels (~ 1300 K).

For $P/D=1.75$, a pin outer diameter of 5.7 mm, a clad thickness of 0.35 mm a radial fuel clad gap of 50 microns and a fuel porosity of 15 percent, inert matrix fractions yielding $k = 0.97$ and a radial power peaking factor less than 1.3 were calculated to 50 volume percent in the outer fuel zone, 60 percent in the middle, and 66 percent in the inner zone. The resulting power profile is exemplified over a radial cut of the core in Figure 4.

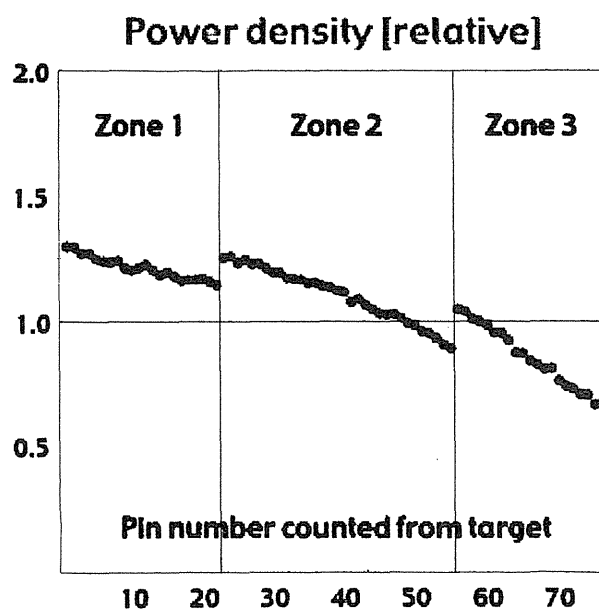


Fig. 4: Radial power profile in the nitride fuelled ADS here investigated.

In Table 1, neutronic safety parameters of this core configuration are displayed. Note the very small effective delayed neutron fraction, which in combination with a vanishing Doppler feedback and a positive void coefficient makes sub-critical operation of the core mandatory. The coolant void worth is large and positive, which requires careful consideration of possible voiding mechanisms, like introduction of gas bubbles into the core.

Table 1: Safety parameters of the nitride fuelled ADS.

Delayed neutron fraction (β)	240 pcm
Effective delayed neutron fraction (β_{eff})	180 pcm
Neutron generation time (Λ)	0.71 μs
Coolant temperature coefficient	+0.50 pcm/K
Fuel axial expansion coefficient	-0.24 pcm/K
Grid radial expansion coefficient	-1.11 pcm/K
Coolant void worth (core only)	+4150 pcm
Coolant void worth (core + upper plenum)	+ 880 pcm

Using these temperature coefficients, the fuel temperatures during a transient over-current accident were calculated. Assuming that a proton beam power increase of 45% is necessary to compensate for reactivity losses during burn-up, the full current could in principle be inserted by accident at beginning of life. Even for such a large over power, the calculated fuel temperature in the hottest fuel pin stays below 1900 K. Considering that the calculated americium pressure at 1900 K is less than one millibar, this type of accident should have no severe consequence for the nitride core, as long as clad integrity is maintained.

5. Irradiation testing

Several irradiations of uranium free nitride fuel are under way in the world today. As part of a CEA-MINATOM collaboration two helium bonded ($\text{Pu}_{0.4}\text{Zr}_{0.6}\text{N}$) pins are irradiated in BOR-60 at moderate linear power ($\sim 25 \text{ kW/m}$). In early 2004, the pins had reached 11% actinide burnup without any sign of clad failure. Within the CONFIRM project, irradiation of four ($\text{Pu,Zr}\text{N}$) pins with 20 and 30 atomic percent plutonium will take place in Studsvik. The pins were delivered from PSI to Studsvik in December 2003. The CONFIRM irradiation will be made in a hafnium shielded NaK capsule, enabling to test the performance at higher linear power, tentatively 40-50 kW/m. As there is some concern that fission gas bubble leakage may lead to loss of conductance, the experimental rig is presently redesigned to pressurise the NaK, so that any clad failure would cause the pins to be filled by the coolant. After the

experimental set-up has been approved by the authorities the pins will be irradiated for 14 cycles, with an expected burn-up of 12 percent actinides. Post-irradiation examination will then be made as part of the EC 6th Framework Programme project EUROTRANS.

In the FUTURIX project, sodium bonded (Pu,Am,Zr)N pins are to be irradiated in Phenix. The fuel pellets will be fabricated by Los Alamos and then transported to ITU, where the pins are filled with sodium before insertion into Phenix in late 2006.

6. Conclusions

As described in the present review, progress has been made in Europe concerning the development of fabrication processes for uranium free nitride fuels. With assistance of thermo-chemical modeling it was shown that the quality of the produced material could be improved by performing decarburization and sintering under nitrogen atmosphere. The thermal conductivity of (Pu,Zr)N has been measured, and four (Pu,Zr)N fuel pins have been fabricated by PSI for irradiation in Studsvik at high linear power. Safety analysis has shown that the suggested nitride fuel ADS core would survive the standard set of design extension conditions, with a remaining question mark for the consequences of clad breach.

Acknowledgments

The author appreciates the kind hospitality of JAERI, where this review was compiled. Many people have contributed to the work here described, in particular Mike Mignanelli, Roger Thetford, Sylvie Pillon, Jean-Pierre Ottaviani, Virginie Basini, Marco Streit, Franz Ingold, Asun Fernandez, Rudy Konings, Mikael Jolkkonen, Marcus Eriksson, Jerzy Cetnar, Jesper Kierkegaard, Johan Flygare and Anders Lind. Financial support from the EC CONFIRM project, SKB and JAERI is gratefully acknowledged.

References

1. J. Wallenius and M. Eriksson, submitted to *Nucl. Tech.* (2004).
2. K. Tsujimoto et al, *J. Nucl. Sci. Tech.* **41**, 21 (2004).
3. M. Jolkkonen, M. Streit and J. Wallenius, *J. Nucl. Sci. Tech.* **41**, 457 (2004).
- 4.
5. R. Thetford and M. Mignanelli, *J. Nucl. Mat.* **320**, 44 (2003).
6. Y. Arai et al, *J. Nucl. Mat.* **195**, 37 (1992).
7. R. Margevicius, LA-UR-03-0415, Los Alamos National Laboratory (2003).
8. M. Takano et al, In Proc. GLOBAL 2003, New Orleans, October 2003.
9. M. Eriksson et al, submitted to *Nucl. Tech.* (2004).

This is a blank page.

2. Session B: Present State of the Technology Development in Japan

2.1 Research and Development of Nitride Fuel Cycle Technology in Japan

Kazuo MINATO¹, Yasuo ARAI¹, Mitsuo AKABORI¹, Masayoshi UNO²,
Yoshihisa TAMAKI³, Kunihiro ITOH⁴

¹ Japan Atomic Energy Research Institute

² Graduate School of Engineering, Osaka University

³ Mitsubishi Materials Corporation

⁴ Nuclear Development Corporation,



This is a blank page.

Research and Development of Nitride Fuel Cycle Technology in Japan

Kazuo MINATO¹, Yasuo ARAI¹, Mitsuo AKABORI¹,
Masayoshi UNO², Yoshihisa TAMAKI³, Kunihiro ITOH⁴

¹ Japan Atomic Energy Research Institute, Tokai-mura, Ibaraki-ken, 319-1195 Japan

² Graduate School of Engineering, Osaka University, Suita-shi, Osaka, 565-0871 Japan

³ Mitsubishi Materials Corporation, Naka-machi, Ibaraki-ken, 311-0102 Japan

⁴ Nuclear Development Corporation, Tokai-mura, Ibaraki-ken, 319-1111 Japan

minato@popsvr.tokai.jaeri.go.jp

Abstract

The research on the nitride fuel was started for an advanced fuel, (U,Pu)N, for fast reactors, and the research activities have been expanded to minor actinide bearing nitride fuels. The fuel fabrication, property measurements, irradiation tests and pyrochemical process experiments have been made. In 2002 a five-year-program named *PROMINENT* was started for the development of nitride fuel cycle technology within the framework of the Development of Innovative Nuclear Technologies by the Ministry of Education, Culture, Sports, Science and Technology of Japan. In the research program *PROMINENT*, property measurements, pyrochemical process and irradiation experiments needed for nitride fuel cycle technology are being made.

1. Introduction

The research on the nitride fuel was started for an advanced fuel for fast reactors. Fuel fabrication, property measurements, irradiation tests and pyrochemical process experiments of (U,Pu)N fuel have been made, and these activities have been expanded to minor actinides (MA: Np, Am, Cm) bearing nitride fuels for transmutation of these elements. The main player in this field in Japan is the Japan Atomic Energy Research Institute (JAERI). The nitride fuel has good potentials. The melting point of the nitride fuel is higher than the metal fuel and comparable to the oxide fuel. The thermal conductivity of the nitride fuel is higher than the oxide fuel and comparable to the metal fuel. The nitride fuel supports a hard neutron spectrum needed for fissions of the minor actinides. The actinide mononitrides would form solid solution, which could accommodate a wide range of the combination and composition of actinides. Highly enriched N-15 would have to be used for the nitride fuel in order to prevent the formation of hazardous C-14. By applying pyrochemical process in the treatment of spent fuel, N-15 could be readily recovered and recycled.

For the development of nitride fuel cycle technology, a five-year-program named *PROMINENT* was started in 2002 within the framework of the Development of Innovative Nuclear Technologies by the Ministry of Education, Culture, Sports, Science and Technology of Japan. In the research program *PROMINENT*, property measurements, pyrochemical process and irradiation experiments needed for nitride fuel cycle technology are being made.

In the present paper, the research and development of nitride fuel cycle technology in Japan is reviewed and the research program *PROMINENT* is introduced.

2. Fast reactor and transmutation fuels

The research activities of the nitride fuel fabrication, property measurements, pyrochemical process experiments and irradiation tests for fast reactors and for transmutation before starting the research program *PROMINENT* are summarized briefly in this chapter.

2.1 Fuel fabrication

Actinide nitrides of UN, PuN and NpN with high-purity have been produced from respective oxides with carbothermic reduction method, and the high-density pellets of UN, PuN and NpN and their solid solutions (U,Pu)N, (U,Np)N and (Np,Pu)N were successfully fabricated [1-4]. AmN, (Pu,Cm)N, (Am,Y)N and (Am,Zr)N were also synthesized with carbothermic reduction method though the batch sizes of them were in the order of ten mg[5-7]. The U-free fuel pellets with inert matrix materials (Pu,Zr)N and PuN+TiN were fabricated for irradiation tests [8]. Figure 1 shows (Am,Zr)N and (Pu,Zr)N pellets.

Fabrication of mixed nitride fuel pellets with high-purity and high-density in the (U)-Pu-Np-Am-Cm system is needed for the next step for the nitride fuel development.

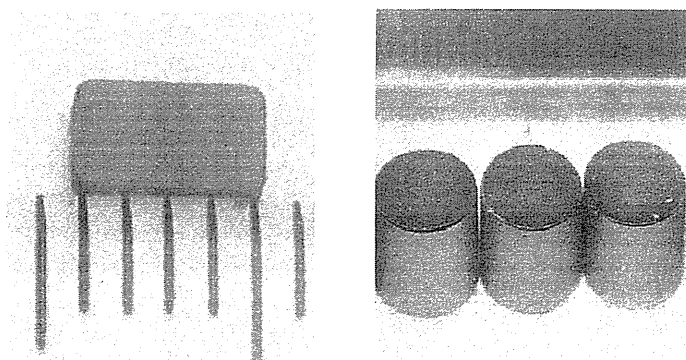


Fig. 1 (Am,Zr)N (left) and (Pu,Zr)N (right).

2.2 Property measurements

Vaporization behaviors of UN, NpN, PuN and the solid solutions of (U,Pu)N and (Np,Pu)N were studied with Knudsen-effusion high temperature mass-spectrometry [9-11]. The specific heat capacities of UN, NpN and PuN were measured with a differential scanning calorimeter [12]. Preliminary experiments of the thermal expansion measurements of UN by high-temperature X-ray diffraction were made. The thermal diffusivities of UN, NpN, PuN and the solid solutions of (U,Pu)N, (U,Np)N and (Np,Pu)N were measured by the laser-flash method and the thermal conductivities were determined as a function of temperature [13-15]. Figure 2 shows thermal conductivities for the UN-NpN-PuN system as a function of composition at 1273 K.

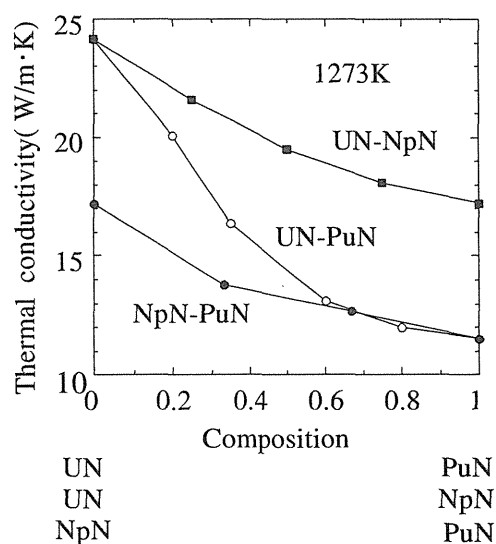


Fig. 2 Thermal conductivities of (U,Pu)N, (U,Np)N and (Np,Pu)N.

The properties for Am and/or Cm bearing nitrides were not available. These properties data are needed to design the MA-bearing fuels and to understand the irradiation behavior of them.

2.3 Pyrochemical process

The pyrochemical process developed by ANL for the metal fuel was applied to the nitride fuel. Electrolyses of UN, NpN and PuN in LiCl-KCl eutectic melt were made, and electro-depositions of U, Np and Pu metals on solid cathodes were carried out [16-18]. Electrode reactions of Np and Pu at liquid Cd and Bi electrodes were studied, and recovery of Pu into liquid Cd was made successfully [19]. As a feasibility test of N-15 recycling, dissolutions of DyN and NdN in LiCl-KCl by CdCl₂ were made, and nitrogen could be recovered as N₂, as shown in Fig.3 [20]. During the electrolysis of UN and PuN, nitrogen evolving as N₂ was observed and nitrogen could be recovered more than 90% as N₂.

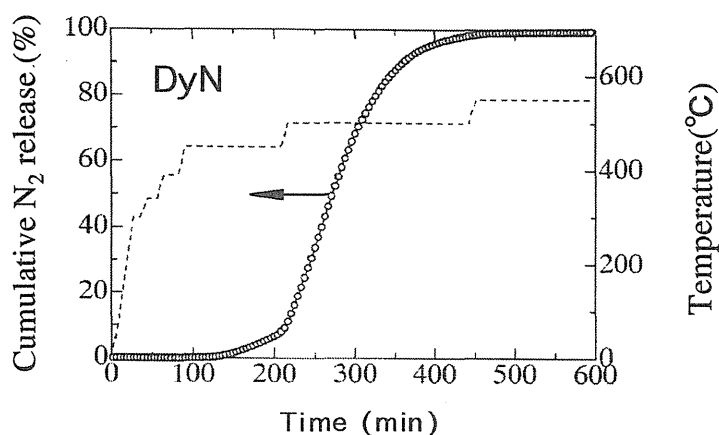


Fig. 3 Evolving behavior of N_2 gas.

For the next step, the electrolysis behavior and electrode reactions for Am and Cm need to be clarified, and re-nitridation of actinide elements recovered in the liquid metal cathode should be made.

2.4 Irradiation tests

Irradiation tests of He-bonded (U,Pu)N fuel pins have been carried out. Four fuel pins of (U,Pu)N were irradiated in the Japan Materials Testing Reactor (JMTR) [21], and two fuel pins of (U,Pu)N were irradiated in the fast test reactor JOYO under the joint research with the Japan Nuclear Cycle Development Institute (JNC). The irradiation behavior of the fuels was found to be good up to 5.5%FIMA. The irradiation tests of U-free fuels (Pu,Zr)N and PuN+TiN are under irradiation in JMTR. Irradiation tests of MA-bearing fuels are needed for the next step.

3. Research program *PROMINENT*

The research program *PROMINENT* was started in November 2002 and is to be valid till March 2007. The purpose of the program is to clarify the feasibility of an innovative nuclear fuel cycle including minor actinides recycling based on the nitride fuel and pyrochemical reprocessing. In the program, the fuel fabrication and pyrochemical process technologies are developed and the fuel properties and irradiation behavior are studied for the MA-bearing fuels, as shown in Fig. 4.

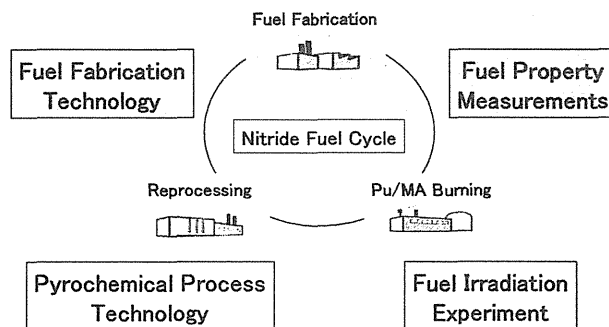


Fig. 4 Research areas in the program *PROMINENT*.

3.1 Fuel fabrication technology

Nitride is hard to be sintered and Am vaporizes easily during fabrication. One of the objectives is to fabricate high-density and high-purity nitride pellets. To survey a suitable fabrication condition, lanthanide elements are used as surrogates for actinide elements, which aims to accelerate the experiments. Mixed nitrides of the Np-Pu-Am-Cm-N system will be fabricated with the carbothermic reduction method. The other objective is to fabricate simulated burnup fuels, where non-radioactive fission product elements are added to uranium nitride. These fuels are supplied to the property measurements and pyrochemical reprocessing tests to support the understanding and modeling of the properties of irradiated nitride fuels and the development of pyrochemical process.

3.2 Fuel property measurements

The handling of minor actinides nitrides is not as easy as that of uranium nitride because of their radioisotopic nature. The size of the specimens containing minor actinides is small, and the number of specimens available is also small. The property measurements of minor actinides nitrides take a longer time since equipments for property measurements are in glove boxes and/or even in hot cells. One of the objectives is to measure thermal properties of Np-Pu-Am-Cm mixed nitrides. For this purpose, new equipments are installed in glove boxes. The second objective is to measure thermal and mechanical properties of the burnup simulated fuels. These measurements support the understanding and modeling of properties of MA-bearing nitride fuels as a function of burnup. The third objective of this area is to develop micro-indentation technique for mechanical property measurements of MA-bearing nitride fuels.

3.3 Pyrochemical process

To develop the pyrochemical process for the nitride fuel, experiments are carried out with MA-bearing nitride and burnup simulated fuels. One of the objectives is to understand the behavior of Am, Cm and fission products at anode and cathode during electrolysis. The other objective is to understand re-nitridation behavior of actinide elements recovered in liquid Cd and to fabricate fuel pellets with recovered actinide nitride. For the enrichment of N-15, the enrichment level of N-15 is evaluated taking account of C-14 production and the cost of enrichment. The process of N-15 recovery in the pyrochemical process and fuel fabrication process is discussed.

3.4 Irradiation experiment

MA-bearing nitride fuel has not been irradiated in fast neutron spectrum. We participate in the irradiation program FUTURIX, where MA-bearing nitride fuels are to be irradiated in Phenix. JAERI will make a contract with CEA on this subject.

Acknowledgements

This paper contains some results obtained within the framework of the Development of Innovative Nuclear Technologies by the Ministry of Education, Culture, Sports, Science and Technology of Japan.

References

1. Y. ARAI, S. FUKUSHIMA, K. SHIOZAWA, M. HANDA, *J. Nucl. Mater.*, **168**, 280 (1989).
2. Y. SUZUKI, Y. ARAI, Y. OKAMOTO, T. OHMICHII, *J. Nucl. Sci. Technol.*, **31**, 677 (1994).
3. Y. ARAI, Y. SUZUKI, M. HANDA, "Research on Actinide Mononitride Fuel," *Proc. Int. Conf. Global '95*, Versailles, France, Sept. 11-14, 1995, Vol. 1, p. 538 (1995).
4. Y. SUZUKI, T. OGAWA, Y. ARAI, T. MUKAIYAMA, "Recent Progress of Research on Nitride Fuel Cycle in JAERI," *Proc. 5th OECD/NEA Information Exchange Meeting on Actinide and Fission Product P&T*, Mol, Nov. 25-27, 1998, p. 213 (1999).
5. M. TAKANO, A. ITOH, M. AKABORI, T. OGAWA, S. KIKKAWA, H. OKAMOTO, "Synthesis of Americium Mononitride by Carbothermic Reduction Method," *Proc. Int. Conf. Global '99*, Jackson Hole, Wyoming, Aug. 29-Sept. 3, 1999, CD-ROM (1999).
6. M. TAKANO, A. ITOH, M. AKABORI, T. OGAWA, et al., *J. Nucl. Mater.*, **294**, 24 (2001).
7. A. ITOH, M. AKABORI, M. TAKANO, et al., *J. Nucl. Sci. Technol.*, **Suppl. 3**, 737 (2002).
8. Y. ARAI, K. NAKAJIMA, *J. Nucl. Mater.*, **281**, 244 (2000).
9. Y. SUZUKI, A. MAEDA, Y. ARAI, T. OHMICHII, *J. Nucl. Mater.*, **188**, 239 (1992).
10. K. NAKAJIMA, Y. ARAI, Y. SUZUKI, *J. Nucl. Mater.*, **247**, 33 (1997).
11. K. NAKAJIMA, Y. ARAI, Y. SUZUKI, *J. Alloys Comp.*, **271-273**, 666 (1998).
12. K. NAKAJIMA, Y. ARAI, *J. Nucl. Sci. Technol.*, **Suppl. 3**, 620 (2002).
13. Y. ARAI, Y. SUZUKI, T. IWAI, T. OHMICHII, *J. Nucl. Mater.*, **195**, 37 (1992).
14. Y. ARAI, Y. OKAMOTO, Y. SUZUKI, *J. Nucl. Mater.*, **211**, 248 (1994).
15. Y. ARAI, K. NAKAJIMA, Y. SUZUKI, *J. Alloys Comp.*, **271-273**, 602 (1998).
16. F. KOBAYASHI, T. OGAWA, M. AKABORI, Y. KATO, *J. Am. Ceram. Soc.*, **78**, 2279 (1995).
17. O. SHIRAI, T. IWAI, K. SHIOZAWA, Y. SUZUKI, et al., *J. Nucl. Mater.*, **277**, 226 (2000).
18. O. SHIRAI, M. IIZUKA, T. IWAI, Y. SUZUKI, Y. ARAI, *J. Nucl. Sci. Technol.*, **37**, 676 (2000).
19. O. SHIRAI, M. IIZUKA, T. IWAI, Y. SUZUKI, Y. ARAI, *J. Electroanal. Chem.*, **490**, 31 (2000).
20. F. KOBAYASHI, T. OGAWA, M. TAKANO, M. AKABORI, A. ITOH, K. MINATO, S. TAKAHASHI, "Dissolution of Metal Nitrides in LiCl-KCl Eutectic Melt," *Proc. Int. Conf. Global '99*, Jackson Hole, Wyoming, Aug. 29-Sept. 3, 1999, CD-ROM (1999).
21. Y. ARAI, Y. SUZUKI, T. IWAI, A. MAEDA, T. SASAYAMA, K. SHIOZAWA, T. OHMICHII, *J. Nucl. Sci. Technol.*, **30**, 824 (1993).

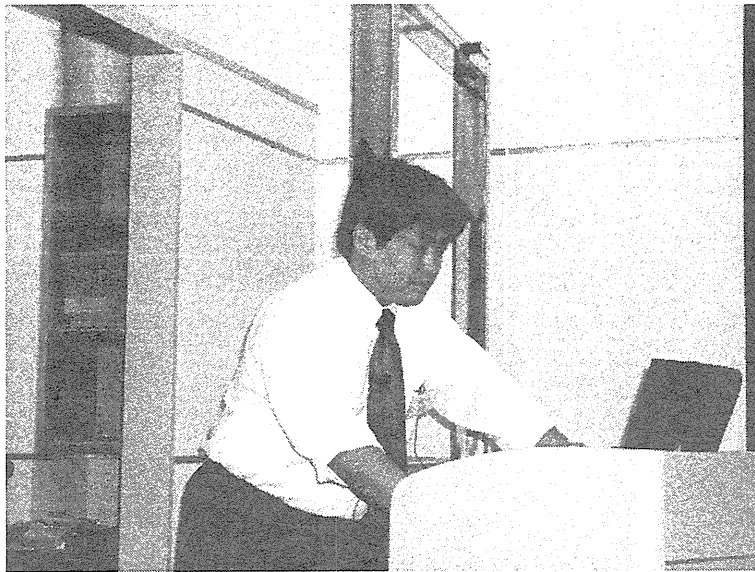


3. Session B-1: Fabrication Technology

3.1 Fabrication of Minor Actinide Nitrides

Masahide TAKANO, Akinori ITOH, Mitsuo AKABORI, Yasuo ARAI,
Kazuo MINATO

Japan Atomic Energy Research Institute



This is a blank page.

Fabrication of Minor Actinide Nitrides

Masahide TAKANO, Akinori ITOH, Mitsuo AKABORI,
Yasuo ARAI, Kazuo MINATO

Japan Atomic Energy Research Institute, Tokai-mura, Ibaraki-ken, 319-1195, Japan

E-mail: takano@poppsvr.tokai.jaeri.go.jp

Abstract

Within the framework of the *PROMINENT* program, minor actinide nitride containing Pu, Am and Cm was prepared by carbothermic reduction of the oxide mixture in N₂ gas flow at 1250 °C. Residual carbon was successfully removed by heating in N₂+4%H₂ mixed gas flow at 1500 °C. The product was a single phase solid solution (Pu,Am,Cm)N without any oxide phases. For the fabrication of Zr-containing nitride, simultaneous nitridation of the mixture of minor actinides and zirconium oxides was attempted by the same way. The product consisted of two phases with NaCl-type structure and had a high carbon content. The two phases are considered to be solid solutions with different (Pu+Am+Cm)/Zr ratios.

1. Introduction

In the concept of fuel cycle based on nitride fuel and pyrochemical reprocessing, carbothermic reduction method is to be applied for the fabrication of nitride fuels containing minor actinides (MAs). In this method, a compacted mixture of the respective oxides and carbon powders is heated in N₂ gas flow to produce a single-phase nitride, which normally contains some amounts of oxygen and carbon as impurities.

In case of U-free nitride fuel, MAs need to be diluted with a material inert to neutron, in order to control the linear power rate and burnup swing of k_{eff} of a core. Some nitrides such as YN, TiN and ZrN are under consideration as candidate materials. TiN and ZrN are chemically stable and has low vapor pressures at high temperatures. And also the mutual solubility among MA nitrides and ZrN would be expected. If MA nitrides form a solid solution with ZrN, the hydrolytic features of MA nitrides and vaporization of Am at high temperatures may be moderated.¹⁾ For these aspects, we regard ZrN as a primary candidate for matrix at this stage.

As for the method to fabricate MA nitrides diluted with ZrN matrix, we have attempted the simultaneous nitridation of a mixture of MA and zirconium oxides to simplify the fabrication process.

In the present paper, results of the recent fabrication experiments on (Pu,Am,Cm)N and (Pu,Am,Cm,Zr)N are overviewed as well as the works before we started the *PROMINENT* program.

2. Outline of fabrication works before *PROMINENT* program

Fabrication of UN, PuN and (U,Pu)N have been originally studied along with the carbides for FBR fuels since early 1980's at JAERI. UN and PuN with high purity were fabricated by carbothermic reduction of their dioxides at about 1550 °C in N₂+8%H₂ mixed gas flow. Solid solutions of (U,Pu)N were obtained by simultaneous carbothermic reduction of UO₂+PuO₂ mixtures, or by heating the compacted mixtures of UN and PuN. Densities up to 95 %TD of the sintered (U,Pu)N pellets were achieved.²⁾

Since 1990's, nitride fuels have also been studied for the transmutation of minor actinides. At first, fabrication of NpN was successfully demonstrated by the similar way.³⁾ Formation of the solid solutions (U,Np)N and (Np,Pu)N was confirmed.⁴⁾

Handling of transplutonium elements, Am and Cm, are very limited in the amount due to the higher radioactive toxicity and also neutron emission. We have fabricated AmN and (Cm,Pu)N in a several ten milligram scale at WASTE-F of JAERI. For the fabrication of AmN, the reaction temperature in N₂ gas flow was lowered to 1300 °C to avoid the vaporization loss of Am during nitridation. Subsequently the excess carbon was removed at 1500 °C in N₂+4%H₂ mixed gas flow.⁵⁾ The low oxygen (0.05 wt%) and carbon (less than 0.02 wt%) in AmN was achieved. The lattice parameter of AmN was found to increase with the oxygen content by the formation of Am(N,O) solid solutions. Although the runs for (Cm,Pu)N fabrication are fewer, similarly low carbon content was achieved and the formation of the solid solution was confirmed.⁶⁾ In addition, the lattice parameters of (Pu,Cm)N increased rapidly after preparation and saturated within ~5 days because of the self-irradiation damage induced by alpha-decay of ²⁴⁴Cm with a short half-life.⁷⁾

Fabrication of some nitrides containing the diluent was attempted. Sintered pellets of (Pu,Zr)N solid solutions were obtained by heating the compacted mixture of PuN and commercially available ZrN powders at 1730 °C, while the heating of PuN+TiN mixture did not yielded the solid solution.⁸⁾ (Am,Y)N solid solutions were obtained from the mixtures of AmO₂ and Y₂O₃ by the same way as the fabrication of AmN. In the carbothermic nitridation of AmO₂+ZrO₂ mixtures at 1300 and 1500 °C, single phase of (Am_{0.1}Zr_{0.9})N was obtained but (Am_{0.3}Zr_{0.7})N consisted of two phases with different Am/Zr ratios.⁹⁾ The lattice parameters of fabricated (Pu,Zr)N, (Am,Y)N and (Am,Zr)N solid solutions are shown in Fig. 1.

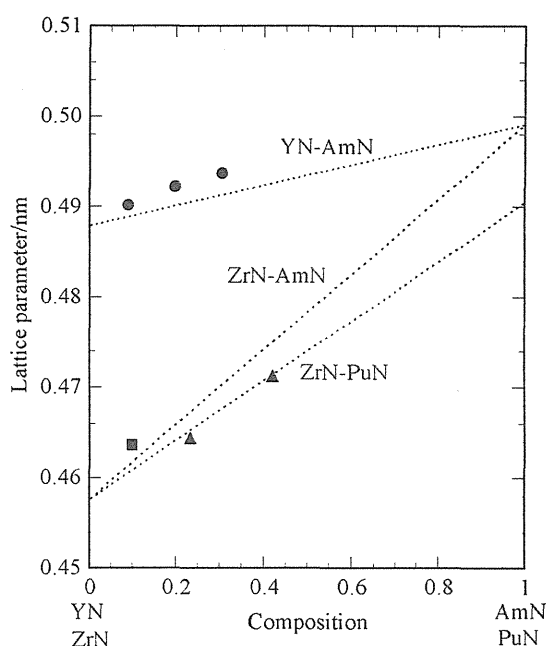


Fig. 1 Lattice parameters of fabricated (Pu,Zr)N, (Am,Zr)N and (Am,Y)N.
Dot lines show Vegard's law.

3. Fabrication of (Pu,Am,Cm)N and (Pu,Am,Cm,Zr)N

Within the framework of the *PRPMINENT* program, we started the fabrication of MA nitrides, which have more complex compositions. (Pu,Am,Cm)N and (Pu,Am,Cm,Zr)N were fabricated by the simultaneous carbothermic reduction of the respective oxide mixtures in approximately 40 mg scale. Powders of $^{243}\text{Am}_2\text{O}_3$, $(^{240}\text{Pu}, ^{244}\text{Cm})\text{O}_2$, ZrO_2 and amorphous carbon were used as starting materials. Compositions of the mixtures are summarized in Table 1. The C/M ratios shown are equivalent to about 200 and 130 % of the theoretically required carbon amounts for the reduction of each mixture, respectively.

Table 1 Composition of TRU and zirconium oxide mixtures

Expected product	Pu/Am/Cm/Zr molar ratio	C/M molar ratio
(Pu,Am,Cm)N	0.450 / 0.336 / 0.214 / 0	3.78
(Pu,Am,Cm,Zr)N	0.134 / 0.099 / 0.063 / 0.704	2.58

The mixtures were compacted into tablets with 4 mm in diameter by a pressure of 200 MPa. Then each tablet in a tungsten crucible was heated at 1250~1300 °C in N_2 gas flow for nitridation. The carbothermic reaction is formally represented by,



CO gas yielded by the reaction was monitored by infrared spectroscopy. After the CO gas release subsided, the temperature was raised up to 1500 °C and the gas flow was replaced with $\text{N}_2+4\%\text{H}_2$ for removal of the excess carbon. The decarburization was continued until the CO gas release subsided again. The CO gas release during the whole process is shown in Fig. 2. For both samples, the temperature of 1250 °C was regarded enough for nitridation from the CO gas release behavior.

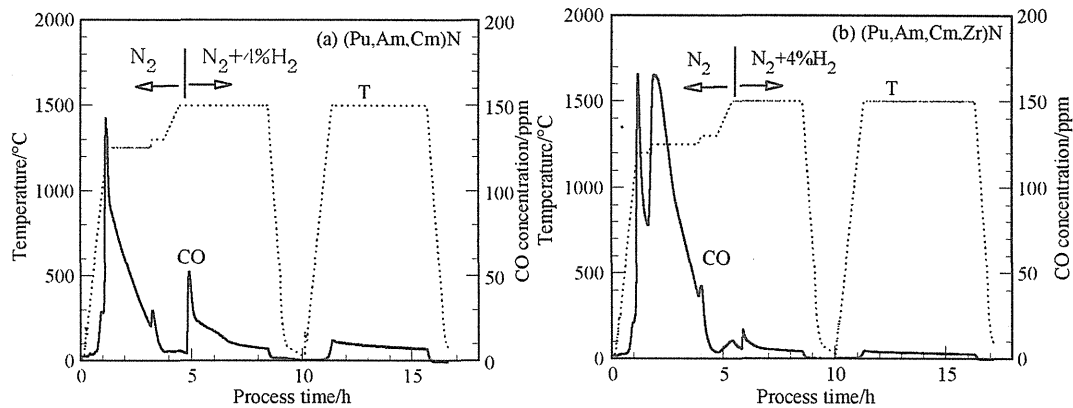


Fig. 2 CO gas release during carbothermic reduction for the fabrication of (a) (Pu,Am,Cm)₃N and (b) (Pu,Am,Cm,Zr)₃N.

X-ray diffraction with Cu-K α radiation was carried out to identify the phase of the products and to determine the lattice parameters. The lattice parameters of the nitrides increased with time after preparation because of the self-irradiation damage. The “undamaged” lattice parameters were estimated by extrapolating the lattice parameters to time=0. Nitrogen, oxygen and carbon contained in the products were also determined by chemical analyses.

X-ray diffraction profiles of (Pu,Am,Cm)N and (Pu,Am,Cm,Zr)N are shown in Fig. 3. (Pu,Am,Cm)N was single phase with NaCl-type structure, and any oxide phases were not recognized. The undamaged lattice parameter was 0.4956 nm, which agreed reasonably with 0.4960 nm calculated by Vegard’s law using the values for PuN¹⁰⁾, AmN and CmN¹¹⁾. The residual carbon content was less than 0.05 wt%. The low carbon content means the excess carbon was successfully removed in $\text{N}_2+4\%\text{H}_2$ mixed gas flow at 1500 °C.

On the other hand, the product containing zirconium consisted of two phases with NaCl-type structure. Oxygen and carbon contents were 0.15 and 1.31 wt%, respectively. The high carbon content suggests that the excess carbon remained as carbonitride. It is known that ZrN can form carbonitride, $\text{Zr}(\text{N}_{1-x}\text{C}_x)$, with a wide range of x values.¹²⁾ Judging from the calculated peak positions of the constituent nitrides and ZrC shown in the figure, these two phases are considered to be solid solutions

with different (Pu+Am+ Cm)/Zr ratios. The factors affecting the mutual solubility among TRU nitrides and ZrN fabricated by the carbothermic reduction should be studied further.

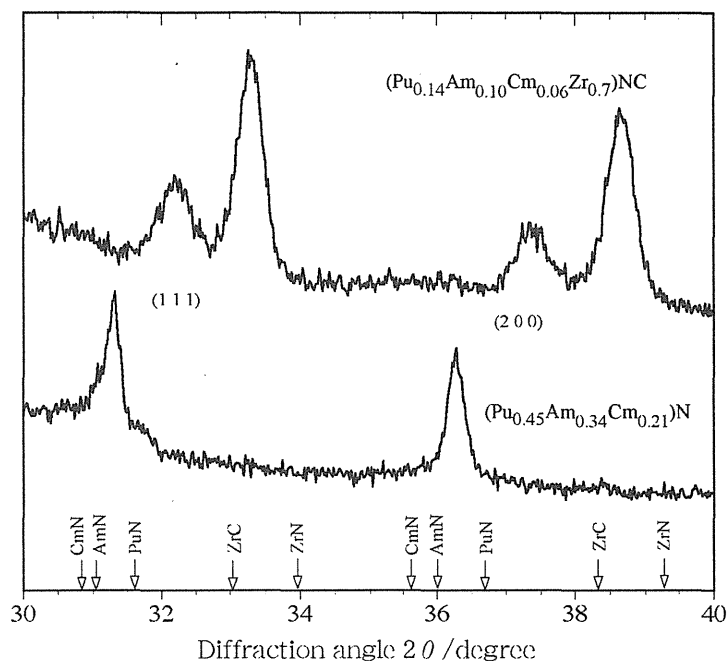


Fig. 3 X-ray diffraction profiles of (Pu,Am,Cm)N and (Pu,Am,Cm,Zr)N.

4. Conclusions

Within the framework of the *PROMINENT* program, (Pu,Am,Cm)N and (Pu,Am,Cm,Zr)N were fabricated by carbothermic reduction of mixtures of the respective oxides. Formation of the single phase solid solution, (Pu,Am,Cm)N, with very low carbon content was achieved. However, the Zr-containing nitride fabricated by the same way consisted of two phases and had high carbon content. The reason will be further examined.

Acknowledgements

This paper contains some results obtained within the framework of the Development of Innovative Nuclear Technologies by the Ministry of Education, Culture, Sports, Science and Technology of Japan.

References

1. M. TAKANO, A. ITOH, M. AKABORI, K. MINATO, "Study on the Stability of AmN and (Am,Zr)N," *Proc. Int. Conf. Global 2003*, New Orleans, USA, Nov. 16-20, 2003, CD-ROM (2003).
2. Y. ARAI, S. FUKUSHIMA, K. SHIOZAWA, M. HANDA, *J. Nucl. Mater.*, **168**, 280 (1989).

3. Y. SUZUKI, Y. ARAI, Y. OKAMOTO, *J. Nucl. Sci. Technol.*, **31**, 677 (1994).
4. Y. SUZUKI, Y. ARAI, *J. Alloys Comp.*, **271-273**, 577 (1998).
5. M. TAKANO, A. ITOH, M. AKABORI, T. OGAWA, S. KIKKAWA, H. OKAMOTO, "Synthesis of Americium Mononitride by Carbothermic Reduction Method," *Proc. Int. Conf. Global'99*, Jackson Hole, USA, Aug. 29-Sep. 3, 1999, CD-ROM (1999).
6. M. TAKANO, A. ITOH, M. AKABORI, T. OGAWA, M. NUMATA, H. OKAMOTO, *J. Nucl. Mater.*, **294**, 24 (2001).
7. M. TAKANO, A. ITOH, M. AKABORI, T. OGAWA, M. NUMATA, M. KIZAKI, *J. Nucl. Sci. Technol.*, **Suppl. 3**, 842 (2002).
8. Y. ARAI, K. NAKAJIMA, *J. Nucl. Mater.*, **281**, 244 (2000).
9. A. ITOH, M. AKABORI, M. TAKANO, T. OGAWA, M. NUMATA, F. ITONAGA, *J. Nucl. Sci. Technol.*, **Suppl. 3**, 737 (2002).
10. N.J. BRIDGER, R.M. DELL, AERE-R-5411 (1967).
11. D.A. DAMIEN et al., CONF 780823-8 (1978).
12. V.V. KOSUKHIN et al., *Izvestiya Akademii Nauk SSSR, Neorganicheskie Materialy*, **23**(1), 63 (1987).

3.2 Fabrication of Lanthanide Nitride Pellets and Simulated Burnup Fuels

Kazuhiko YAMASAKI¹, Yoshihisa TAMAKI¹, Masahide TAKANO²,
Mitsuo AKABORI², Kazuo MINATO², Yasuo ARAI²

¹Mitsubishi Materials Corporation

²Japan Atomic Energy Research Institute



This is a blank page.

Fabrication of Lanthanide Nitride Pellets and Simulated Burnup Fuels

Kazuhiko YAMASAKI¹, Yoshihisa TAMAKI¹, Masahide TAKANO²

Mitsuo AKABORI², Kazuo MINATO², Yasuo ARAI²

¹Mitsubishi Materials Corporation, Naka-machi, Naka-gun, Ibaraki-ken, 311-0102, Japan,

²Japan Atomic Energy Research Institute, Tokai-mura, Naka-gun, Ibaraki-ken, 319-1195, Japan

E-mail address: kazuyama@mmc.co.jp

Abstract

Recent progress in the fabrication technique for the nitride fuel pellets, which is a part of the development of nuclear fuel cycle based on the nitride fuel and pyrochemical process, is described. Firstly, we reported here the parametric study for fabrication of the sintered pellets of DyN and (Dy,Zr)N. Dy was used as Am simulant and Zr was chosen as a dilutant for minor actinide (MA) transmutation. The results showed that the increase in milling time for DyN pellet fabrication, and sintering temperature for (Dy_{0.4}Zr_{0.6})N was the most effective to obtain high densities of sintered pellets. And then, we performed the fabrication experiment of simulated burnup fuels, which contained Nd as simulated rare earth fission product (FP) and Pd as simulated noble metal FP in UN matrix. For such fuels, Nd was found to be solely in solid solution, however precipitation along the grain boundaries was observed in case of Pd.

1. Introduction

Nitride fuel is a promising candidate for transmutation of MA because of its excellent thermal and neutronic properties [1,2]. The advantages of nitride fuel have been confirmed through the recent research on the application of pyrochemical process to the nitride fuel cycle.

The present paper describes recent progress of the fabrication technique of nitride pellets, which is a part of the development of nuclear fuel cycle based on the nitride fuel and pyrochemical process. In the first half of this paper, the parametric study for fabrication of the sintering pellets of (Dy,Zr)N and DyN was reported. Dy was used as simulated Am known to cause difficulties to prepare the high-density pellets. Zr was a dilutant needed in order to fabricate the actual fuel for transmutation of MA. In the second half, the fabrication of simulated burnup fuels, which contained Nd as simulated rare earth FP or Pd as simulated noble metal FP in UN matrix, was studied.

2. Fabrication of lanthanide nitride pellets

Dysprosium and zirconium nitrides were synthesized from metals as follows. First metals were hydrided and finely milled in the mortar. The Dysprosium hydride powder was heated at 1573K, and the zirconium hydride powder was heated at 1573-1673K in flowing N_2 gas for nitridation. X-ray diffraction analysis confirmed the formation of DyN and ZrN.

Solid solutions of (Dy,Zr)N were prepared by mechanical blending method, where DyN and ZrN powders were mixed at a molar ratio of 4:6. The mixed powder was compacted into green pellets and heated at 1873K in flowing N_2 gas. The formation of $(Dy_{0.4}Zr_{0.6})N$ was confirmed by X-ray diffraction analysis.

The parametric study to fabricate sintered pellets from the synthesized nitride powders was also performed. DyN and $(Dy_{0.4}Zr_{0.6})N$ were ball-milled and formed into green pellets by pressing. Then, the pellets were sintered in flowing N_2 . Tables 1 and 2 show conditions and result of DyN and $(Dy_{0.4}Zr_{0.6})N$ pellet fabrication experiment. It was confirmed that densities of sintered pellets increased with milling time, pressing pressure, sintering temperature and time. Among these parameters, milling time in the DyN experiment was seen to be the most effective to obtain the high densities of sintered pellets and about 90%TD was the highest density in the present study. On the other hand, sintering temperature in $(Dy_{0.4}Zr_{0.6})N$ was seen to be the most effective and about 94%TD was the highest.

Table 1 Result of the fabrication experiment

of DyN pellets

(1) Effect of milling time

Sintering temperature : 1773K / Pressing pressure : 300MPa

Grinding time (h)	Sintering time (h)		
	5	10	15
20	77.35	79.26	81.14
40	80.97	81.19	82.48
80	89.03	89.34	90.11

(2) Effect of sintering temperature

Pressing pressure : 300MPa / Milling time : 40 hours

Temperature (K)	Sintering time (h)		
	5	10	15
1773	80.97	81.19	82.48
1873	81.06	81.40	82.48
1973	81.34	81.55	82.72

(3) Effect of pressing pressure

Sintering temperature : 1773K / Milling time : 40 hours

Pressure (MPa)	Sintering time (h)		
	5	10	15
200	78.61	80.67	81.65
300	80.97	81.19	82.48
400	81.48	81.88	82.83

Table 2 Result of the fabrication experiment

of $(Dy_{0.4}Zr_{0.6})N$ pellets

(1) Effect of milling time

Sintering temperature : 1773K / Pressing pressure : 300MPa

Grinding time (h)	Sintering time (h)		
	5	10	15
20	74.75	77.24	78.07
40	76.01	78.73	80.00
80	76.79	79.71	80.95

(2) Effect of sintering temperature

Pressing pressure : 300MPa / Milling time : 80 hours

Temperature (K)	Sintering time (h)		
	5	10	15
1773	76.79	79.71	80.95
1873	85.53	88.35	89.39
1973	92.07	93.59	93.91

(3) Effect of pressing pressure

Sintering temperature : 1773K / Milling time : 80 hours

Pressure (MPa)	Sintering time (h)		
	5	10	15
200	76.82	79.77	80.73
300	76.79	79.71	80.95
400	79.11	81.93	83.03

3. Fabrication of simulated burnup fuels

3.1 Uranium-neodymium-nitride pellets

Solid solutions of (U,Nd)N were prepared by carbothermic reduction method[3]. An amount of added Nd_2O_3 was that in ratio of NdN to (U,Nd)N as 1.7 or 8.0wt%, which

corresponded to the amount of rare earth FP in 50 or 200 GWD/t burnup fuels. The powders of UO_2 , Nd_2O_3 and active carbon were mixed at a molar ratio $\text{C}/(\text{U}+\text{Nd})$ of 2.4. The mixed powder was compacted into green pellets and heated at 1773K in flowing N_2 gas for carbothermic reduction and successively heated in flowing N_2 -5% H_2 gas to remove the residual carbon. X-ray diffraction analysis revealed the complete solid solution of (U,Nd)N. After conversion to (U,Nd)N, the pellets were so fragile that they were crushed easily with spatula. The obtained coarse (U,Nd)N powder was mixed with hexane as dispersion agent and milled in the WC ball mill. After milling and removing hexane under reduced pressure, the solution of polyethylene glycol in trichloroethylene as binder was added to the milled powder and the mixture was formed into green pellets under the pressure of about 200MPa. The green pellets were sintered for 4 hrs at 2073K in flowing Ar.

Characteristics of the produced pellets are summarized in Table 3. The carbon content was found to be less than 2000ppm and that of oxygen was less than 5000ppm. The density of the produced pellets was near 95%TD. X-ray diffraction analysis indicated the mixed nitride solid solution without remarkable residual oxides. A ceramography of the sintered pellet is shown in Fig.1.

Table 3 Characteristics of (U,Nd)N pellets

Nd concentration (wt%)	1.7	8.0
Diameter (mm)	8.7-8.8	8.5-8.6
Height (mm)	9.9-10.1	9.7-10.0
Content of carbon (ppm)	1149	1892
Content of oxygen (ppm)	3701	4391
Content of Nitrogen (wt%)	5.62	5.67
N/(U+Nd) (molar ratio)	1.01	0.98
Lattice parameter (nm)	0.4898	0.4913
Density (%TD)	93.8	95.1

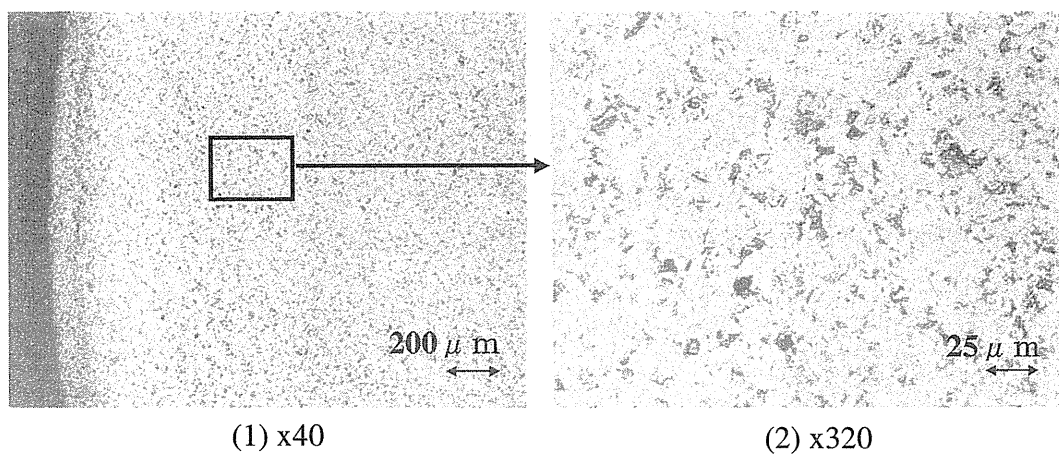


Fig.1 A ceramography of (U,Nd)N pellet (8.0wt%Nd) after sintering

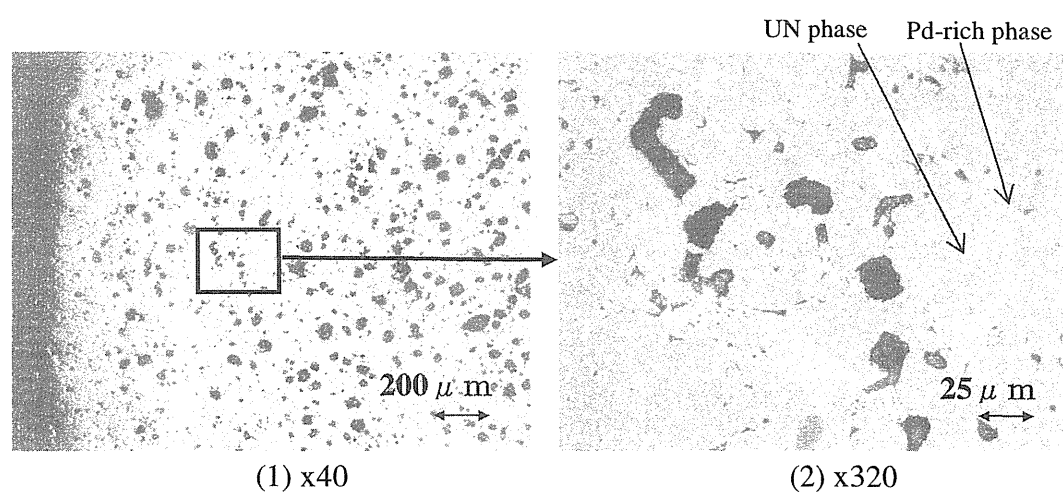
3.2 Uranium-palladium-nitride pellets

As the first step of U-Pd nitride pellets fabrication, UN powder was synthesized by carbothermic reduction[3]. Powders of UO_2 and active carbon were mixed at a molar ratio C/U of 2.4 and pressed into the green pellets. The pellets were heated at 1773K in flowing N_2 gas for carbothermic reduction, then in flowing N_2 -5% H_2 gas to remove the residual carbon. After conversion to UN, the pellets were so fragile that they were crushed easily with spatula. And then, the coarse UN powder was mixed with hexane as dispersion agent and milled in the WC ball mill. After milling and removing hexane under reduced pressure, Pd powder was added to the milled UN powder in ratio of 0.97wt% or 4.6wt%, which corresponded to the amount of noble metal FP in 50 or 200 GWD/t burnup fuels, and mixed by V-type mixer. Then, the solution of polyethylene glycol in trichloroethylene as binder was also added and the mixture was formed into green pellets under the pressure of about 200MPa. The green pellets were sintered for 8 hrs at 2073K in flowing Ar.

Characteristics of the produced pellets are summarized in **Table 4**. The carbon contents were less than 2000ppm and the oxygen contents were less than 5000ppm. The densities of the produced pellets were above 85%TD. A ceramography of the sintered pellet is shown in **Fig.2**. We have also examined the electron probe microanalysis image and found that Pd-rich phase was precipitated mainly along the UN grain boundaries ((2) in **Fig.2**). The X-ray diffraction analysis also indicated that the sintered pellets had two phases of UN phase and Pd-metal or UPd_3 intermetallic compound phase. Previous study showed the possibility to form UPd_3 phase [4], although X-ray diffraction analysis was not able to distinguish between two phases.

Table 4 Characteristics of the UN pellets containing Pd

Pd concentration (wt%)	0.97	4.6
Diameter (mm)	9.0-9.1	8.6-8.7
Height (mm)	9.7-10.0	9.4-9.9
Content of carbon (ppm)	1509	1304
Content of oxygen (ppm)	3274	4243
Content of Nitrogen (wt%)	5.27	4.93
N/U (molar ratio)	1.04	1.07
Density (%TD)	85.2	89.4

**Fig.2** A ceramography of UN pellet containing 4.6wt%Pd after sintering

4. Summary

The fabrication of the MA simulated pellets of DyN and (Dy,Zr)N was parametrically studied. Dy was used as the simulated Am, and Zr was a candidate of diluted material for MA transmutation. The results showed that the increase in milling time for DyN pellet fabrication and sintering temperature for (Dy_{0.4}Zr_{0.6})N was the most effective to obtain high densities of sintered pellets.

The fabrication of simulated burnup fuels which contained Nd as simulated rare earth FP and Pd as simulated noble metal FP in UN matrix was done successfully. For such fuels, Nd was found to be solely in solid solution, however precipitation along the grain boundaries was observed in case of Pd.

Acknowledgements

This study was carried out within the framework of the Development of Innovative Nuclear Technologies by the Ministry of Education, Culture, Sports, Science and Technology of Japan.

References

1. T. Mukaiyama, M. Kubota, T. Takizuka, Y. Suzuki, T. Ogawa, T. Osugi, M. Mizumori, Proceedings 4th OECD/NEA Int. Mtg. on Actinide and Fission Product Partitioning and Transmutation, Mito, Oct. 1996, P80.
2. T. Mukaiyama, M. Kubota, T. Takizuka, T. Ogawa, M. Mizumoto, H. Yoshida, Proceedings of International Conference on Global'95, Versaille, France, 110(1995)
3. Y. Arai, Y. Suzuki, H. Handa, Proceedings of International Conference on Global'95, Versaille, France, 538(1995)
4. H. Kleykamp, S. Kang, Z. Metallkd, **82**, 844(1991)



4. Session B-2: Property Measurements

4.1 Properties of Minor Actinide Nitrides

**Masahide TAKANO, Akinori ITOH, Mitsuo AKABORI, Yasuo ARAI,
Kazuo MINATO**

Japan Atomic Energy Research Institute

This is a blank page.

Properties of Minor Actinide Nitrides

Masahide TAKANO, Akinori ITOH, Mitsuo AKABORI,
Yasuo ARAI, Kazuo MINATO

Japan Atomic Energy Research Institute (JAERI)
Tokai-mura, Naka-gun, Ibaraki-ken 319-1195, JAPAN
akabori@popsvr.tokai.jaeri.go.jp

Abstract

The present status of the research on properties of minor actinide nitrides for the development of an advanced nuclear fuel cycle based on nitride fuel and pyrochemical reprocessing is described. Some thermal stabilities of Am-based nitrides such as AmN and (Am,Zr)N were mainly investigated. Stabilization effect of ZrN was clearly confirmed for the vaporization and hydrolytic behaviors. New experimental equipments for measuring thermal properties of minor actinide nitrides were also introduced.

1. Introduction

Nitrides fuel has been widely studied as one of advanced fuels of fast reactors, because actinide nitrides have many advantages compared with the oxides, such as higher heavy-metal density, good thermal properties, miscibility among the actinide nitrides, and so on. Recently, large R & D efforts devoted to transmutation of long-lived radioactive elements including minor actinides (MA) are being done in Japan in the frame of the OMEGA program, for the management of high level, long-lived radioactive waste. The Japan Atomic Energy Research Institute (JAERI) has proposed the concept for transmutation of MA elements using accelerator-driven systems (ADS) [1], where MA nitride is adopted as a fuel material of the sub-critical core.

The research and development of nitrides fuel as an advanced fuel of fast reactors at JAERI included fabrication technologies, property measurements, irradiation tests and electrorefining. In this frame work, some thermal properties such as vaporization, heat capacity, thermal conductivity and thermal expansion were measured in UN, PuN, NpN and their solid solutions of (U,Pu)N, (U,Np)N and (Np,Pu)N.

Significant experience exists for U-based or Pu-based nitrides, but there is a lack of knowledge about the characteristics for MA-based nitrides as U-free fuels for ADS. The main disadvantage related to the use of MA-based nitrides fuel is relatively lower thermal stability, in particular, high-temperature stability in terms of vaporization in fabrication processes and reactor accidents. The addition of an inert matrix to improve the thermal properties of MA-based nitrides fuel has been suggested. ZrN is thought to be one of candidate materials for Am-based nitrides.

In the study the properties of UN, PuN, NpN and their solid solutions are overviewed, and the present status on property measurements of MA-based nitrides is summarized.

2. Properties of U, Np and Pu nitrides

Vaporization behavior of U-, Np-, Pu-based nitrides was investigated by a Knudsen-effusion mass-spectrometry [2-4]. UN vaporizes incongruently precipitating liquid uranium while PuN vaporizes congruently. For NpN, the vapor pressure of Np(g) was similar to that of Np(g) over liquid Np metal. The vapor pressures of UN, NpN, and PuN increase in this order at an identical temperature.

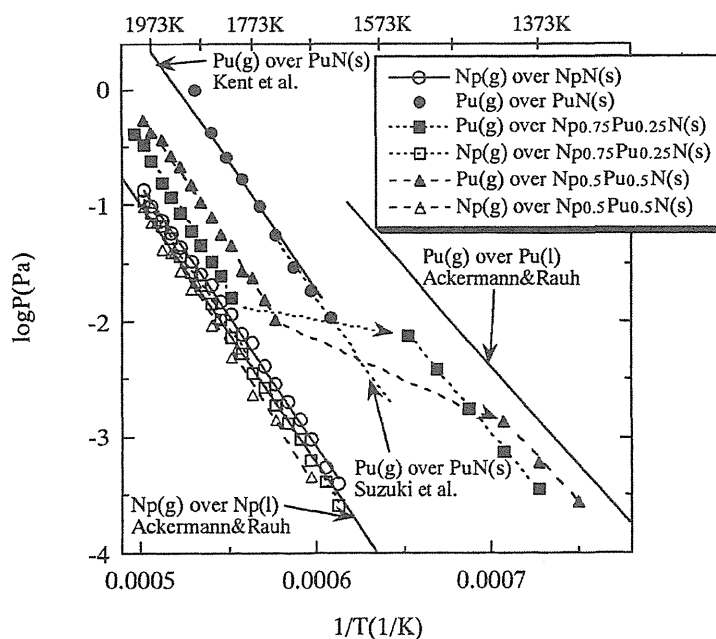


Fig.1 Vaporization behavior of (Np,Pu)N solid solutions

For (U,Pu)N, the partial pressures of U(g) and Pu(g) depended on the composition of the solid solutions. (U,Pu)N vaporized congruently and no liquid phase formed under the experimental conditions. For (Np,Pu)N as shown in Fig.1, the vapor pressures of Np(g) over solid solutions of (Np,Pu)N showed a similar temperature dependence to that over Np(l), which suggested the precipitation of liquid neptunium during the measurements. On the other hand, rather complicated temperature dependence

was found for Pu(g) over the solid solutions (Np,Pu)N. At temperatures higher than 1773 K the vapor pressures of Pu(g) reflected those over (Np,Pu)N being influenced by the Pu/(Np+Pu) ratio in solid phase, while at temperatures lower than 1473 K the vapor pressures of Pu(g) observed were those over liquid plutonium that may have been precipitated during the measurements..

The specific heat capacities of UN, NpN, and PuN were measured with a differential scanning calorimeter (DSC) in the temperature range from 323 to 1023 K [5]. The heat capacities of UN and PuN measured in this study agreed with the data in the literature within experimental errors. The heat capacity of NpN was found to be nearly the same as those of UN and PuN.

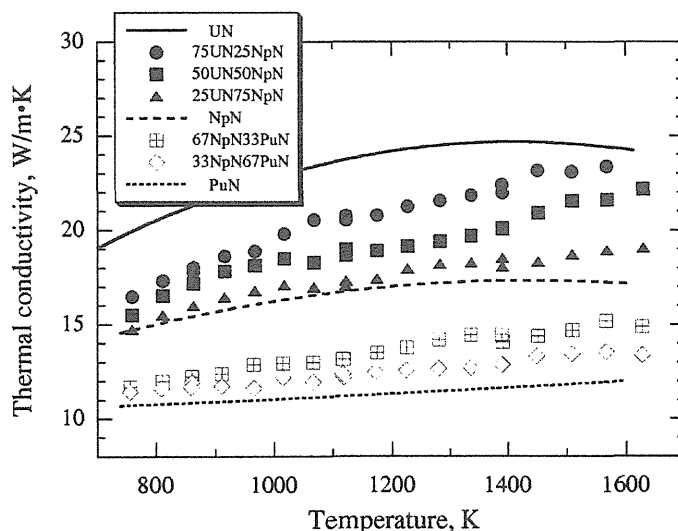


Fig.2 Thermal conductivity of (U,Np)N and (Np,Pu)N solid solutions

The thermal diffusivities of UN, NpN, PuN and the solid solutions of (U, Pu)N, (U, Np)N, and (Np, Pu)N were measured by the laser-flash method from 740 to 1630 K and the thermal conductivities were determined as a function of temperature, as shown in Fig.2 [6-8]. The thermal conductivities of the actinide nitrides gradually increase with temperature over the temperature range investigated. For these nitrides, the electronic component contributes dominantly to the total thermal conductivity, and the increase in the thermal conductivity is due to the increase in the electronic component. It is also found that the thermal conductivity decreases with increasing atomic number from UN to PuN. It is probable that the decrease is caused by the decrease in the electronic component to the thermal conductivity.

3. Properties of minor actinide nitrides

3.1 Hydrolytic behavior

Hydrolytic behavior of Am-based nitrides, AmN and (Am,Zr)N solid solution, was investigated by measuring the weight change in ambient air. The weight gains are shown in Fig.3 as a function of exposure time in air. The weight gain of AmN was rapid compared with that of (Am,Zr)N and saturated within 20 hours. The volume increase during exposure to air was considerably large, and the color of AmN changed from black into light brown. From the weight gain and the chemical analysis of C,N and O before and behind the exposure, the main product was considered to be a hydroxide, $\text{Am}(\text{OH})_3$. The increase in carbon content from 0.3 to 2 wt% suggests that a part of $\text{Am}(\text{OH})_3$ reacted with CO_2 in the atmosphere to form a hydrooxy-carbonate, AmOHCO_3 and/or a carbonate, $\text{Am}_2(\text{CO}_3)_3$.

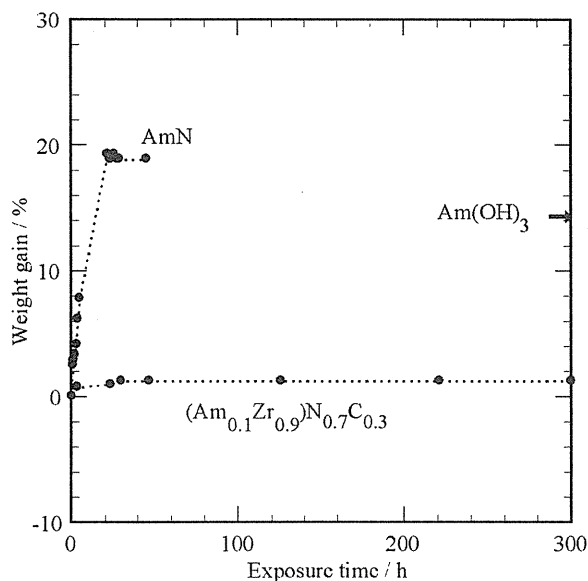


Fig.3 Weight gains of AmN and (Am,Zr)N in air.

For the solid solution of $(\text{Am}_{0.1}\text{Zr}_{0.9})\text{N}$, the weight gain was very small compared with that of AmN, and remained constant at about 1.5 % after 1000 hours. From XRD measurement of the resulted sample, (Am,Zr)N solid solution retained the structure after the long-time exposure in air. Therefore, the result suggested that AmN was significantly stabilized against moisture by the formation of solid solution with ZrN.

3.2 Vaporization behavior

Vaporization behavior of AmN and (Am,Zr)N solid solution in He gas flow was investigated by measuring N_2 release with a gas chromatography. For AmN, nitrogen release was detected above about 1570 K, and large weight loss was found after heating. However, AmN retained the structure

after heating and the metallic phase was not found. For (Am,Zr)N solid solution, the mole fraction of Am/(Am+Zr) decreased from 0.1 to 0.03. The result suggests that selective vaporization of AmN on (Am,Zr)N solid solution occurred.

Fig.4 shows the vaporization behavior of AmN and (Am,Zr)N as a function of temperature, where the rate constant (1/s) is defined from the evaporation rate (mol/s) and the amount of remained AmN (mol). A linear relationship between log (Evaporation rate const.) and reciprocal temperature was clearly found in AmN, but not in (Am,Zr)N. The non-linear relationship for (Am,Zr)N is thought to be mainly due to the decrease of AmN fraction in (Am,Zr)N during heating. It was also found that the addition of ZrN into AmN depressed the vaporization of Am on the nitride.

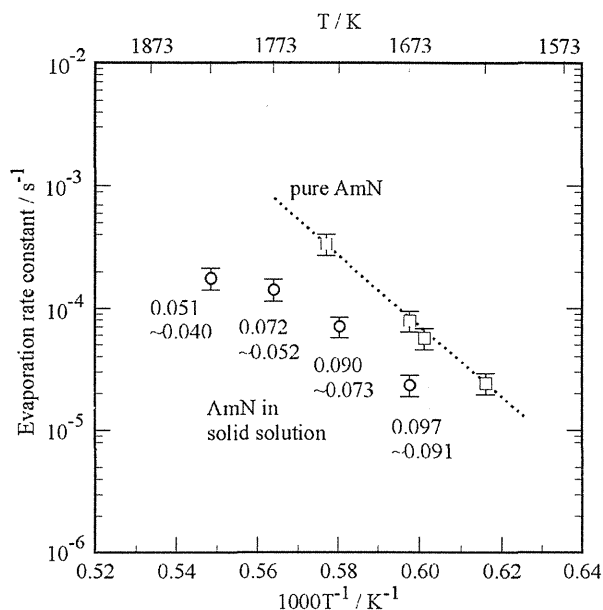


Fig. 4 Arrhenius plots of the evaporation rate constants for AmN and $(\text{Am}_{0.1}\text{Zr}_{0.9})\text{N}_{0.85}\text{C}_{0.15}$.

On the other hand, the equilibrium vapor pressure of Am over AmN was estimated with the Gibbs free energy minimizer ChemSage. It was found that the vapor pressure of Am strongly depends on the partial pressure of N_2 in atmosphere and that high partial pressure of N_2 is very effective to depress the vaporization and loss of Am at high temperature.

4. Installation of experimental equipments

For the purpose of measuring thermal properties such as thermal diffusivity and specific heat capacity of MA nitrides, two experimental equipments were newly installed in WASTEF in the Tokai Research Establishment of JAERI. The thermal diffusivity measuring equipment based on laser flash method was specially designed to make measuring very small samples of MA nitrides and handling the samples in an inert atmosphere possible. Fig.5 shows the equipment before installation and the

Ar-atmosphered inert glove box, in which oxygen and moisture contents are controlled to be below a few ppm.

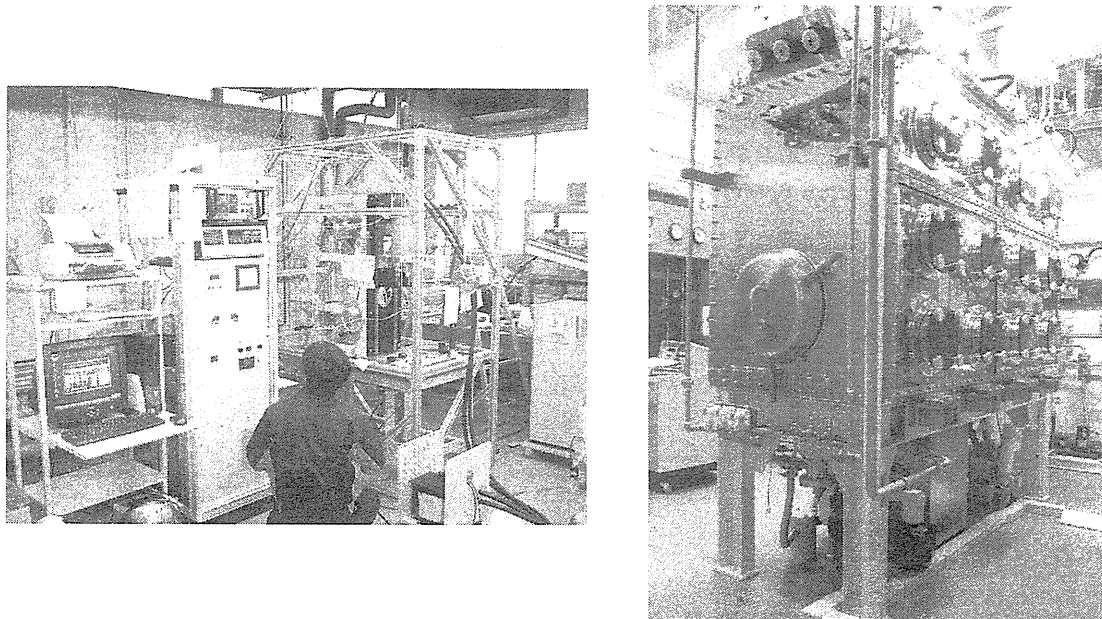


Fig.5 The thermal diffusivity measurement equipment and the inert glove box.

The specific heat capacity measuring equipment based on drop calorimetry method was also installed in an air-atmosphered glove box. It allows to measure the heat capacity of very small samples ($<100\text{mg}$). Fig.6 shows the equipment before installation and the glove box.

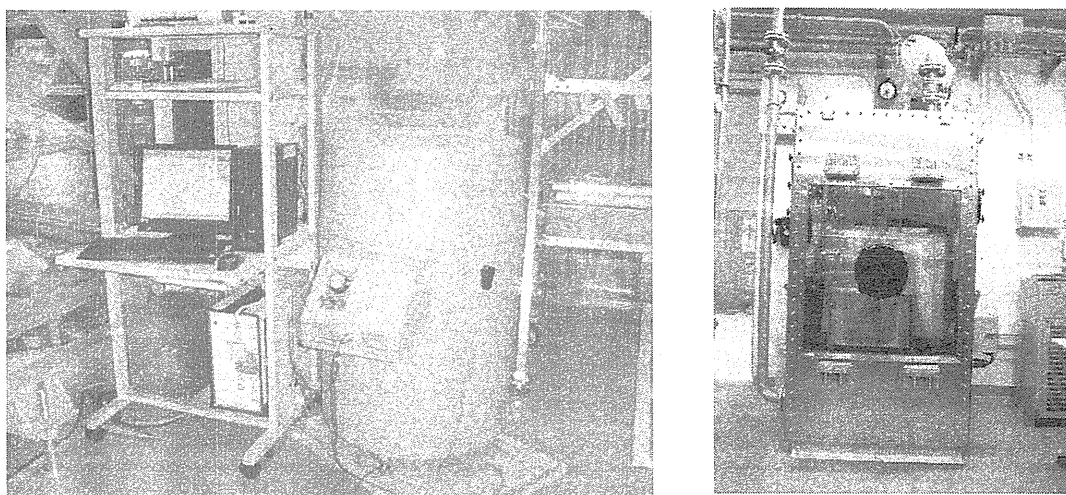


Fig.6 The specific heat capacity measuring equipment and the glove box

Acknowledgements

This paper contains some results obtained within the framework of the Development of Innovative Nuclear Technologies by the Ministry of Education, Culture, Sports, Science and Technology of Japan.

References

1. T.MUKAIYAMA et al., *Partitioning and transmutation program "OMEGA" at JAERI*, Proc. Int. Conf. Global'95, Sept. 11-14, 1995, p.110 (1995).
2. Y. SUZUKI, A. MAEDA, Y. ARAI, and T. OHMICHII, *J. Nucl. Mater.*, **188**, 239 (1992).
3. K. NAKAJIMA, Y. ARAI, and Y. SUZUKI, *J. Nucl. Mater.*, **247**, 33 (1997).
4. K. NAKAJIMA, Y. ARAI, and Y. SUZUKI, *J. Alloys Comp.*, **271-273**, 666 (1998).
5. K. NAKAJIMA and Y. ARAI, *J. Nucl. Sci. Tech.*, **Supplement 3**, 620 (2002).
6. Y. ARAI, Y. SUZUKI, T. IWAI, and T. OHMICHII, *J. Nucl. Mater.*, **195**, 37 (1992).
7. Y. ARAI, Y. OKAMOTO and Y. SUZUKI, *J. Nucl. Mater.*, **211**, 248 (1994).
8. Y. ARAI, K. NAKAJIMA and Y. SUZUKI, *J. Alloys Comp.*, **271-273**, 602 (1998).

This is a blank page.



4.2 Properties of Simulated Burnup Fuels

Masayoshi UNO*, Ken KUROSAKI, Shinsuke YAMANAKA, Kazuo MINATO**

Department of Nuclear Engineering, Graduate School of Engineering Osaka University

**Japan Atomic Energy Research Institute



This is a blank page.

Properties of Simulated Burnup Fuels

Masayoshi UNO*, Ken KUROSAKI, Shinsuke YAMANAKA and Kazuo MINATO**

Department of Nuclear Engineering, Graduate School of Engineering Osaka University
Suita Osaka 565-0871 Japan (*Corresponding author; uno@nucl.eng.osaka-u.ac.jp)

**Japan Atomic Energy Research Institute, Department of Materials Science
Research Group for Actinides Science, Tokai-mura, Ibaraki-ken 319-1195, Japan

Abstract

In order to develop the technologies for nuclear fuel cycle based on nitride fuel and pyrochemical reprocessing thermal properties and mechanical properties for UN and (U,Nd)N were measured. Lattice constants for (U,Nd)N obeyed Vegard law and increased with NdN content. Vickers hardness increase with NdN content and thermal conductivity decreased with NdN content.

1. Introduction

In order to develop the technologies for nuclear fuel cycle based on nitride fuel and pyrochemical reprocessing we have a plan to examine various thermal properties and mechanical properties for uranium nitride and uranium nitrides solid solution containing some surrogate elements and/or some FP elements in Osaka University. In the present study Vickers hardness, elastic moduli obtained by ultrasonic pulse echo method and thermal conductivity estimated by experimentally obtained thermal diffusivity and theoretically calculated specific heat for uranium nitride and uranium neodymium nitride solid solution have been discussed.

2. Experimental

Fuel pellets of uranium nitride and uranium neodymium solid solution (2.7 at%Nd and 12.2 at%Nd) were fabricated by the carbothermic reduction of the mixed oxide powders with active carbon at Mitsubishi Material Co. Ltd. Table 1 shows the geometric properties for the samples.

X-ray diffraction was done by Rigaku Rint-2000 diffractometer using Cu-K α radiation at room temperature. Vickers hardness measurement was carried out using a MHT-1 Vickers hardness tester supplied by MATSUZAWA SEIKI Co. The Vickers hardness number, H_V was measured by loading a diamond pyramid-type (with apex 136°) indenter into the surface of the specimen, which is defined by:

$$H_v = \frac{2p_H \sin \phi}{d^2},$$

where d is the mean diagonal length of the diamond-shaped impression made in the indented surface. In the present study, the applied load and loading time were chosen to be 1 kg (9.8 N) and 15 sec, respectively. The measurements were repeated 12 times for all the samples, and the average was figured from the data except for the maximum and minimum values.

Table 1 Geometric properties for the samples

	Shape	Diameter (mm)	Height (mm)	Density (g/cm ³)	Theoretical Density (g/cm ³)	Density (%TD)
UN	Pellet	8.848	9.926	13.21	14.32	92.2
UN + 2.7mol%NdN	Pellet	8.748	10.02	13.31	14.14	94.1
UN + 12.2mol%NdN	Pellet	8.564	9.995	12.86	13.54	95.0

To evaluate the elastic moduli an ultrasonic pulse-echo measurement was carried out at room temperature in air using an Echometer 1062 (NIHON MATECH Inc.). The schematic view of the apparatus is shown in Fig. 1. The sample is cemented to the SiO₂ buffer, and the other end of the buffer is bonded to the 5 MHz transducer connected to the Echometer. The glue joint between the transducer and buffer is Sonicoat-SHN13 (Nichigo Acetylene. Corp.). The longitudinal sound velocity V_L and shear sound velocity V_S are calculated by the following equations [1-5]:

$$V_L = \frac{2L}{T_2 - T_1},$$

$$V_S = \left[\left(\frac{T_3 - T_2}{D} \right)^2 + \left(\frac{T_2 - T_1}{2L} \right)^2 \right]^{-\frac{1}{2}},$$

where T_1 is the reflection time of the longitudinal sound velocity from bottom face of the sample, T_2 is the reflection time of the longitudinal sound velocity from top face of the sample, T_3 is the reflection time of the shear sound velocity from top face of the sample, D is the diameter of the sample, and L is the length of the sample. For isotropic media, the shear modulus G and Young's modulus E are expressed in terms of the measured longitudinal sound velocities V_L and shear sound velocities V_S as:

$$G = \rho V_s^2,$$

$$E = G \left(\frac{3V_L^2 - 4V_s^2}{V_L^2 - V_s^2} \right),$$

where ρ is the sample density.

The measurements were performed three times over changing the sample position, and the error in the sound velocity calculated from t was within 20 m/s.

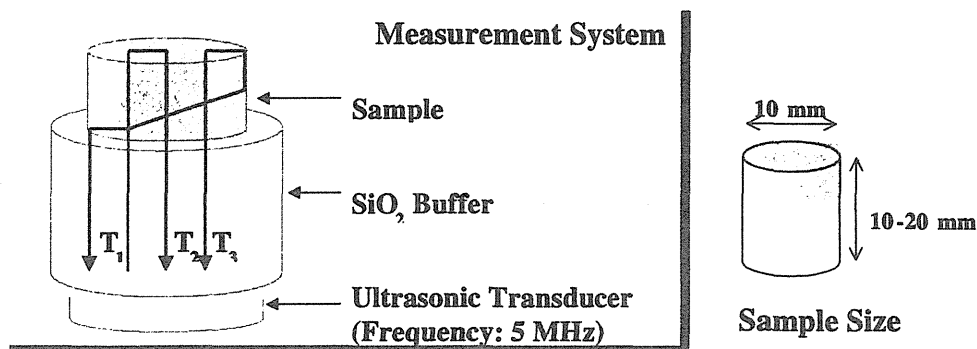


Fig. 1 Schematic diagrams of ultrasonic pulse-echo measurement.

For the thermal diffusivity measurements, the samples with a disc of 1~2 mm in thickness were sliced from the pellet and the end faces were polished with diamond paste. The thermal diffusivities were measured by a laser flash method from room temperature to about 1273 K in vacuum (10^{-4} Pa) by using ULVAC TC-7000 (ULVAC-RIKO Inc.). For the calculation of thermal conductivity of UN, the reported specific heat capacities of UN [6,7] were used. For the calculation of (U,Nd)N the specific heat capacities of the solid solution were calculated by Neumann-Kopp's law using those of UN and NdN.

The thermal conductivity was calculated from the thermal diffusivity (α), specific heat capacity (C_p), and density (ρ) using the following standard expression:

$$\lambda = \alpha C_p \rho$$

The thermal conductivity was normalized to 95 % of the theoretical density using the Maxwell-Eucken relationship [8,9]:

$$\lambda_{95} = \lambda_M \frac{1+2p}{1-p}$$

3. Results and discussion

It was confirmed that the solid solution was one phase and contained no impurity phase. Figure 2 shows the variation of the lattice constant with neodymium content. It is found that the lattice constant increases with the Nd content linearly suggesting that it obeys Vegard law.

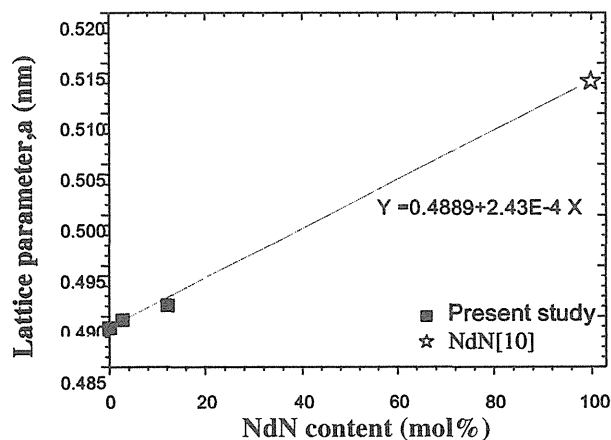


Fig. 2 Variation of lattice constant with NdN content.

The variation of Vickers hardness with NdN content is shown in Fig.3. It is seen that the hardness increases with NdN content. The particle sizes of these samples are in the range of 10 to 30 μm and the size of indentation trace is 50 μm as shown in Fig.4. It is considered that this variation results from NdN content rather than porosity.

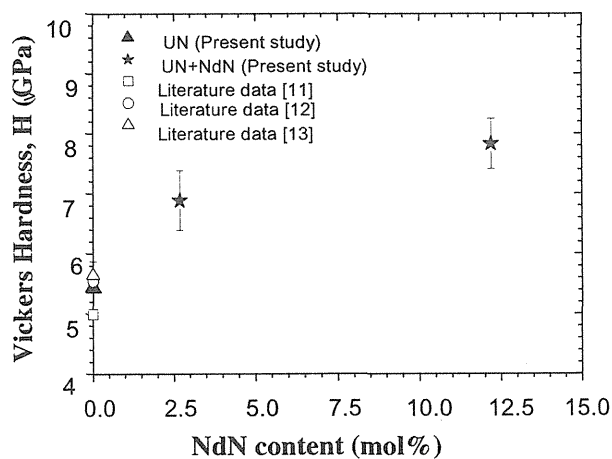


Fig.3 Variation of Vickers hardness with NdN

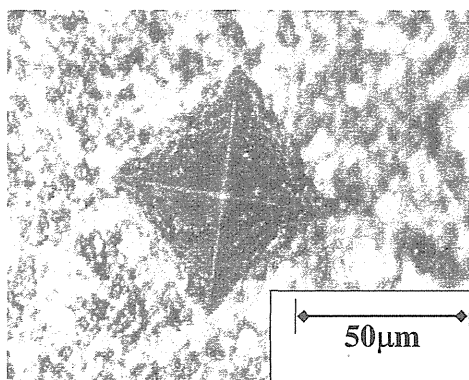


Fig.4 Indentation trace

Figures 5 and 6 show the variations of Young's modulus and shear modulus with porosity, respectively. As shown in these figures both the moduli increase with porosity and we cannot estimate the effect of Nd content on the elastic moduli.

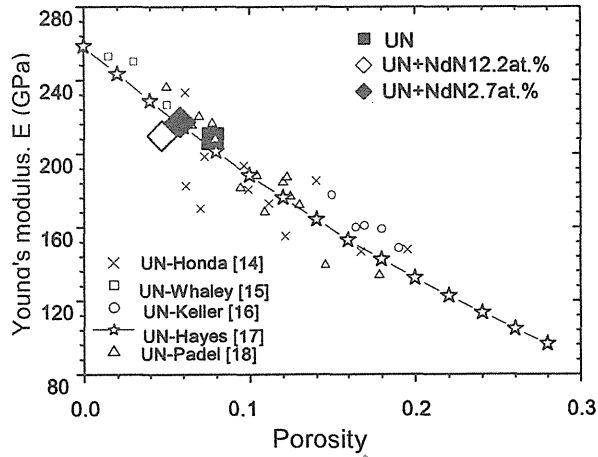


Fig. 5 Variation of Young's modulus with porosity

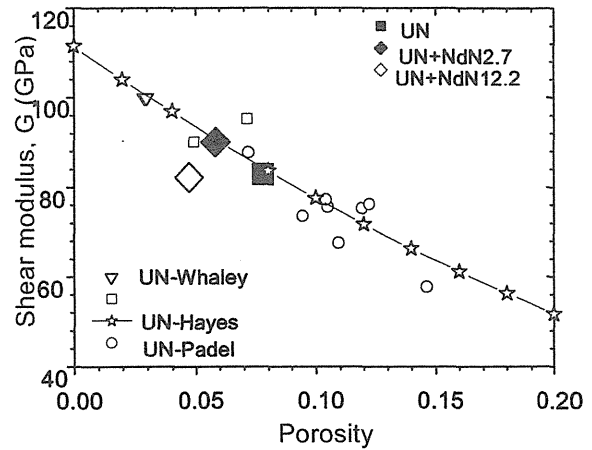


Fig.6 Variation of shear modulus with porosity

The values of thermal conductivity as a function of the temperature are plotted in Fig. 7 with literature data [17,19,20]. The values obtained in the present study are scattered among the literature data and decrease with Nd content.

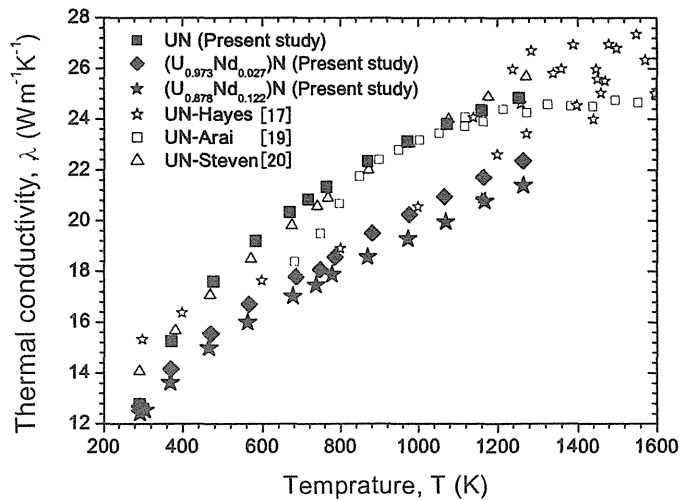


Fig. 7 Thermal conductivity of UN and UN-NdN solid solution.

4. Conclusion

In order to develop the technologies for nuclear fuel cycle based on nitride fuel and pyrochemical reprocessing some properties of UN and (U,Nd)N were measured.

Lattice constants for (U,Nd)N obeyed Vegard law and increased with NdN content. Vickers hardness increased with NdN content. Thermal conductivity of (U,Nd)N estimated by experimentally obtained thermal diffusivity and theoretically calculated specific heat decreased with NdN content. Elastic moduli measured by ultrasonic pulse echo method might decrease with porosity but the dependence of the moduli on NdN content was not obtained.

Acknowledgements

This study was carried out within the framework of the Development of Innovative Nuclear Technologies by the Ministry of Education, Culture, Sports, Science and Technology of Japan. The authors give special thanks to people of Mitsubishi Material Co. Ltd for making UN and (U,Nd)N samples.

References

1. K. Yamada, S. Yamanaka, T. Nakagawa, M. Uno, and M. Katsura, J. Nucl. Mater., 247 (1997) 289.
2. K. Yamada, S. Yamanaka, and M. Katsura, J. Alloys and Compounds, 271-273 (1998) 697.
3. S. Yamanaka, S. Yoshida, K. Kurosaki, M. Uno, K. Yamamoto, and T. Namekawa, J. Alloys and Comp., 327 (2001) 281.
4. S. Yamanaka, H. Kobayashi, and K. Kurosaki, J. Alloys and Comp., 349 (2003) 269.
5. S. Yamanaka, A. Kosuga, and K. Kurosaki, J. Alloys and Comp., 350 (2003) 288.
6. H. Matzke, Science of advanced LMFBR fuels, 1986.
7. S. Yamanaka et al., Journal of Alloys and Compounds, 271-273 (1998) 549-556.
8. Y. Philipponneau, J. Nucl. Mater., 188 (1992) 194.
9. C. Duriez, J.-P. Alessandri, T. Gervais, and Y. Philipponneau, J. Nucl. Mater., 277 (2000) 143.
10. Pearson's Handbook of Crystallographic Data for intermetallic phase, second edition, p. 4480.
11. D. L. Keller, BMI-1633 (1963).
12. R. W. Endeck, BMI-1690, (1970).
13. A. Bauer, Reactor Technology, Vol. 15, 1972.
14. T. Honda, J. Nucl. Sci. Technol., 6 (1968) 59.
15. H. L. Whaley, J. Nucl. Mater., 31 (1968) 345.
16. D. L. Keller, BMI-X-178 (1961).
17. S. L. Hayes and J. K. Peddicord, J. Nucl. Mater., 171 (1990) 262, 289, 300.
18. A. Padel and Ch. de Novion, J. Nucl. Mater., 49 (1973) 91.
19. Y. Arai, Journal of Alloys and Compounds, 271-273 (1998) 577-582
20. B. Steven, Journal of Nuclear Materials, 151 (1988) 313.



4.3 Compressive Creep of Simulated Burnup Fuel

Nobuyuki FUKUDA, Yuji KOSAKA, Kunihiro ITO, Kazuo MINATO*

Nuclear Development Corporation,

*Japan Atomic Energy Research Institute



This is a blank page.

Compressive Creep of Simulated Burnup Fuel

Nobuyuki FUKUDA, Yuji KOSAKA, Kunihiro ITO, Kazuo MINATO*

Nuclear Development Corporation, 622-12 Funaishikawa, Tokai-mura, Ibarakiken 319-1111, Japan

*Japan Atomic Energy Research Institute, Tokai-mura, Ibarakiken 319-1195, Japan

Hukuda@ndc.hq.mhi.co.jp

Abstract

In order to study the nitride fuel mechanical properties, we measured the compressive steady state creep rates of uranium mononitride (UN) and UN containing neodymium which was simulated burnup fuel. The stress exponent “n” and the apparent activation energy “Q” of the creep rate were determined in the range of $27.5 \leq \sigma \leq 200.0$ MPa and $950 \leq T \leq 1500$ °C.

1. Introduction

Uranium mononitride (UN) is one of the potential advanced reactor fuel, therefore determining of the creep behavior of UN is required in order to predict the fuel performance. We measured the steady-state creep rate of UN as well as of (U, Nd)N which was simulating the burnup fuel to estimate the creep rate of irradiated nitride fuel.

2. Experimental

2.1 Specimen characteristics

UN specimens were fabricated by Mitsubishi Materials Corporation using the carbothermic reduction method of UO_2 . The shape of specimen is a columnar of 9 mm diameter and 10 mm height. The main characteristics of the UN specimens are shown in Table 1 and the impurities contents are in Table 2.

Table 1 Main characteristics of UN and (U, Nd) N pellets

	Composition			Density (%T.D.)	Grain size (μm)
	C (ppm)	O (ppm)	N (wt%)		
UN	938	2464	5.68	92.5	17.4
(U _{0.87} , Nd _{0.13})N _{0.97} (Nd 8wt%)	1892	4391	5.67	95.1	10.8

Table 2 Impurities of UN and (U, Nd) N pellets

	Al	Si	Ca	Ti	Cr	Fe	Ni	Cu	Mo	W	Pb
UN	<300	<500	<500	<10	<10	<1000	83	<10	<10	<10	<10
(U _{0.87} , Nd _{0.13})N _{0.97} (Nd 8wt%)	<300	<500	<500	<10	<10	<1000	27	<10	<10	70	<10

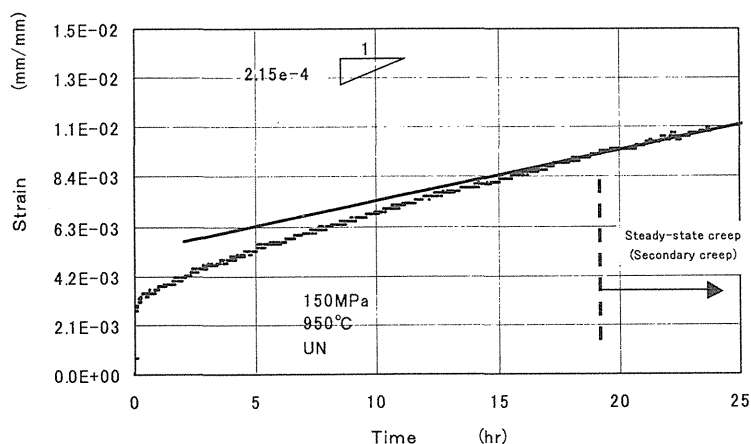
(ppm by weight)

2.2 Experimental apparatus

The apparatus for the creep test consists of a furnace chamber, heaters, compression rods, thermocouples and mechanical linkages to measure compression. The chamber was evacuated to 3×10^{-2} Pa and back-filled to 1 atm with 5% H₂+Ar, then kept the gas flowing continuously to protect specimens against oxidization.

2.3 Creep rate measurement

Steady-state creep rate measurements were carried out at three temperature levels, those are 1200, 1300 and 1500 °C. Applied load was increased in stepwise from lower to higher values, which corresponded to the stress of 27.5, 41.0 and 55.0 MPa under a constant temperature condition during one specimen measurement. We also performed the measurements in the conditions of 150, 165 and 200 MPa at 950 °C to simulate under irradiation condition, in which the fuel stress was evaluated by Faugere et al. [1]. The steady-state creep rate was measured from the linear portion of strain versus time curve as shown in Fig.1. Because the deformation of the specimen induced the slight increase of the cross section, the cross section area was corrected by the following manner at the beginning of each load level for the stress evaluation. Assuming the volume of a specimen remained constant, the corrected cross-section area was deduced by dividing the volume by the strained specimen height at the beginning of each loading step.

**Fig. 1** A typical creep curve of the measurements.

3. Results and discussion

The measurement results of the creep rates are summarized in Table 3 for UN specimens and in Table 4 for (U, Nd)N specimen. The following equation is well known as the conventional expression for the creep rate.

$$\dot{\varepsilon} = A\sigma^n \exp\left(-\frac{Q}{RT}\right),$$

where $\dot{\varepsilon}$: steady state creep rate,

A : empirical constant,

σ : applied stress,

n : stress exponent,

Q : activation energy,

R : gas constant,

T : temperature.

Table 3 Creep rates of UN

No.	Stress (MPa)	Temp. (°C)	Creep Rate (1/hr)
1	27.5	1200	4.33×10^{-4}
	41.0		7.75×10^{-4}
	55.0		1.66×10^{-4}
2	27.5	1300	1.20×10^{-3}
	41.0		3.05×10^{-3}
	55.0		1.17×10^{-2}
3	27.5	1500	1.17×10^{-2}
	41.0		3.14×10^{-2}
	55.0		9.20×10^{-2}
4	150.0	950	2.15×10^{-4}
	165.0		2.07×10^{-4}
	200.0		1.05×10^{-3}

Table 4 Creep rates of (U_{0.87}, Nd_{0.13})N_{0.97}

No.	Stress (MPa)	Temp. (°C)	Creep Rate (1/hr)
5	27.5	1300	5.55×10^{-5}
	55.0		4.02×10^{-4}

Hayes et al. [2] developed the creep rate correlation in the range of $20 \leq \sigma \leq 34$ MPa and $298 \leq T \leq 2523$ K, they concluded as follows:

$$A = 2.054 \times 10^{-3} (1/s) (=7.394 \text{ 1/hr}),$$

$$n = 4.5,$$

$$Q/R = 39369.5 \text{ (} Q = 327338 \text{ (J/mol))}.$$

As shown in Fig.2, the stress exponent of our measurements indicates good agreement with the value of 4.5 at stresses of 41 and 55 MPa with the exception of 27.5 MPa stress. Hayes referred that the stress exponent of 4.5 corresponded to a climb-controlled dislocation glide mechanism. We therefore consider the value of 4.5 and 2.5 corresponded to low temperature (high stress) creep and high temperature (low stress) respectively. Thin lines in Fig.2 show the stress exponent of 2.5 relatively fit the creep rate in the range of $27.5 \leq \sigma \leq 41$ MPa. We therefore obtained these two stress exponents.

A plot of $\log \dot{\epsilon}$ against reciprocal temperature is shown in Fig.3 and the activation energy is deduced from the gradient of these plots. An average value of 265 kJ/mol is obtained for the activation energy of UN. This value is smaller than that of Hayes [2] referred. It is supposed that the differences in stoichiometry, impurities or porosity of specimens should be the cause of the difference, but it is not clear which parameter dominates the cause at present.

The creep rate of (U,Nd)N is lower than that of UN by one-thirtieth of UN. This result implies that impurity element of Nd should suppress the movement of dislocations.

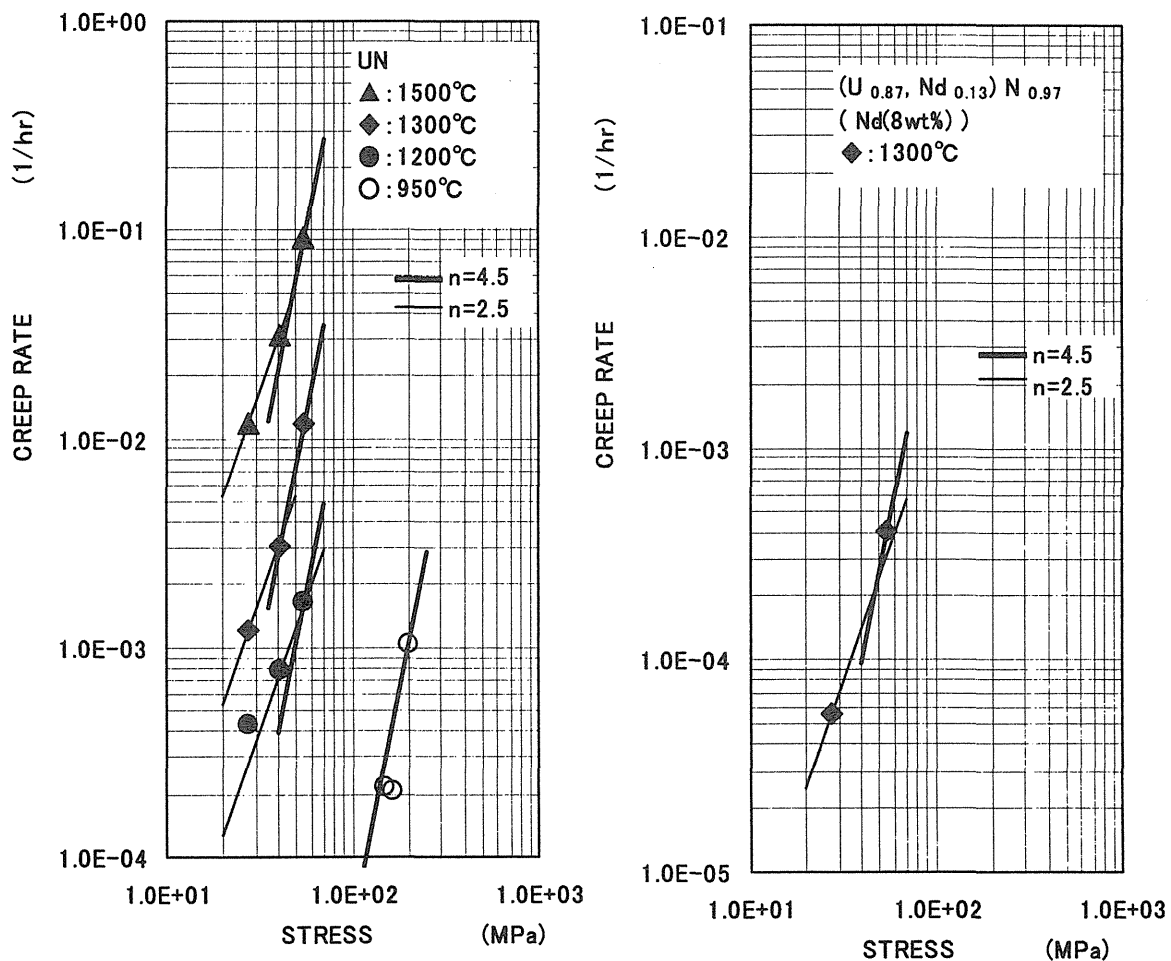


Fig. 2 Creep rate versus stress for UN and (U, Nd)N pellets

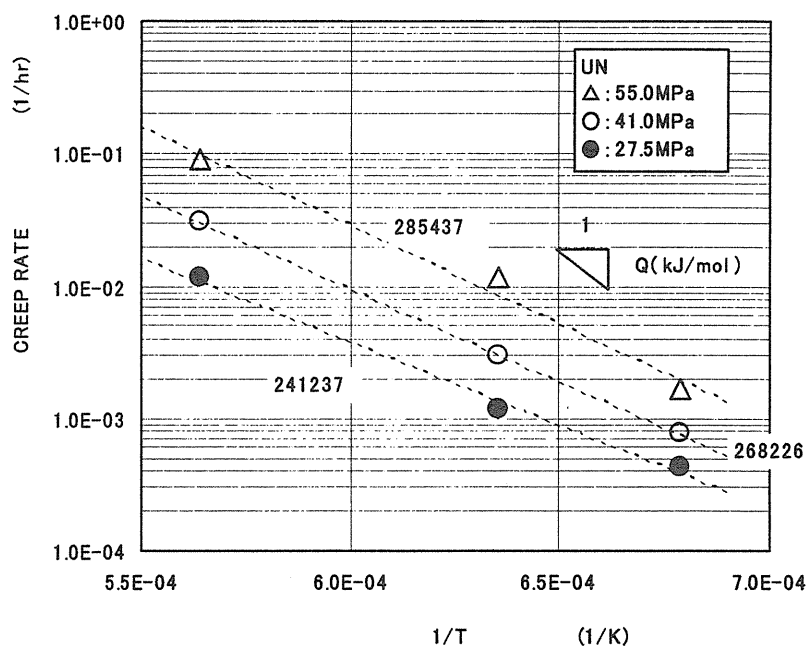


Fig. 3 Activation energy for creep

5. Conclusions

The compressive steady state creep rates of uranium mononitride (UN) and (U,Nd)N were measured from 950 - 1500 °C under applied 27.5 - 200.0MPa. Two stress exponents of 4.5 and 2.5 are deduced from the experimental results of UN depending on the stress conditions. It is revealed that the creep rates of (U, Nd)N are much lower than those of UN, which implies that impurity element of Nd should suppress the movement of dislocations. The activation energy of UN was obtained as 265 kJ/mol, which was smaller than that of Hayes reported [1].

Acknowledgements

This study was carried out within the framework of the Development of Innovative Nuclear Technologies by the Ministry of Education, Culture, Sports, Science and Technology of Japan. The authors gratefully acknowledge the contributions of Iizuka T. and Saito M. for their experimental works.

References

1. J. L. Faugere, et al., ANP(1992) pp.28.1-1~28.1-6
2. S.L. Hayes, J.K. Thomas and K.L. Peddicord, J. Nucl. Mater. 171(1990)271-288.

This is a blank page.



4.4 Molecular Dynamics Studies of Actinide Nitrides

Ken KUROSAKI¹, Masayoshi UNO¹, Shinsuke YAMANAKA¹, Kazuo MINATO²

¹ Department of Nuclear Engineering, Graduate School of Engineering, Osaka University

² Japan Atomic Energy Research Institute,



This is a blank page.

Molecular Dynamics Studies of Actinide Nitrides

Ken KUROSAKI^{1,*}, Masayoshi UNO¹, Shinsuke YAMANAKA¹, Kazuo MINATO²

¹ Department of Nuclear Engineering, Graduate School of Engineering, Osaka University
Suita Osaka 565-0871 Japan

² Japan Atomic Energy Research Institute, Department of Materials Science
Research Group for Actinides Science, Tokai-mura, Ibaraki-ken 319-1195, Japan

* Corresponding author: kurosaki@nucl.eng.osaka-u.ac.jp

Abstract

The molecular dynamics (MD) calculation was performed for actinide nitrides (UN, NpN, and PuN) in the temperature range from 300 to 2800 K to evaluate the physical properties viz., the lattice parameter, thermal expansion coefficient, compressibility, and heat capacity. The Morse-type potential function added to the Busing-Ida type potential was employed for the ionic interactions. The interatomic potential parameters were determined by fitting to the experimental data of the lattice parameter. The usefulness and applicability of the MD method to evaluate the physical properties of actinide nitrides were studied.

1. Introduction

In order to develop the technologies for nuclear fuel cycle based on nitride fuel and pyrochemical reprocessing, it is very important to understand the physical properties of actinide nitrides. In Osaka University, we have carried out the molecular dynamics simulation to evaluate the properties of oxide fuel, such as UO₂, PuO₂, and MOX [1-3]. In the present study, the molecular dynamics (MD) calculation is performed for actinide nitrides (UN, NpN, and PuN), and their thermal and mechanical properties are evaluated.

2. Calculation

The MD calculations for AnN (An: U, Np, Pu) were performed for a system of 512 ions (cation: 256, anion: 256) initially arranged in the NaCl type crystal structure. In the present study, the calculations were performed by a molecular dynamics program based on MXDORTO [4]. The calculations were made in the temperature range from 300 to 2500 K, and in the pressure range from 0.1 MPa to 1.5 GPa.

The temperature and pressure of the system were controlled independently through a simple

velocity scaling method. However, in calculating the thermal conductivity, a combination of the methods proposed by Andersen [5] and Nose [6] was used to control the pressure and temperature.

We employed the semi-empirical two-body potential function proposed by Ida [7] for cation-anion interactions. The potential is a partially ionic model including a covalent contribution [8]:

$$\phi_{ij}(r_{ij}) = \frac{z_i z_j e^2}{r_{ij}} + A_{ij}(b_i + b_j) \exp\left(\frac{a_i + a_j - r_{ij}}{b_i + b_j}\right) - \frac{c_i c_j}{r_{ij}^6} + D_{ij} \left[\exp\left\{-2\beta_{ij}(r_{ij} - r_{ij}^*)\right\} - 2 \exp\left\{-\beta_{ij}(r_{ij} - r_{ij}^*)\right\} \right] \quad (1)$$

where f_0 equals 4.186, z_i and z_j are the effective partial electronic charges on the i th and j th ions, r_{ij} is the interatomic distance, r_{ij}^* is the bond length of the cation-anion pair in vacuum, and a , b , and c are the characteristic parameters depending on the ion species. In this potential function, D_{ij} and β_{ij} describe the depth and shape of this potential, respectively.

The potential parameters were determined by trial and error using the experimental values of the lattice parameters. Using the parameters so obtained, the linear thermal expansion coefficient (α_{lin}), compressibility (β), and heat capacity (C_p) were evaluated.

The values of the interatomic potential parameters used in the present study are summarized in Table 1.

Table 1 Values of the interatomic potential function parameters for UN, NpN, and PuN

Ions	z	a	b	c	D_{ij}	β_{ij}	r_{ij}^*
N	-1.450	1.797	0.080	20			
U	1.450	1.228	0.080	0	(for U-N pairs) 7.00	1.25	2.364
Np	1.450	1.248	0.080	1	(for Np-N pairs) 9.56	1.25	2.364
Pu	1.450	1.196	0.080	0	(for Pu-N pairs) 0.10	0.80	2.453

3. Results and discussion

The temperature dependence of the lattice parameter of UN, NpN, and PuN obtained by the MD calculation controlled at 0.1 MPa is shown in Fig. 1, together with literature data [9-11]. The calculation was performed in the temperature range between 300 K and 3000 K. Although the temperature range of the experimental data is limited for NpN and PuN, the high temperature data are obtained from the MD calculation. The calculated results well agree with literature data.

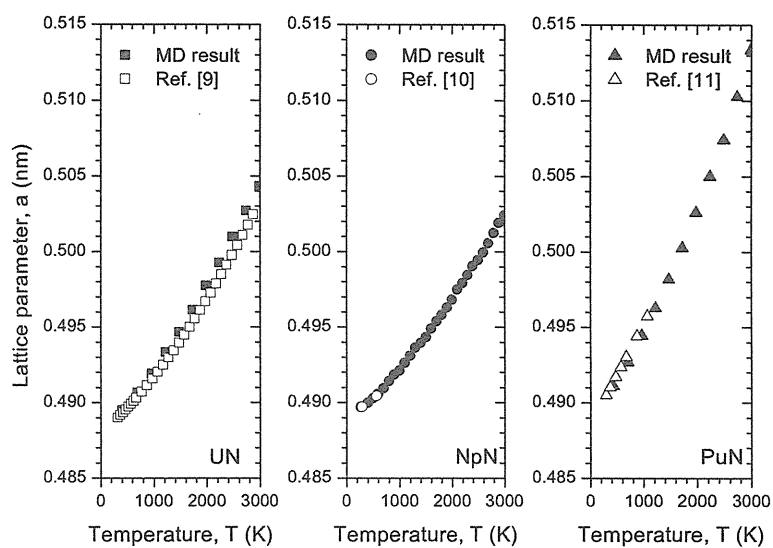


Fig. 1. Temperature dependence of the lattice parameter of UN, NpN, and PuN.

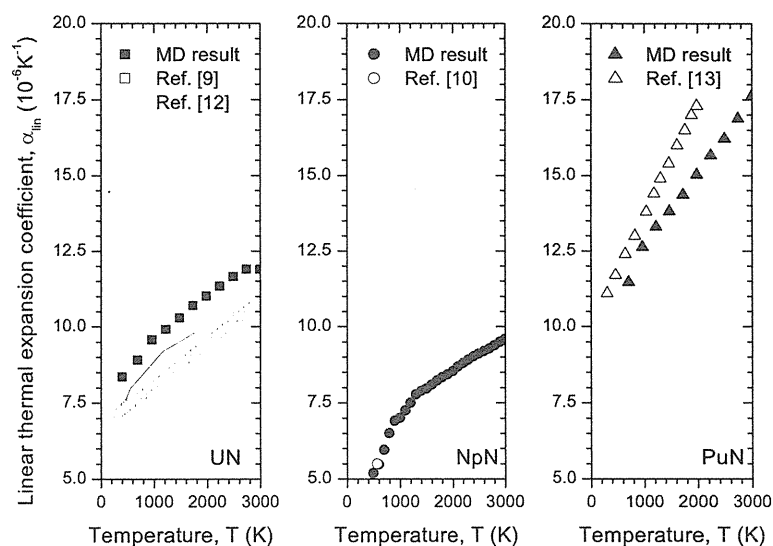


Fig. 2. Temperature dependence of the linear thermal expansion coefficient of UN, NpN, and PuN.

The linear thermal expansion coefficient (α_{lin}) and compressibility (β) of UN, NpN, and PuN can be evaluated from the variation of the lattice parameter with temperature. In case of NpN and PuN, the experimental data for linear thermal expansion coefficient and compressibility are scarcely reported.

The results are shown in Figs. 2 and 3, together with literature data [9,10,12-14]. It is confirmed that the calculated results almost agree with literature data.

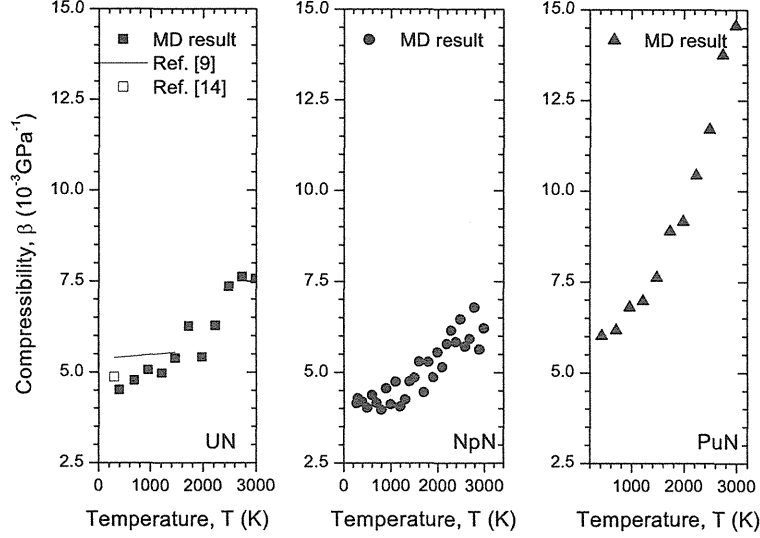


Fig. 3. Temperature dependence of the compressibility of UN, NpN, and PuN.

Although there are electronic contributions in actinide nitride system, we can evaluate only the lattice contribution to the heat capacity by the MD calculation. In the temperature range from 300 K to 3000 K, the heat capacity at constant pressure (C_p) was evaluated as sum of the heat capacity at constant volume (C_v) and lattice dilation term (C_d). The C_v was evaluated from the variation of the internal energy of the system with temperature calculated by the NVT MD simulation. The C_d was evaluated from the following relationship:

$$C_d = \frac{(3\alpha_{lin})^2 VT}{\beta} \quad (2)$$

where V is the molar volume, α_{lin} is the linear thermal expansion coefficient, β is the compressibility, and T is the absolute temperature. The C_d was evaluated by using the calculated values of α_{lin} , V , and β obtained from the NPT MD simulation. The temperature dependence of the calculated $C_v + C_d$ of UN, NpN, and PuN is shown in Fig. 3, together with literature data [15-19]. The calculated values of $C_v + C_d$ are slightly lower than the experimental results. This may be caused by the electronic contributions.

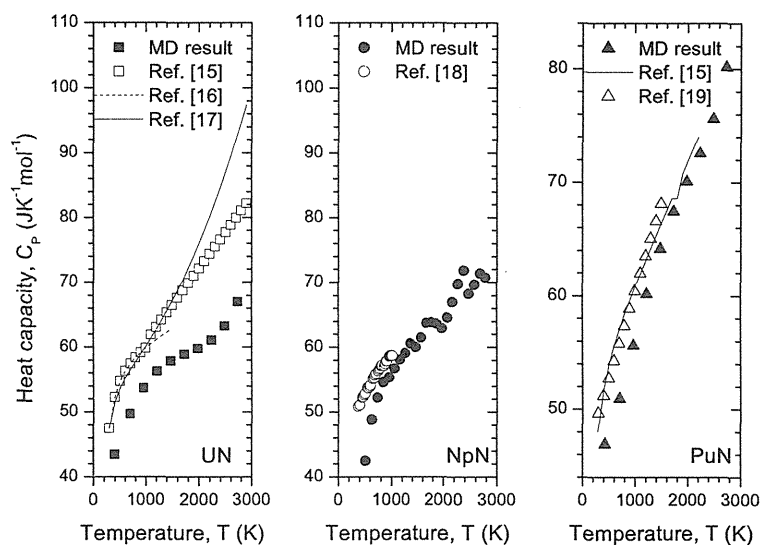


Fig. 4. Temperature dependence of the heat capacity of UN, NpN, and PuN.

4. Conclusion

The lattice parameter, linear thermal expansion coefficient, compressibility, and heat capacity of UN, NpN, and PuN were evaluated with the MD simulation. The interatomic potential parameters were determined from the variation of the lattice parameter with temperature. The calculated results are almost identical with the experimental data. The present study shows that the MD method can be usefully applied to determine the physical properties of actinide nitrides.

Acknowledgements

This study was carried out within the framework of the Development of Innovative Nuclear Technologies by the Ministry of Education, Culture, Sports, Science and Technology of Japan.

References

1. K. Kurosaki, K. Yano, K. Yamada, M. Uno, S. Yamanaka, K. Yamamoto, and T. Namekawa, J. Nucl. Mater., 294 (2001) 160.
2. K. Yamada, K. Kurosaki, M. Uno, and S. Yamanaka, J. Alloys & Comp., 307 (2000) 1.
3. K. Yamada, K. Kurosaki, M. Uno, and S. Yamanaka, J. Alloys & Comp., 307 (2000) 10.
4. K. Kawamura and K. Hirao, "Material Design using Personal Computer", Shokabo, Tokyo, (1994).
5. H. C. Andersen, J. Chem. Phys., 72 (1980) 2384.
6. S. Nose, J. Chem. Phys., 81 (1984) 511.

7. Y. Ida, Phys. Earth Planet Interiors, 13 (1976) 97.
8. P. M. Morse, Phys. Rev., 34 (1929) 57.
9. S. L. Hayes, J. K. Thomas, and K. L. Peddicord, J. Nucl. Mater., 171 (1990) 262.
10. A. T. Aldred, B. D. Dunlap, A. R. Harvey, D. J. G. H. Lander, and M. H. Mueller, Phys. Rev. B 9(9) (1974) 3766.
11. D. F. Carroll, J. Am. Ceram. Soc., 46 (1963) 406.
12. E. O. Speidel and D. L. Keller, BMI-1633, (1963).
13. C. A. Alexander, R. B. Clark, O. L. Krugar, and J. L. Robins, Plutonium and other Actinides 1975, North-Holland, Amsterdam, 1976, p.277.
14. A. Padel and Ch. De. Novion, J. Nucl. Mater., 33 (1969) 40.
15. The SGTE Pure Substance and Solution databases, GTT-DATA SERVICES, (1996).
16. F. L. Oetting and J. M. Leitnaker, J. Chem. Thermodyn., 4 (1972) 199.
17. H. Matzke in: Science of Advanced LMFBR, Amsterdam, North-Holland, 1986, p.106.
18. Y. Arai and Y. Suzuki, J. Nucl. Sci. Technol., Suppl. 3 (2002) 620.
19. F. L. Oetting, J. Chem. Thermodyn., 10 (1978) 941.

4.5 New Technique for Property Measurement of Small Sized Specimen

Hajime FUJII, Yuji KOSAKA, Kunihiro ITO, Kazuo MINATO**

Nuclear Development Corporation

**Japan Atomic Energy Research Institute



This is a blank page.

New Technique for Property Measurement of Small Sized Specimen

Hajime FUJII*, Yuji KOSAKA, Kunihiro ITO, Kazuo MINATO**

Nuclear Development Corporation, 622-12 Funaishikawa, Tokaimura, Ibaraki 319-1111, Japan

**Japan Atomic Energy Research Institute, Tokai-mura, Ibarakiken 319-1195, Japan

hajime_fujii@mhi.co.jp

Abstract

The test method applying indentation technique for obtaining thermo-mechanical properties of small-sized specimen such as minor actinide nitride fuels has been investigated. Especially, the relationship between indentation creep rate and steady state uniaxial creep rate has been studied. Indentation creep experiments have been conducted on Aluminum at 625 and 682K, and UO₂, at 673, 773, and 873K. It is confirmed that (1) stress exponent n and apparent activation energy Q of power-law creep formula can be confirmed using the Al specimen. (2) modification coefficient should be introduced in comparison of indentation creep rate and uniaxial creep rate, and (3) modification coefficient might be different from material.

1. Introduction

In the nitride fuel cycle system, nitride fuel with minor actinides can be available only with small-sized test specimen because of handling limitation. Instrumented indentation has been widely used to extract elastic and elastoplastic properties at low temperatures and to estimate creep properties at high temperatures for metallic materials. Especially, instrumented micro indentation creep technique with conical indenter can give creep properties, such as stress exponent and apparent activation energy of power-law creep for bulk materials¹. According to Takagi et al.¹, (i)the indentation creep strain field below indenter show self-similar in a constant-load indentation creep test, except for the short transient period at the initial loading stage, (ii)the indentation creep rate, $\dot{\epsilon}_{in} = \dot{u}/u$, is in proportion to representative creep strain rate, $\dot{\epsilon}$, and (iii)representative flow stress $\bar{\sigma}_m$ at the plastic region below indenter can be approximately written as $\bar{\sigma}_m \cong p_m/3$, where p_m is indentation pressure. The objective of this study in the fuel cycle system is to establish the method to evaluate high temperature creep properties of uranium nitride based fuels by means of indentation technique. However, (a)the theory to correlate the steady state uniaxial creep strain rate of bulk material with indentation creep

* Present address: Mitsubishi Heavy Industries, Ltd., 1-1-1 Wadasaki-cho, Hyogo-ku, Kobe, 652-8585 Japan, hajime_fujii@mhi.co.jp

experiment result, and (b) whether it is adequate to apply indentation creep technique to ceramic materials, are not clear.

In the present study, the relationship between indentation creep rate and steady state uniaxial creep rate with metallic materials, and applicability of indentation creep method to ceramic materials, have been investigated.

2. Experimental

Pure aluminum (99.999%, Furuya metals) and sintered uranium dioxide, UO_2 (density 10.7g/cm^3) were used in the experiment. Aluminum specimens were sliced from approximately 6mm-dia round bar into 3mm thickness in columnar shape. UO_2 specimens were sliced from approximately 8mm-dia columnar pellets into 2mm thickness. They were carefully machined parallel in both ends using special jigs and emery papers.

In the indentation creep measurements, the instrumented micro indenter ($\mu\text{IT-1}$, ULVAK-RIKO) was used. The specimen was introduced in the chamber, and the diamond indenter tip with conical shape was pressed perpendicularly into a heated specimen by an electromagnetic force in Ar gas atmosphere. For protection of diamond indenter tip, maximum heating temperature was limited below 1073K at any stage of experiment. The indentation depth was detected by measuring the displacement of the indenter column with a linear variable differential transformer (LVDT). Indentation creep tests were carried out under following test conditions.

<u>Material</u>	<u>Test temperatures</u>	<u>Indentation load</u>	<u>Indentation time</u>
Al	625, 682K	0.39N	1200s
UO_2	673, 773, 873K	1.96 ~ 4.90N	20 ~ 65hr

3. Results

Fig.1 shows indentation displacement curves with time for Al and UO_2 samples. Except for the short transient period at the initial loading stage, gently increase of displacement is observed.

Here, average equivalent stress in the plastic region below indenter can be defined as $\bar{\sigma}_m \cong p_m / 3$, where p_m is indentation pressure. Assuming that the plastic strain rate of the material at representative point follows power-law creep formula below,

$$\dot{\varepsilon} = A_1 \left(\frac{\bar{\sigma}}{E} \right)^n \exp \left(-\frac{Q}{RT} \right)$$

Indentation displacement rate \dot{u} can be described as follows.

$$\dot{u} = A_2 u \left(\frac{F}{Eu^2} \right)^n \exp \left(-\frac{Q}{RT} \right)$$

Or, introducing "indentation creep rate" $\dot{\epsilon}_{in} = d \ln u / dt = \dot{u} / u$, it can be described as

$$\dot{\epsilon}_{in} = A_3 \left(\frac{\bar{\sigma}_m}{E} \right)^n \exp \left(-\frac{Q}{RT} \right)$$

Based on the above formula, Fig. 2 shows double logarithm plot of indentation creep rate and estimated average equivalent stress, where the slope represents stress exponent. From Fig.2 (1), stress exponent of Al at the temperature and stress region was obtained as 5.0, and it is comparable with the value of 4.6 reported by Fujiwara². Fig.3 shows Arrhenius plot of indentation creep rate and reciprocal temperature. According to the Fig.3(1), the apparent activation energy of Al is deduced to be comparable with 141kJ/mol of Fujiwara². Fig.2 (1) also compares the results from indentation creep experiment and those from uniaxial creep experiments³.

Fig.2(2) shows the large difference of the creep stress exponents of UO_2 in the different stress levels, namely 15~18 for high stress region and 2 for low stress region, which is probably due to different dominant creep mechanisms.

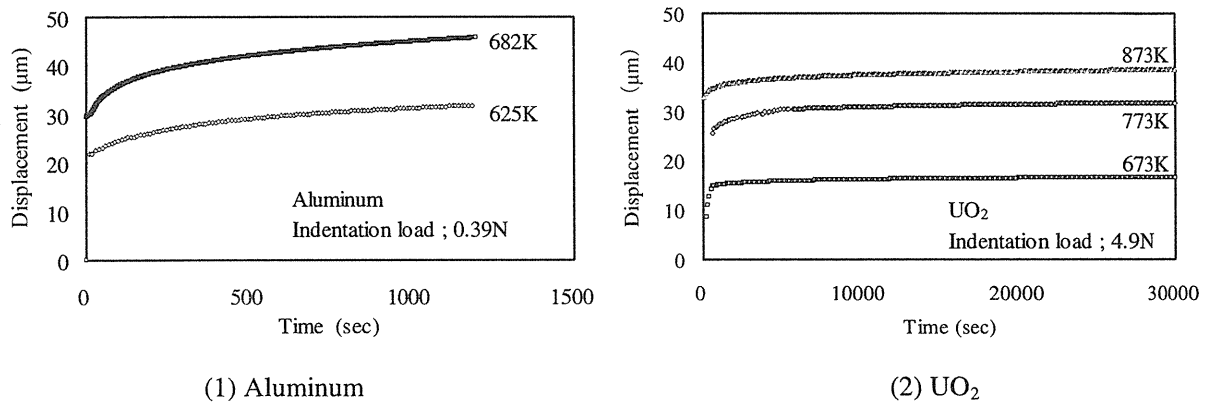


Fig. 1 Indentation creep curves with a constant load

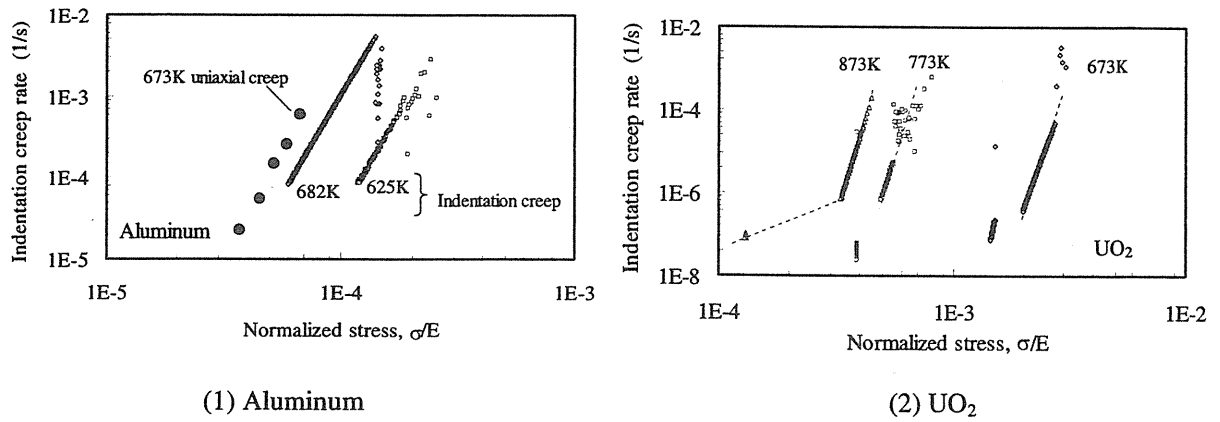


Fig. 2 Indentation creep rate with Normalized stress

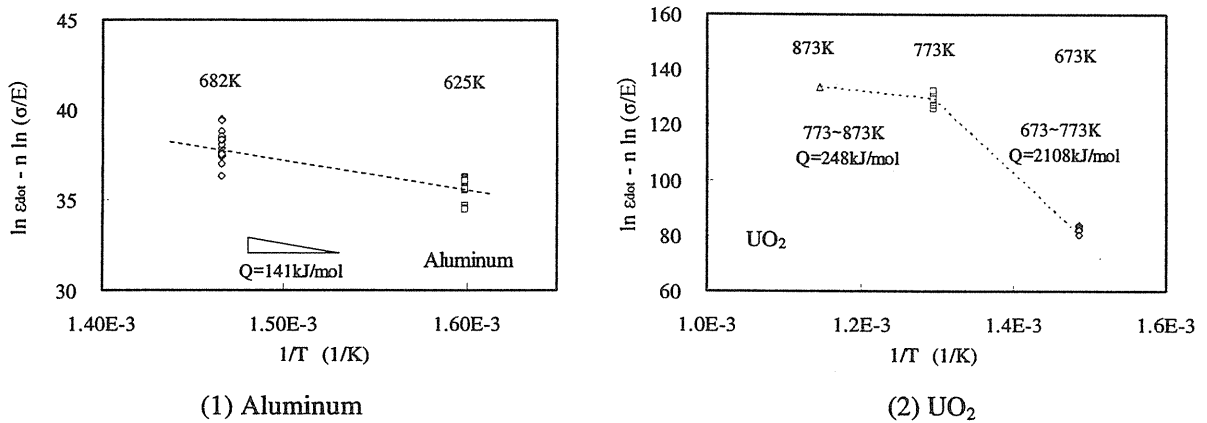


Fig. 3 Indentation creep rate with reciprocal temperature

4. Discussion

4.1 Relationship between indentation creep rate and uniaxial creep rate

Based on indentation creep technique, it is possible to obtain creep parameters, such as stress exponents and activation energy. Takagi et al showed the adequacy of the method by comparing detailed modeled FEM creep analysis and indentation creep experimental data¹. Fig.4 shows the comparison of indentation creep rate and uniaxial creep rate of Al-Mg alloy, where the data are extracted from ref.¹. As shown in the figure, transition stress from indentation creep where the dominant creep mechanism to change is comparable with those from uniaxial creep. On the other hand, indentation creep rate is larger than uniaxial creep rate. Therefore, it is necessary to introduce modification coefficient α in comparison of indentation creep rate and uniaxial creep rate, $\dot{\epsilon} = \alpha \dot{\epsilon}_{in}$. Poisl et al⁴ reported a coefficient of 0.09 based on the indentation of single crystal Se. Fig.4 gives α

coefficient of the value of about 0.25 for Mg-Al alloy. Additionally, based on our experimental data, Fig.2(1) suggests α coefficient of over 1 for Al. The reason for the difference in modification coefficient among the materials might be attributed to material viscosity differences but is not clear at present and further investigation is required. Therefore, in order to estimate uniaxial (steady state) creep rate from indentation creep test results, it is necessary to obtain uniaxial creep data at least at several points for setting modification coefficient α .

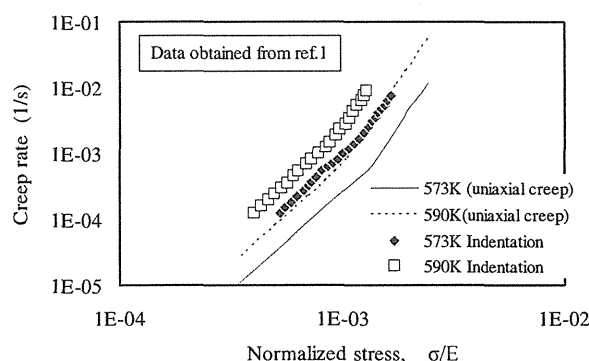


Fig. 4 Comparison of creep rate from uniaxial creep and indentation creep

4.2 Application of indentation creep technique to ceramic materials

Since UO_2 hardly creeps at low temperature, most of the steady state creep data of UO_2 are available at temperature range above 1273K. At temperature region of above 1273K, dominant creep mechanism at low stress region (below about 30MPa) is diffusion controlled (stress exponent; $n=1$), and at high stress region is dislocation glide controlled ($n=5$). According to the indentation creep experiments, it is found that n is in the range of 15-18 for high stress region at 673-873K and n almost equivalent to 2 for low stress region at 873K. This difference of stress exponents in different stress levels might be attributed to different dominant creep mechanisms, but the discrepancy between indentation creep and uniaxial creep is not clear because of the lack of uniaxial creep data of UO_2 at such a low temperature region.

As described in chapter 4.1, it is possible to obtain creep rate parameters of material by the indentation creep experiment, but in order to estimate uniaxial (steady state) creep rate from indentation creep test results, it is necessary to obtain uniaxial creep data at least at several points for setting modification coefficient. At present, uniaxial creep data of ceramic materials such as UO_2 and UN can be available only at high temperature region (above 1273K). Therefore, we are planning to develop improved indentation equipment to expand the operation temperature range above 1273K, in order to obtain indentation creep data and to compare the result with those of uniaxial creep data.

5. Conclusions

The relationship was investigated between indentation creep rate and steady state uniaxial creep rate on the metallic materials. The indentation creep experiments were conducted on Aluminum at 625 and 682K, and UO₂, at 673, 773, and 873K. It is confirmed that (1) stress exponent n and apparent activation energy Q of power-law creep formula can be confirmed with Al. (2) modification coefficient should be introduced in comparison of indentation creep rate and uniaxial creep rate, and (3) modification coefficient might be different from material.

Acknowledgements

This study was carried out within the framework of the Development of Innovative Nuclear Technologies by the Ministry of Education, Culture, Sports, Science and Technology of Japan. The author would acknowledge Professor Fujiwara of Nihon University for his invaluable suggestion and discussions.

References

1. H. TAKAGI, et. al., *Philosophical Magazine*, **83**, 35 (2003).
2. M. FUJIWARA, *Journal of Japan Institute of Light Metals*, **52**, 6 (2002).
3. K. MARUYAMA, Ed., "*Material science of high temperature strength (revised edition)*", Uchida Rokakuho (2002)
4. W.H. POISL, et.al., *Journal of Materials Research*, **10**, 8 (1995).



5. Session B-3: Pyrochemical Process

5.1 Pyrochemical Reprocessing of Nitride Fuel

Yoshihisa NAKAZONO, Takashi IWAI, Yasuo ARAI

Japan Atomic Energy Research Institute



This is a blank page.

Pyrochemical Reprocessing of Nitride Fuel

Yoshihisa NAKAZONO, Takashi IWAI, Yasuo ARAI

Japan Atomic Energy Research Institute
3607 Narita-cho, Oarai-machi, Ibaraki-ken, 311-1394, Japan
arai@popsvr.tokai.jaeri.go.jp

Abstract

Electrochemical behavior of actinide nitrides in LiCl-KCl eutectic melt was investigated in order to apply pyrochemical process to nitride fuel cycle. The electrode reaction of UN and (U,Nd)N was examined by cyclic voltammetry. The observed rest potential of (U,Nd)N depended on the equilibrium of U^{3+}/UN and was not affected by the addition of NdN of 8 wt.%.

1. Introduction

Pyrochemical process has several advantages over conventional wet process for reprocessing the spent fuel with high radiation dose and decay heat [1-2]. Especially for nitride fuel cycle with N-15 enriched nitrogen, pyrochemical process will have technical feasibility of recovering expensive N-15 as nitrogen gas. Therefore application of pyrochemical process to nitride fuel cycle has been carried out in JAERI and electrochemical behavior of UN, NpN, PuN and (U,Pu)N has been investigated so far [3-7]. However, the effect of fission products on the electrochemical behavior of nitride fuel has not been reported so far. In this study, the electrochemical behavior of (U,Nd)N containing NdN of 8wt.% was examined by cyclic voltammetry in comparison with that of UN.

2. Experimental

2.1 Samples

UN and (U,Nd)N specimens used in this study were prepared by carbothermic reduction of UO_2 and Nd_2O_3 , of which detailed procedures are reported elsewhere [8]. The X-ray diffraction patterns showed an almost single phase of NaCl-type structure and the densities of sintered UN and (U,Nd)N pellets were 13.3 and 12.8 g/cm³, namely 92.3 and 94.7 %TD, respectively. Fragments of the pellets (~1g) were subjected to cyclic voltammetry.

2.2 Apparatus

Figure 1 shows the schematic of electrochemical cell and heating furnace used in this study. In order to avoid the reaction of the specimens with oxygen and moisture, the apparatus shown in Fig.1 is installed in the glovebox with high-purity argon gas atmosphere [9]. Fragments of the nitride pellets wound with Ta-wire were used as a working electrode. The counter electrode was Mo-wire of 1mm ϕ in diameter. The reference Ag/AgCl electrode consisted of Ag wire immersed in the LiCl-KCl eutectic melt containing 1 wt.% of AgCl. Temperature of the salt phase was measured by a calibrated Chromel-Alumel thermocouple. Cyclic voltammograms were obtained using a voltammetric analyzer, Potentiostat/Galvanostat Model 273A (Seiko EG&G), at a scan rate of 100 mV/s. The concentration of UCl_3 in the LiCl-KCl eutectic melt was determined by ICP-AES.

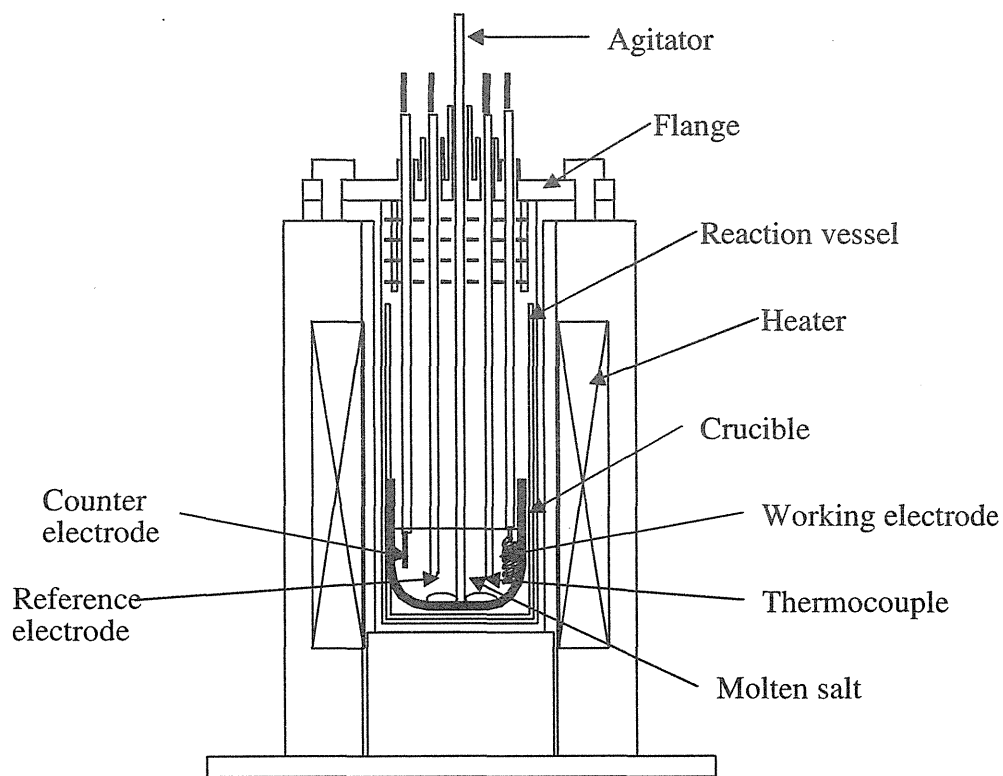


Fig. 1 Schematic of electrochemical cell

3. Results and discussion

Cyclic voltammograms of UN and (U,Nd)N obtained in the LiCl-KCl eutectic melt at 773 K are shown in Fig. 2. The rest potential of the surface of (U,Nd)N was -0.72 V, which almost agrees with that of UN in the literature [7]. Anodic current was observed for UN and (U,Nd)N at more positive potential than -0.8~-0.9 V vs. the reference Ag/AgCl electrode. These currents corresponded to the dissolution of U into the melt as trivalent ion shown in equation (1),



Accordingly, U in UN and (U,Nd)N dissolved at an almost similar potential under the present experimental condition.

On the other hand, small anodic and cathodic peaks were observed in the cyclic voltammogram of (U,Nd) as shown in Fig. 2. The peaks observed at -1.16 V and -1.26 V vs. the Ag/AgCl reference electrode possibly corresponded to the dissolution and deposition of Nd in (U,Nd)N shown in equation (2),



Equilibrium potential of NdN in the (U,Nd)N, however, could not be determined in this study, since the Nd content in the melt was too low to be quantitatively analyzed by ICP-AES.

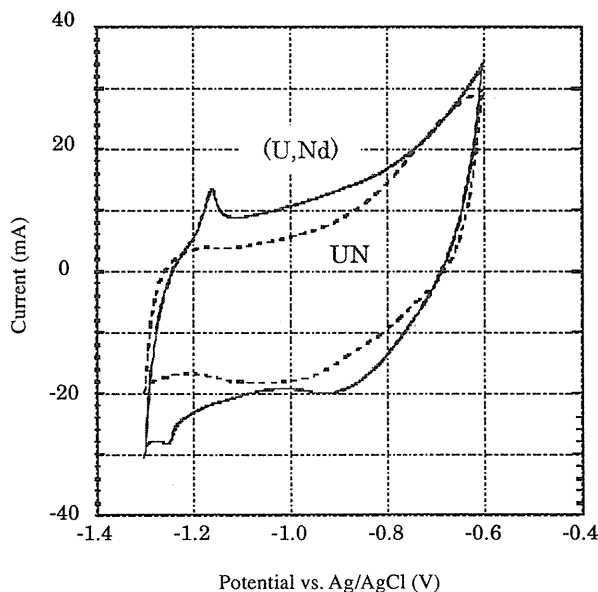


Fig. 2 Cyclic voltammograms of UN and (U,Nd)N at 773 K
(Scan rate: 100mV/s)

4. Conclusions

Electrochemical behavior of UN and (U,Nd)N containing NdN of 8wt.% in LiCl-KCl eutectic melt was investigated by cyclic voltammetry in order to examine the effect of addition of rare earth elements in nitride fuel. Anodic currents indicating dissolution of U into the melt as trivalent ion were observed at more positive potential than -0.8~-0.9 V vs. the Ag/AgCl reference electrode for both specimens. Anodic and cathodic peaks observed at -1.16 and -1.26V vs. the Ag/AgCl reference electrode possibly corresponded to the dissolution and deposition of Nd in (U,Nd)N. It is suggested from the present results that separation of U and rare earth elements is probable by the potential controlled electrolysis in the melt.

Acknowledgements

This study was carried out within the framework of the Development of Innovative Nuclear Technologies by the Ministry of Education, Culture, Sports, Science and Technology of Japan. The authors also wish to express deep gratitude to Dr. O. Shirai of Research Reactor Institute of Kyoto University for helpful discussion.

References

1. T. OGAWA, Y. ARAI, "Nitride/Pyroprocess for MA Transmutation and Fundamental Database", *Proc. OECD/NEA Workshop on Pyrochemical Separation, Mar. 14-15, 2000, Avignon*, pp 157-164.
2. Y. ARAI, T. OGAWA, "Research on Nitride Fuel and Pyrochemical Process for MA Transmutation", *Proc. 6th OECD/NEA Information Exchange Meeting on Actinide and Fission Product Partitioning and Transmutation, Dec. 11-13, 2000, Madrid (CD-ROM)*.
3. F. KOBAYASHI, T. OGAWA, et al., "Anodic Dissolution of Uranium Mononitride in LiCl-KCl Eutectic Melt", *J. Am. Ceram. Soc.*, **78**, 2279 (1995).
4. O. SHIRAI, T. IWAI, et al., "Electrochemical Behavior of Actinide Ions in LiCl-KCl Eutectic Melts", *J. Alloys Comp.*, **271-273**, 685 (1998).
5. O. SHIRAI, T. IWAI, et al., "Electrolysis of Plutonium Nitride in LiCl-KCl Eutectic Melts", *J. Nucl. Mater.*, **277**, 226 (2000).
6. O. SHIRAI, M. IIZUKA, et al., "Recovery of Neptunium by Electrolysis of NpN in LiCl-KCl Eutectic Melts", *J. Nucl. Sci. Technol.*, **37**, 676 (2000).
7. O. SHIRAI, K. UOZUMI, et al., "Recovery of U by Electrolysis of UN in LiCl-KCl Eutectic Melts", *J. Nucl. Sci. Technol.*, **Supplement 3**, 745 (2002).
8. K. YAMASAKI, et al., "Fabrication of Lanthanide Nitride Pellets and Simulated Burnup Fuels", *Symposium on Nitride Fuel Cycle Technology (this Symposium)*, Jul. 28, 2004, Tokai.
9. Y. ARAI, T. IWAI, et al., "Design and Installation of Gloveboxes with Inert Gas Atmosphere for Molten Salt Electrolysis and Preparation of Alloy Samples", *JAERI-Tech 97-002* (1997). (in Japanese)



5.2 Renitridation of Recovered Pu in Liquid Cd

Takashi IWAI, Yoshihisa NAKAZONO, Yasuo ARAI

Japan Atomic Energy Research Institute



This is a blank page.

Renitridation of Recovered Pu in Liquid Cd

Takashi IWAI, Yoshihisa NAKAZONO, Yasuo ARAI

Japan Atomic Energy Research Institute

Oarai, Higashi-ibarakigun, Ibaraki 311-1394, Japan

E-mail address: iwait@oarai.jaeri.go.jp

Abstract

Renitridation of plutonium recovered in liquid cadmium cathodes by electrorefining of nitride fuel was investigated. It was not successful by the bubbling of nitrogen gas into Pu-Cd melt. On the other hand, it was proved that plutonium mononitride powder was obtained with high efficiency of recovery under the nitridation-distillation combined process.

1. Introduction

Plutonium is recovered in liquid cadmium cathodes by electrorefining in molten salt in pyrochemical process of nitride fuels. Development of the renitridation method for converting the recovered plutonium to nitride is very important. The conditions of the renitridation process, the characterization of the plutonium nitride obtained by renitridation and the efficiency of recovery in the renitridation process were investigated.

The results of the renitridation of uranium in U-Cd were reported before by Akabori [1] and Kasai [2]. Their methods were the static contact with nitrogen gas and U-Cd melt, or the bubbling of nitrogen gas into U-Cd melt. But, the result for plutonium was not reported. Therefore, we tried first the bubbling methods for uranium and plutonium in U-Cd or Pu-Cd melt. Next, we planned and examined a new method of renitridation by nitridation-distillation combined process.

2. Experimental

2.1 Bubbling of nitrogen

The apparatus for the bubbling method is shown in Fig.1. LiCl-KCl eutectic salt was used to prevent the evaporation of cadmium. The content of uranium in U-Cd melt was 0.52wt%, which is below 2.3wt%, the solubility limit of uranium in liquid cadmium at 773K. Under the bubbling process, a small amount of U-Cd melt was sampled and the content of uranium was analyzed by an inductivity coupled plasma and atomic emission spectroscopy (ICP-AES). The flow rate of the nitrogen gas was

15cc/min and the total amount of the nitrogen gas was 40 liters, which was 5000 times more than the quantity for renitridation of uranium contained in the U-Cd melt.

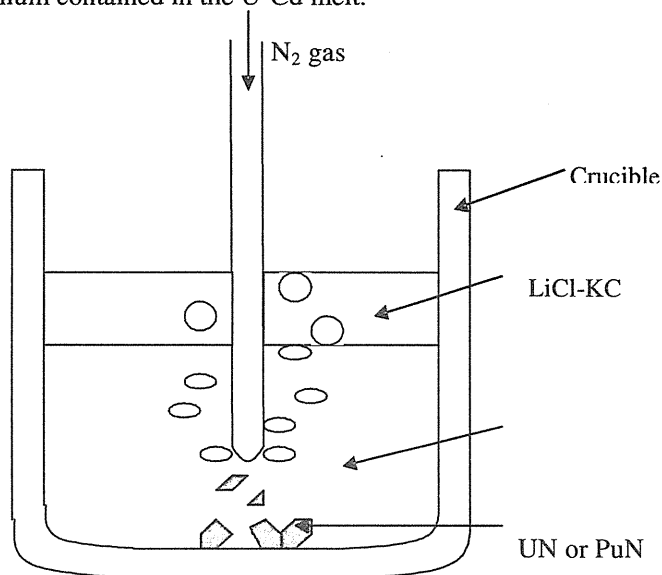


Fig.1 Apparatus for bubbling

2.2 Bubbling of nitrogen gas into Pu-Cd melt

The content of plutonium in Pu-Cd melt was 1.57 wt%, which is below 3.6 wt%, the solubility limit of plutonium in liquid cadmium at 773K. Under the bubbling process, a small amount of Pu-Cd melt was sampled and the content of plutonium was analyzed by ICP-AES. The flow rate of the nitrogen gas was 15cc/min and the total amount of the nitrogen gas was 80 liters, which was 3000 times more than the quantity for renitridation of plutonium contained in the Pu-Cd melt.

2.3 Renitridation by nitridation-distillation combined process

A new method for renitridation of plutonium in Pu-Cd melt was examined. In order to enhance the activity of plutonium in Pu-Cd melt and make renitridation successfully, two process, which were the distillation of cadmium from Pu-Cd melt and the nitridation of plutonium, were combined and practiced simultaneously. The experiment was carried out at 973K using an apparatus shown in Fig.2. Plutonium content of the sample used for this test was 12wt%. The flow rate of the nitrogen gas was 15cc/min and the weight of the sample was measured during the experiment.

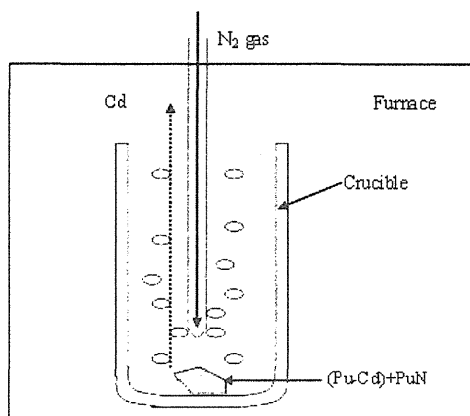


Fig.2 Apparatus for nitridation-distillation combined process

3. Results and discussion

Under bubbling process, the change of the uranium content in the U-Cd melt is shown in Fig.3. The content of uranium in U-Cd melt was decreased rapidly by bubbling of nitrogen gas and reached nearly zero at about 3000 times equivalent of nitrogen gas. It indicates that the renitridation of uranium was completed and this bubbling method was proved useful.

The change of the plutonium content in the Pu-Cd melt under bubbling process is shown in Fig.4. The content of plutonium decreased slowly and about 90% of the initial content of plutonium remained in Pu-Cd melt after the bubbling. This means that renitridation of plutonium in Pu-Cd melt did not proceed. The different results for uranium and plutonium cases may be caused by the difference of the activities. The activity of uranium in U-Cd melt at 773K is estimated as 75. On the other hand, that of plutonium in Pu-Cd melt is 0.00014 which is very smaller than that of uranium [3]. Therefore, the renitridation of plutonium by bubbling method was not successful.

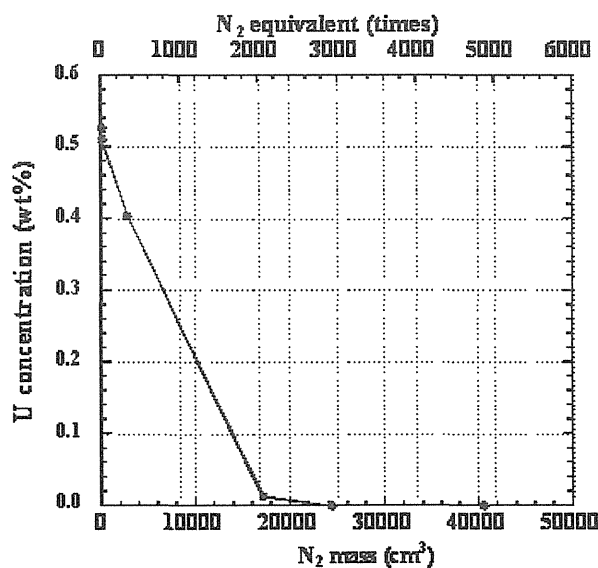


Fig.3 The change of U content under bubbling

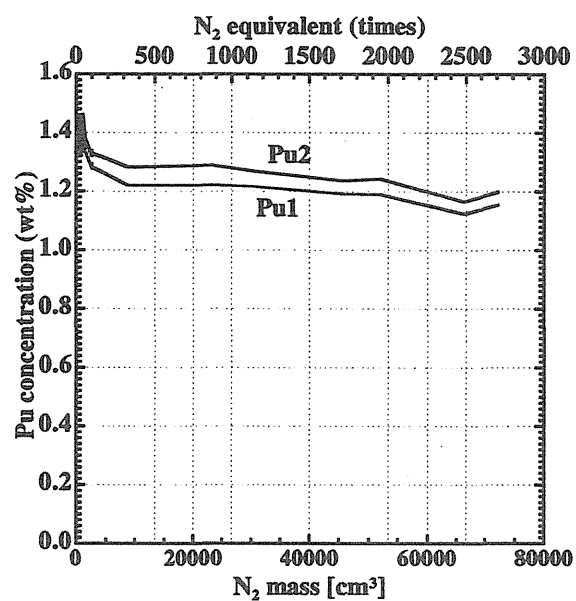


Fig.4 The change of Pu content under bubbling

The result by a new method, which is the nitridation-distillation combined process, was successful. The X-ray diffraction pattern of the recovered material from the crucible is shown in Fig.5 and agreed with that of plutonium mononitride (PuN). The efficiency of the recovery of PuN by renitridation estimated from the material balance is upper than 99%.

The new method is very useful because plutonium mononitride powder can be obtained by a single process.

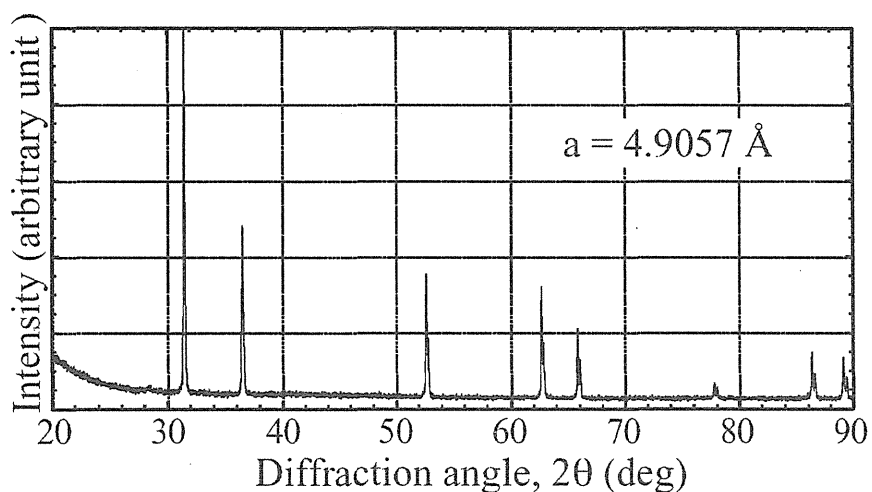


Fig.5 X-ray diffraction pattern of PuN recovered by nitridation-distillation combined process

4. Summary

Nitrogen gas bubbling process and nitridation-distillation combined process were investigated for the renitridation of plutonium recovered in liquid cadmium cathode. Using the nitrogen gas bubbling process, the renitridation of uranium in U-Cd melt was completed rapidly, however the renitridation of plutonium in Pu-Cd melt proceeded very slowly and a large part of plutonium remained in the melt. These results were caused by the difference of the activities of uranium and plutonium in the melt. Using the nitridation-distillation combined process, all of plutonium was converted to plutonium nitride of high purity. This method is very useful and very simple because plutonium mononitride powder can be obtained by a single process.

Acknowledgements

This study was carried out within the framework of the Development of Innovative Nuclear Technologies by the Ministry of Education, Culture, Sports, Science and Technology of Japan. The authors also wish to express deep gratitude to T.Kato of Central Research Institute of Electric Power Industry for helpful discussion.

References

1. M.Akabori, A.Itoh, T.Ogawa, J. Nucl., Mater., **248**,338—342(1997).
2. Y.Kasai, I.Takehi, S.Noro, S.Yonezawa, T.Higashi, K.Tozawa, Proc. GLOBAL'99, Aug. 29-Sep. 3, 1999, Jackson Hole (1999).
3. M.Kurata, Y.Sakamura, T.Matsui, J. Alloys and Compounds, **234**, 83—92 (1996).

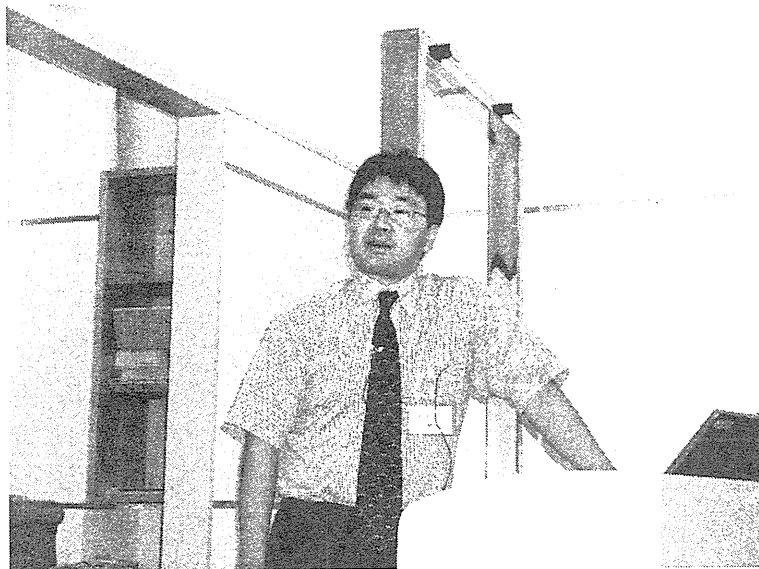
This is a blank page.



5.3 Experiments of Pyrochemical Process with Americium

Hirokazu HAYASHI, Kazuo MINATO

Japan Atomic Energy Research Institute



This is a blank page.

Experiments of Pyrochemical Process with Americium

Hirokazu HAYASHI, Kazuo MINATO

Department of Materials Science, Japan Atomic Energy Research Institute,
Tokai-mura, Naka-gun, Ibaraki-ken, 319-1195, Japan
hhayashi@popsvr.tokai.jaeri.go.jp

Abstract

Experiments of pyrochemical process of minor actinide nitrides are scheduled. Experimental procedures of electrochemical study of the molten salts containing minor actinides (10-100mg) were established. Preliminary study with a rare earth element used as a surrogate was carried out in the hot cells using master-slave manipulators.

1. Introduction

Experimental study of pyrochemical process of nitrides containing minor actinides (Am, Cm) requires the facility having not only shielding for γ -ray and neutron but also ability to keep a high purity inert gas atmosphere; because minor actinide nitrides or chlorides can easily react with oxygen or water vapor in an atmosphere. Experimental procedures in the facility were established and preliminary study with a rare earth element used as a surrogate of minor actinides was carried out after preparation of the experiments using master-slave manipulators in the hot cells.

2. Experimental

2.1 Apparatus

The electrochemical cell was set in a vertical well type furnace hanging on the floor of the hot cell. A crucible having salt sample was set in the furnace. The sample was heated under an inert gas flow after setting a cover of the furnace having the electrodes. The cover has 5 holes for electrodes, which are appropriate for the experiments. Solid metal electrodes, liquid cadmium electrodes, reference electrodes, anodes for dissolving nitride pellets were designed and manufactured. Figure 1 shows a schematic diagram of the apparatus.

2.2 Preliminary study with a rare earth element

Experimental procedures including transferring and setting of the samples and apparatus were established. Preliminary study with lanthanum used as a surrogate was carried out after preparation of the experiments using master-slave manipulators and in-cell cranes in the hot cells.

Electrochemical measurements were carried out for $\text{LaCl}_3\text{-LiCl-KCl}$ system with $X(\text{LaCl}_3)=8.5 \times 10^{-4}$ at 450°C . Electrochemical measurements were carried out with a Solartron 1280 Electrochemical measurement unit. The working electrode was consisted of $1\text{mm}\phi$ tungsten wire. Another tungsten wire was used as the counter electrode. The reference electrode was consisted of a silver wire ($1\text{mm}\phi$) dipped in the $\text{AgCl}(X(\text{AgCl})=0.0413)\text{-LiCl-KCl}$ placed in a mulite tube. Potentials were measured versus the reference electrode. Temperatures of the molten salt sample were measured with R type thermocouple set in an alumina tube.

3. Results and discussion

Figure 2 shows a typical cyclic voltammogram; it has a single group of signals around -2.2V , which is close to the lower limit of the electrochemical window. The signals correspond to redox reactions of La(III)/La(0) . The lower limit signals around -2.6V correspond to electrodeposition of lithium contained in the solvent; the higher limit signal around $+1.1\text{V}$ corresponds to evolution of chlorine gas. The positions of these signals are in good agreement with the reported values. EMF of La(III)/La(0) couple was also measured. La metal was deposited in situ on a tungsten electrode by coulometry at a constant potential of about -2.3V for about 5 seconds. Figure 3 shows the evolution of the measured potential of the La deposited electrode after the coulometry at -2.3V for 5 seconds. The potential indicated a stable value (-2.29V) for about 80 seconds and then changed to the rest potential of the tungsten electrode gradually. The standard potential of the electrochemical couple $E^0(\text{La(III)/La(0)})$ was calculated from the measured EMF of the galvanic cell: $\text{Ag(s)}|\text{AgCl}, \text{LiCl-KCl} \parallel \text{LiCl-KCl}, \text{LaCl}_3 | \text{La(s)}$, which is given by

$$\text{EMF} = E_{\text{La}} - E_{\text{ref}} = E^0(\text{La(III)/La(0)}) + 2.3(\text{RT}/3\text{F})\log[\text{La(III)}] - E_{\text{ref}}, \quad (1)$$

where E_{ref} is the potential of the $\text{Ag}|\text{AgCl}$ reference electrode; the value reported in [1] was used. $E^0(\text{La(III)/La(0)})$ was calculated to -3.22V , which is close to the values of $E^0(\text{La(III)/La(0)})$ reported in literature [1-3].

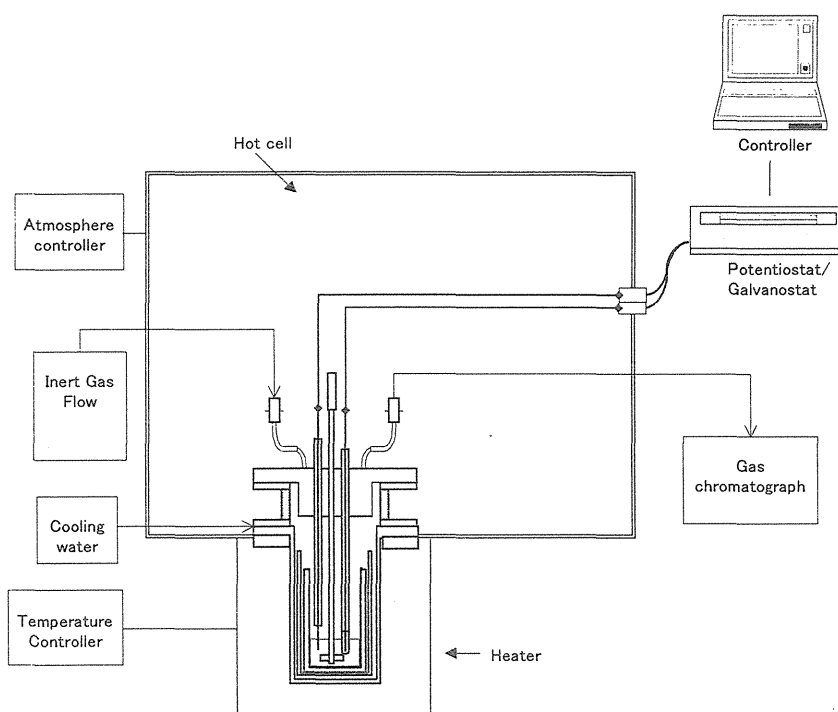


Fig. 1 Schematic diagram of the apparatus.

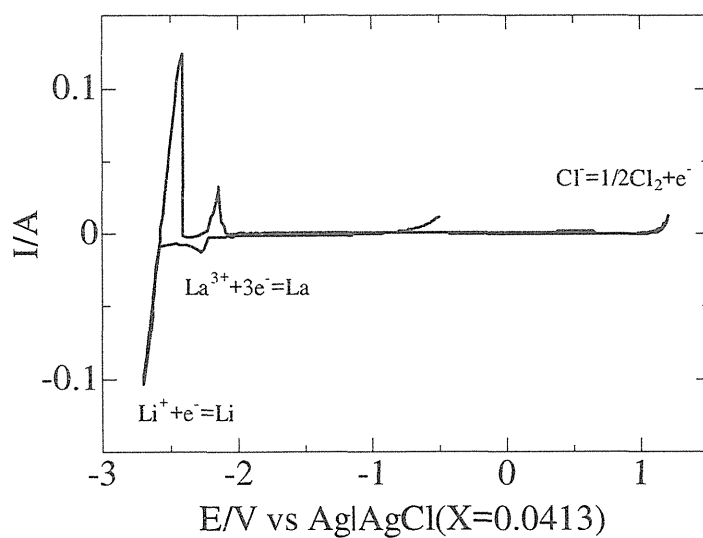


Fig. 2 Cyclic voltammogram obtained for $\text{LaCl}_3\text{-LiCl-KCl}$ system with $X(\text{LaCl}_3) = 8.5 \times 10^{-4}$ at 450°C .

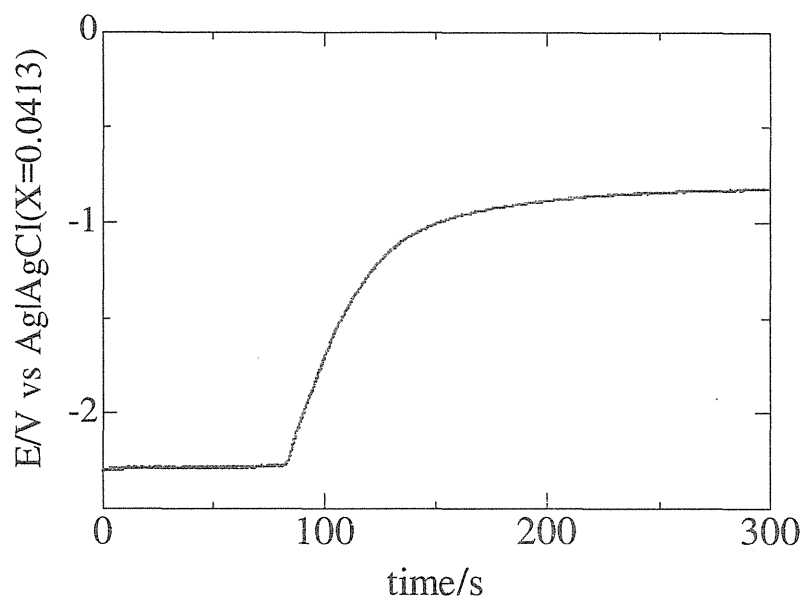


Fig. 3 Potential of the La deposited electrode after the coulometry at -2.3V for 5 seconds of $\text{LaCl}_3\text{-LiCl-KCl}$ system with $X(\text{LaCl}_3)=8.5 \times 10^{-4}$ at 450°C .

4. Summary

To prepare the experiments of the electrolyses of minor actinide nitride, experimental procedures in the hot cell facility were established and preliminary study with a rare earth element used as a surrogate was carried out.

Acknowledgements

This study was carried out within the framework of the Development of Innovative Nuclear Technologies by the Ministry of Education, Culture, Sports, Science and Technology of Japan.

References

1. T. INOUE et al. CRIEPI report T57 (1998).
2. Y.Castrllejo, M.R.Bermejo, R.Pardo, A.M.Martinez, *J. Electroanal. Chem.*, **545**, 141 (2003).
3. S.P.Fusselman, et.al., *Jounal Electrochem. Soc.*, **146**, 2573 (1999).



5.4 Influence of N-15 Enrichment on Neutronics, Costs and C-14 Production in Nitride Fuel Cycle Scenarios

Janne WALLENIOUS¹, Yasuo ARAI², Kazuo MINATO²

¹ Department of Nuclear and Reactor Physics, Royal Institute of Technology (KTH)

² Japan Atomic Energy Research Institute

This is a blank page.

Influence of N-15 Enrichment on Neutronics, Costs and C-14 Production in Nitride Fuel Cycle Scenarios

Janne WALLENIOUS¹, Yasuo ARAI², Kazuo MINATO²

¹ Department of Nuclear and Reactor Physics, Royal Institute of Technology (KTH)

AlbaNova University Centre, S-106 91 Stockholm Sweden

janne@neutron.kth.se

² Japan Atomic Energy Research Institute, Tokai-mura, Ibaraki-ken, 319-1195 Japan

Abstract

The C-14 production for different closed fuel cycle scenarios has been investigated. If nitride fuel is used in fast reactors and ADSs dedicated to management of plutonium and minor actinides, an N-15 enrichment level of about 99% is required for the nitride cores to produce the same amount of C-14 as the oxide cores in the power park. The corresponding cost penalty for fuel fabrication is estimated to be larger than 25%. If reprocessing is included in the costs for fuel operations, the penalty is of the order of 5-10%, provided that a closed gas cycle is implemented for the fabrication. If nitride fuels are used only for minor actinide management in ADS, the required enrichment level is about 93%, and the cost penalty is less than 10%.

1. Introduction

C-14 released from reactors and reprocessing plants today is one of the five major sources of dose to the public deriving from commercial nuclear power. It is primarily produced in reactions of neutrons with N-14 and O-17 nuclides present in fuel and coolant, with the exception of graphite moderated reactors, where neutron capture on C-13 becomes important.

C-14 is a beta-emitter with a half-life of approximately 5750 years. It is present in the atmosphere due to interactions with cosmic ray neutrons. The naturally occurring C-14 contributes with about 10 $\mu\text{Sv/y}$ to the exposure of humans. It is estimated that the release of C-14 from reprocessing plants gives a dose of about 1 $\mu\text{Sv/y}$ to most exposed group¹⁾. These numbers may be compared to the average dose commitment due to natural radiation sources, being of the order of several thousands $\mu\text{Sv/y}$. Still, it is considered that introduction of new C-14 sources into the environment should be restricted. Since the implementation of nitride fuel in fast reactors could increase the C-14 releases from nuclear power facilities by orders of magnitude, it is therefore necessary to analyse the impact of potential nitride fuel cycle scenarios on production and release of C-14 into the biosphere.

In this report, the C-14 production in oxide and nitride fuel reactors dedicated to transmutation of plutonium and minor actinides is calculated and compared to the C-14 production in light water reactors. In the case of reactors with nitride fuel, the level of N-15 enrichment required for the C-14 production to be comparable of oxide fuel reactors in the nuclear power park is suggested, and corresponding cost penalties are estimated.

2. Fuel cycle scenarios

Four different closed fuel cycle scenarios have been investigated, assuming the following power parks, in accordance with the NEA report on ADS and FRs in advanced fuel cycles²⁾.

- (#1) 63% LWRs and 37% FRs with oxide fuel for Pu+MA management
- (#2) 63% LWRs and 37% FRs with nitride fuel for Pu+MA management
- (#3) 76% LWRs with single MOX recycle, 19% FRs with oxide fuel for Pu-management and 5% ADS with nitride fuel for MA management (Double strata fuel cycle).
- (#4) 82% LWRs with single MOX recycle, 13% FRs with uranium-free (Pu,Zr)N fuel for Pu-management and 5% ADS with nitride fuel for MA management .

The fast reactor design in scenarios (#1)-(#3) was based on the high burnup CAPRA core design, introducing $^{11}\text{B}_4\text{C}$ moderator pins in order to achieve acceptable reactivity coefficients for fuels with low uranium content^{3,4)}. The uranium free fast reactor in the fourth case was specially designed for the present study.

Detailed 3-dimensional Monte Carlo modelling of the fast reactors in all scenarios has been made in order to provide a basis for the calculations. The neutronic safety case for each of these designs is included in the report. Results for the ADS were taken from a previous work⁵⁾.

3. Neutronics

Table 1 shows the core parameters adopted for the fast reactor calculations. It can be noted that the higher linear power for the nitride fuels is compensated for by a larger pin pitch and lower number of fuel pins per sub-assembly. In the oxide cores, the number of fuel sub-assemblies were adjusted in order to obtain an approximately critical core in the hot state with shutdown assemblies withdrawn. The configuration of control assemblies versus shutdown assemblies for the nitride cores was not yet investigated.

Table 1 Core parameters adopted for the fast reactor calculations

Core (scenario)	CAPRA-Pu+MA (#1)	CAPRA-Pu (#3)	FR-nitride-Pu+MA (#2)	FR-nitride-Pu (#4)
Core power	3600 MWth	3600 MWth	1500 MWth	800 MWth
Clad diameter	5.45/6.35 mm	5.45/6.35 mm	5.00/5.72 mm	5.00/5.72 mm
Pellet diameter	2.16/5.27 mm	2.16/5.27 mm	0.00/4.80 mm	0.00/4.80 mm
Fuel porosity	10%	10%	15%	15%
Pin P/D	1.205	1.205	1.338	1.338
Fuel pins/SA	336	336	336	133
¹¹ B ₄ C pins/SA	133	133	133	336
SA-FTF	167.6/176.4 mm	167.6/176.4 mm	167.6/176.4 mm	167.6/176.4 mm
SA pitch	181.4 mm	181.4 mm	181.4 mm	181.4 mm
Fuel SA	346	346	103	103
Control SA	24	24	6	6
Shutdown SA	9	9	-	-
Linear power	31 kW/m	31 kW/m	43 kW/m	58 kW/m
U-fraction	67%	67%	67%	0%
Pu-fraction	29%	33%	29%	30%
MA-fraction	4%	0%	4%	0%

Neutronic safety parameters were calculated for these cores at BOL using MCNP4C in conjunction with the JEF2.2 neutron cross section library, with the exception of the effective delayed neutron fraction, for which ENDFB/VI was used. A detailed pin by pin model was implemented for both core and axial plenum regions, in order to obtain correct values for sodium void worths. The results are displayed in Table 2. As expected, the addition of 4% minor actinides to the fuel of the CAPRA core leads to a reduction of the Doppler feedback by 25%. Combined with a 50% increase in the coolant void coefficient and a decrease in the effective delayed neutron fraction, the safety case for this CAPRA core (where the minor actinides was homogeneously distributed in the fuel) is questionable. Similar conclusions were arrived to in a study made by CEA using less sophisticated methods of calculation⁶⁾.

Table 2 Calculated neutronic safety parameters at BOL

Core	CAPRA- Pu+MA	CAPRA- Pu	FR-nitride- Pu+MA	FR-nitride- Pu
Beta-effective	310 pcm	380 pcm	350 pcm	360 pcm
Neutron generation time	1.45 μ s	1.52 μ s	1.25 μ s	3.33 μ s
Doppler constant	890 pcm	1260 pcm	750 pcm	1070 pcm
Coolant void coefficient	+0.22 pcm/K	+0.14 pcm/K	+0.18 pcm/K	-0.84 pcm/K
Coolant void worth	+460 pcm	-70 pcm	+220 pcm	- 4570 pcm

It is very interesting to note that the uranium free nitride core with (Pu,Zr)N fuel provides both an acceptable effective delayed neutron fraction, a significant Doppler feedback and a negative sodium void coefficient. Apparently, the increased moderator inventory enables Pu-240 to take over the role of U-238 as provider of fuel temperature feedback. The removal of U-238 further yields a decrease in coolant void coefficient and void worth that can be understood from the sharp fast fission threshold in U-238. What is most surprising is the high value of beta-effective, which needs to be analysed in more detail. A beta-effective equal to 360 pcm in conjunction with the calculated values of neutron generation time, Doppler constant and void coefficient would indeed allow for this reactor to be operated in a critical mode.

The cost penalty related to the use of nitride fuels for transmutation purposes could be reduced, if multirecycling of plutonium would be done in uranium free cores. The above results thus merit a more detailed investigation of the operational and safety performance of such a system.

4. C-14 production

Both oxygen and nitrogen contribute to the production of ^{14}C in the systems here investigated. In the burnup calculations performed with MCB, all possible transmutation trajectories leading to the formation of ^{14}C are taken into account. Explicit cross sections were calculated for the following reactions: $^{14}\text{N}(\text{n,p})^{14}\text{C}$, $^{15}\text{N}(\text{n,d})^{14}\text{C}$, $^{16}\text{O}(\text{n},^3\text{He})^{14}\text{C}$, and $^{17}\text{O}(\text{n},\alpha)^{14}\text{C}$.

Table 3 displays the core averaged cross section at BOL for all cores studied in the present report. The statistical error from the Monte Carlo procedure is estimated to less than 1%, with exception for the $^{16}\text{O}(\text{n},^3\text{He})^{14}\text{C}$ reaction, having a statistical uncertainty of about 10%. From the figures, it is clear that the cross sections do not vary much from one fuel type to the other. In the uranium free core, which thanks to the larger moderator inventory has a considerably softer spectrum, the $^{14}\text{N}(\text{n,p})^{14}\text{C}$ reaction is larger by 10%. The cross section most sensitive to the spectrum is for the $^{15}\text{N}(\text{n,d})^{14}\text{C}$ reaction, which

varies by up to 20%. It can be noted that the largest cross section is found for $^{17}\text{O}(\text{n},\alpha)^{14}\text{C}$, which consequently is the most important contributor to ^{14}C production in fast neutron oxide fuel reactors. In earlier works ⁷⁾, a considerably lower value for this cross section has been quoted, which has lead to an underestimation of calculated ^{14}C production rates in FBRs.

Table 3 Core averaged cross sections for ^{14}C production at BOL

Reaction	CAPRA-Pu+MA	CAPRA-Pu	FR-nitride-Pu+MA	FR-nitride-Pu
$^{14}\text{N}(\text{n},\text{p})^{14}\text{C}$	14.2 mb	14.0 mb	14.5 mb	15.8 mb
$^{15}\text{N}(\text{n},\text{d})^{14}\text{C}$	6.8 μb	6.2 μb	7.9 μb	6.6 μb
$^{16}\text{O}(\text{n},^3\text{He})^{14}\text{C}$	0.07 μb	0.05 μb	0.06 μb	0.06 μb
$^{17}\text{O}(\text{n},\alpha)^{14}\text{C}$	31.3 mb	30.5 mb	34.4 mb	31.4 mb

Burnup calculations were made using 10 burnup zones, and detailed modeling of control rod withdrawal. The difference in core and spectrum averaged cross sections at EOC is about 10 percent for all of the cores. Table 4 shows the resulting average production rates of C-14, in units of grams per GW year electric. For the nitride cores, the composition of natural nitrogen was used in the calculation. In the case of the oxide fuels, a nitrogen impurity of 200 ppm light atoms was assumed. Since the concentration of ^{17}O in natural oxygen is 400 ppm and the $^{17}\text{O}(\text{n},\alpha)^{14}\text{C}$ cross section is twice as large as the $^{14}\text{N}(\text{n},\text{p})^{14}\text{C}$ cross section, about 80 percent of the ^{14}C produced in the oxide fuels was due to the ^{17}O , and 20% to ^{14}N impurities.

Table 4 Average production rates of ^{14}C

Core	^{14}C production
CAPRA-Pu+MA (200 ppm light atoms natural nitrogen)	2.9 g/(GWe year)
CAPRA-Pu (200 ppm light atoms natural nitrogen)	3.3 g/(GWe year)
FR-nitride- Pu+MA (natural nitrogen)	1330 g/(GWe year)
FR-nitride- Pu+MA (99% N-15)	13.3 g/(GWe year)
FR-nitride-Pu (natural nitrogen)	1000 g/(GWe year)
FR-nitride-Pu (99% N-15)	10.0 g/(GWe year)
ADS-MA (natural nitrogen)	1300 g/(GWe year)
ADS-MA (99% N-15)	13.0 g/(GWe year)

The corresponding number for the C-14 production rate in LWRs is approximately 4 g/(GWe year) in the fuel, and 2 g/(GWe year) in the coolant ⁷⁾. The specific C-14 production in the nitride cores

is thus more than two orders of magnitude larger than in reactors with oxide fuel. Full release of this carbon inventory from reprocessing facilities would tenfold the dose to the most exposed group, and is thus probably not acceptable, even if natural background sources still would dominate the dose commitment. Hence use of N-15 enriched nitrogen and/or carbon trapping appears mandatory for the application of nitride fuels in the back end of the fuel cycle to be viable. The cross sections for C-14 production in the nitride cores were recalculated adopting nitrogen enriched to 50% and 99% with N-15, and it was found that self-shielding effects were small (less than 2% change in the $^{14}\text{N}(n,p)^{14}\text{C}$ cross section). Hence we may use linear scaling rules for the specific production rate as function of N-15 enrichment.

Table 5 ^{14}C production in the fuel cycle scenario (#1) assuming a total electricity production of 100 GWe year

Reactor type	Power fraction	Production rate	Total production
LWRs	63.2%	6.0 g/(GWe year)	380 g
CAPRA-Pu+MA	36.8%	2.9 g/(GWe year)	110 g
Sum	100%		490 g

Summing the contributions to the C-14 production of each reactor in the pure oxide fuel cycle scenario (#1) one obtains the following figures shown in Table 5, assuming a total electricity production of 100 GWe*year in the reactor park.

Note that for the LWRs, the C-14 produced in the coolant is included, as it is typically released to the biosphere. C-14 appearing in cladding is assumed not to be released in any of the cases. Introducing nitride fuels into the cycle, we may then calculate the relative increase in C-14 releases as function of N-15 enrichment in the respective core. Let us ad hoc assume that an increase of C-14 production by a factor of two is acceptable, i.e. the hypothetical 100 GWe power park would be allowed to release one kg C-14 (4500 Ci) per effective power year. In scenario (#2), where nitride fuel is used for both Pu and MA management in fast reactors, we arrive at an enrichment level of 98.7% for the nitride fuel production as shown in Table 6.

Table 6 ^{14}C production in the fuel cycle scenario (#2) assuming a total electricity production of 100 GWe*year

Reactor type	Power fraction	N-15enrichment	Production rate	Total production
LWRs	63.2%	Natural	6.0 g/(GWe year)	380 g
FR-nitride-Pu+MA	36.8%	98.7%	16.8 g/(GWe year)	620 g
Sum	100%			1000 g

In scenario (#3), where nitride fuel is used only for MA management in ADS, the required enrichment level stays at 92.8% as shown in Table 7.

Table 7 ^{14}C production in the fuel cycle scenario (#3) assuming a total electricity production of 100 GWe*year

Reactor type	Power fraction	N-15enrichment	Production rate	Total production
LWRs	75.8%	Natural	6.0 g/(GWe year)	450 g
CAPRA-Pu	19.0%	Natural	3.3 g/(GWe year)	60 g
ADS-MA	5.2%	92.8%	93.6 g/(GWe year)	490 g
Sum	100%			1000 g

Finally in scenario (#4), where nitride fuel is used for Pu management in a uranium free fast reactor core as well as for MA management in ADS, the average enrichment level should be 97.4% as shown in Table 8.

Table 8 ^{14}C production in the fuel cycle scenario (#4) assuming a total electricity production of 100 GWe*year

Reactor type	Power fraction	N-15enrichment	Production rate	Total production
LWRs	82.0%	Natural	6.0 g/(GWe year)	490 g
FR-nitride-Pu	13.0%	97.4%	26 g/(GWe year)	340 g
ADS-MA	5.0%	97.4%	33.8 g/(GWe year)	170 g
Sum	100%			1000 g

5. Cost estimation

The use of nitrogen enriched in N-15 for nitride fuel fabrication will obviously result in a cost penalty. Due to the presence of minor actinides in the fuels here investigated, the relative magnitude of this penalty will be smaller than for classical FBRs. CEA has estimated that the cost for N-15 production, which today is about 80 Euro/g, could drop to 8-12 Euro/g if the production rate is increased to the order of tons per year⁷⁾. The estimation was made for an enrichment target of 99.9%. If the standard formula for Separative Work would be valid in the case of this high enrichments, cost would be approximately proportional to the enrichment level, and hence no substantial gain would result from lowering the enrichment level by a few percent.

In an NEA assesment, estimated costs for fabrication and reprocessing of fuels containin minor actinides are provided⁸⁾. For an IFR type of metallic fuel, the estimated cost for fabrication is 2300 \$/kg-HM and that for reprocessing 7500 \$/kg-TRU. Corresponding estimates for ADS fuels are 7000 \$/kg-HM and 11000 \$/kg-TRU, respectively⁹⁾. Uncertainties are obviously large, of the order of $\pm 50\%$. Since 62 grams of N-15 is the minimum theoretical mass required to fabricate one kg of nitride fuel, the cost penalty for the fabrication itself would be substantial for the fast reactor fuels here investigated – larger than 25%, using the average cost estimate. If one would include the cost of reprocessing in the reference cost, however, the penalty becomes less severe, approximately 5-10%. Here one must remember that this conclusion is based on the assumption that losses of N-15 in the fabrication facility would be negligible. The open gas cycle used in existing fabrication lines yields losses of 95-99%, which would raise the cost penalty to completely unacceptable values. Implementation of closed gas cycles therefore is mandatory. Concerning recovery of N-15 in the stage of reprocessing, it could reduce the cost penalty furhter, if the cost of recovery is substantially less than that of the original enrichment.

Acknowledgements

This study was carried out within the framework of the Development of Innovative Nuclear Technologies by the Ministry of Education, Culture, Sports, Science and Technology of Japan.

References

1. S.E. BEATY, *Energy & Environment* **6**, 383 (1995).
2. *Accelerator-driven systems and fast reactors in advanced nuclear fuel cycles*, NEA (2002).
3. G. GASTALDO, M. ROME, J.C. GARNIER, Capra core optimisation by use of $^{11}\text{B}_4\text{C}$, in Proc. GLOBAL 95, Paris (1995).
4. H.M. BEAUMON et al, CAPRA core studies, high burn-up core – conceptual study, in Proc. GLOBAL 97, Yokohama (1997).
5. J. WALLENIS, S. PILLON, N-15 requirement for 2nd stratum ADS nitride fuels, in Proc. AccApp/ADTT, ANS (2001).
6. J. TOMMASI et al, *Nucl. Technol.*, **111**, 133 (1995)
7. S. PILLON, J. WALLENIS, Note Technique SESC/LIAC 01-020, CEA (2001).
8. *Trends in the nuclear fuel cycle: economic, environmental and social considerations*, NEA (2001).
9. D. WESTLÉN, A cost benefit analysis of accelerator driven transmutation systems, KTH (2001).

Appendix

A.1 Program

July 28, 2004

Opening Session

9:30	Opening address	Toru Ogawa	JAERI
------	-----------------	------------	-------

Session A:

Present State of the Technology Development in the World

	Chairperson:	Yasuo Arai	JAERI
9:40	Investigations of nitride fuels for fast reactors in Russia	Liudmila Zabudko	IPPE (Russia)
10:25	Research and development of nitride fuel cycle technology in Europe	Janne Wallenius	KTH (Sweden)
11:10	Research and development of nitride fuel cycle technology in US - Information from literature -	Kazuo Minato	JAERI

Session B:

Present State of the Technology Development in Japan

	Chairperson:	Koji Sato	JNC
11:30	Research and development of nitride fuel cycle technology in Japan	Kazuo Minato	JAERI
11:50	Lunch		

Session B-1:

Fabrication Technology

	Chairperson:	Koji Sato	JNC
13:00	Fabrication of minor actinide nitrides	Masahide Takano	JAERI
13:30	Fabrication of lanthanide nitride pellets and simulated burnup fuels	Kazuhiko Yamasaki	MMC

Session B-2:**Property Measurements**

	Chairperson:	Tadafumi Koyama	CRIEPI
13:50	Properties of minor actinide nitrides	Masahide Takano	JAERI
14:20	Properties of simulated burnup fuels	Masayoshi Uno	Osaka Univ.
14:40	Compressive creep of simulated burnup fuel	Nobuyuki Fukuda	NDC
15:00	Molecular dynamics studies of actinide nitrides	Ken Kurosaki	Osaka Univ.
15:20	New technique for property measurement of small sized specimen	Hajime Fujii	NDC
15:40	Break		

Session B-3:**Pyrochemical Process**

	Chairperson:	Osamu Shirai	KURRI
16:00	Pyrochemical reprocessing of nitride fuel	Yasuo Arai	JAERI
16:30	Renitridation of recovered Pu in Liquid Cd	Takashi Iwai	JAERI
16:50	Experiments of pyrochemical process with Americium	Hirokazu Hayashi	JAERI
17:10	Influence of N-15 enrichment on neutronics, costs and C-14 production in Nitride Fuel Cycle Scenarios	Janne Wallenius	KTH (Sweden)

Closing Session

17:30	Closing address	Shinsuke Yamanaka	Osaka Univ.
-------	-----------------	-------------------	-------------

A.2 List of Participants

Liudmila ZABUDKO

Department of Nuclear Power Plants
Institute for Physics and Power Engineering
Bondarenko sq., 1, Obninsk, Kaluga reg.,
249033, RUSSIA

Janne WALLENIS

Department of Nuclear and Reactor Physics
Royal Institute of Technology,
AlbaNova University Centre
S-106 91 Stockholm, Sweden

J. ADACHI

Department of Nuclear Engineering
Osaka University
Suita, Osaka 565-0871, Japan

I. AMAMOTO

O-arai Engineering Center
Japan Nuclear Cycle Development Institute
Narita, Oarai, Ibaraki 311-1393, Japan

S. ARAI

Hill Research

Y. ARAI

Department of Nuclear Energy System
Japan Atomic Energy Research Institute
Narita, Oarai, Ibaraki 311-1394, Japan

H. FUJII

Kobe Shipyard & Machinery Works
Mitsubishi Heavy Industries, Ltd.
Hyogo, Kobe, Hyogo 652-8585, Japan

M. FUJIWARA

College of Engineering
Nihon University
Tamura, Koriyama, Fukushima 963-8642, Japan

N. FUJIOKA

O-arai Engineering Center
Japan Nuclear Cycle Development Institute
Narita, Oarai, Ibaraki 311-1393, Japan

N. FUKUDA

Nuclear Fuel and Core Research & Development
Department
Nuclear Development Co.
Tokai, Ibaraki 319-1111, Japan

T. HARAMI

Synchrotron Radiation Research Center
Japan Atomic Energy Research Institute
Mikazuki, Hyogo 679-5148, Japan

H. HAYASHI

Department of Materials Science Research
Japan Atomic Energy Research Institute
Tokai, Ibaraki 319-1195, Japan

M. INOUE

O-arai Engineering Center
Japan Nuclear Cycle Development Institute
Narita, Oarai, Ibaraki 311-1393, Japan

A. ITOH

Department of Materials Science Research
Japan Atomic Energy Research Institute
Tokai, Ibaraki 319-1195, Japan

K. ITO

Nuclear Fuel and Core Research & Development
Department
Nuclear Development Co.
Tokai, Ibaraki 319-1111, Japan

T. IWAI

Department of Nuclear Energy System
Japan Atomic Energy Research Institute
Narita, Oarai, Ibaraki 311-1394, Japan

T. KATO

Central Research Institute of Electric Power
Industry
Iwadokita, Komae, Tokyo 201-8511, Japan

F. KAWAMURA

Hitachi, Ltd.
Saiwai, Hitachi, Ibaraki 317-8511, Japan

Y. KOSAKA

Nuclear Fuel and Core Research & Development
Department
Nuclear Development Co.
Tokai, Ibaraki 319-1111, Japan

T. KOYAMA

Nuclear Technology Research Laboratory
Central Research Institute of Electric Power
Industry
Iwadokita, Komae, Tokyo 201-8511, Japan

K. KUROSAKI

Department of Nuclear Engineering
Osaka University
Suita, Osaka 565-0871, Japan

N. MASAKI

Department of Materials Science Research
Japan Atomic Energy Research Institute
Tokai, Ibaraki 319-1195, Japan

K. MINATO

Department of Materials Science Research
Japan Atomic Energy Research Institute
Tokai, Ibaraki 319-1195, Japan

M. MISUMI

Kawasaki Heavy Industries, Ltd.
Hamamatsu, Minato, Tokyo 105-6116, Japan

K. MORIKAWA

Mitsubishi Materials Co.
Mukohyama, Naka, Ibaraki 311-0102, Japan

Y. MORI

Mitsubishi Heavy Industries, Ltd.
Yokohama, Kanagawa 220-8401, Japan

M. NAKADA

Department of Materials Science Research
Japan Atomic Energy Research Institute
Tokai, Ibaraki 319-1195, Japan

K. NAKAMURA

Central Research Institute of Electric Power
Industry
Iwadokita, Komae, Tokyo 201-8511, Japan

K. NAKAJIMA

Department of Nuclear Energy System
Japan Atomic Energy Research Institute
Narita, Oarai, Ibaraki 311-1394, Japan

Y. NAKAZONO

Department of Nuclear Energy System
Japan Atomic Energy Research Institute
Narita, Oarai, Ibaraki 311-1394, Japan

T. NISHI

Department of Materials Science
Japan Atomic Energy Research Institute
Tokai, Ibaraki 319-1195, Japan

T. OGATA

O-arai Engineering Center
Japan Nuclear Cycle Development Institute
Narita, Oarai, Ibaraki 311-1393, Japan

T. OGAWA

Preparations Office for JAERI-JNC Integration
Japan Atomic Energy Research Institute
Uchisaiwai, Chiyoda, Tokyo 100-0011, Japan

Y. OKAMOTO

Department of Materials Science
Japan Atomic Energy Research Institute
Tokai, Ibaraki 319-1195, Japan

M. OSAKA

O-arai Engineering Center
Japan Nuclear Cycle Development Institute
Narita, Oarai, Ibaraki 311-1393, Japan

H. OTOBE

Department of Materials Science
Japan Atomic Energy Research Institute
Tokai, Ibaraki 319-1195, Japan

K. SATO

O-arai Engineering Center
Japan Nuclear Cycle Development Institute
Narita, Oarai, Ibaraki 311-1393, Japan

T. SATO

Nuclear Technology and Education Center
Japan Atomic Energy Research Institute
Tokai, Ibaraki 319-1195, Japan

T. SATO

Department of Materials Science
Japan Atomic Energy Research Institute
Tokai, Ibaraki 319-1195, Japan

H. SHIBATA

Department of Materials Science
Japan Atomic Energy Research Institute
Tokai, Ibaraki 319-1195, Japan

O. SHIRAI

Kyoto University Research Reactor Institute
Kyoto University
Kumatori, Osaka 590-0494, Japan

Y. SHIRASU

Department of Materials Science
Japan Atomic Energy Research Institute
Tokai, Ibaraki 319-1195, Japan

M. TAKANO

Department of Materials Science
Japan Atomic Energy Research Institute
Tokai, Ibaraki 319-1195, Japan

K. TANAKA

O-arai Engineering Center
Japan Nuclear Cycle Development Institute
Narita, Oarai, Ibaraki 311-1393, Japan

K. TANAKA

Department of Materials Science
Japan Atomic Energy Research Institute
Tokai, Ibaraki 319-1195, Japan

K. TSUJIMOTO

Center for Proton Accelerator Facilities
Japan Atomic Energy Research Institute
Tokai, Ibaraki 319-1195, Japan

M. UMENO

Center for Proton Accelerator Facilities
Japan Atomic Energy Research Institute
Tokai, Ibaraki 319-1195, Japan

M. UNO

Department of Nuclear Engineering
Osaka University
Suita, Osaka 565-0871, Japan

S. YAMANAKA

Department of Nuclear Engineering
Osaka University
Suita, Osaka 565-0871, Japan

K. YAMASAKI

Mitsubishi Materials Co.
Mukohyama, Naka, Ibaraki 311-0102, Japan

T. YAMASHITA

Department of Nuclear Energy System
Japan Atomic Energy Research Institute
Tokai, Ibaraki 319-1195, Japan

M. YAMAWAKI

Tokai University
Japan Atomic Energy Research Institute

R. YUMOTO

PESCO Co. Ltd

This is a blank page.

A.3 Viewgraphs

Investigations of nitride fuels for fast reactors in Russia

L. M. Zabudko, V. M. Poplavsky (IPPE, Russia)

Research and development of nitride fuel cycle technology in Europe

J. Wallenius (KTH, Sweden)

This is a blank page.

INVESTIGATIONS OF NITRIDE FUELS FOR FAST REACTORS IN RUSSIA

L.M.Zabudko, V.M.Poplavsky
Institute for Physics and Power Engineering (IPPE), Obninsk,
RUSSIA

International Symposium on Nitride Fuel Cycle,
Tokai, JAPAN, 28 -29 July 2004

Introduction

The following features could be achieved in optimized fast reactor with sodium coolant and nitride fuel, what meets modern requirements to advanced nuclear installations:

- zero reactivity excess per fuel burn-up ensuring any refueling interval;
- zero value of sodium void reactivity effect (SVRE) at sodium loss;
- possibility to use special technology without separation of uranium, plutonium and minor actinides. The technology should improve fuel cycle economics and ensure proliferation resistance.

2

Introduction

The core basic design of the BN-800 reactor and the design proposals for the advanced BN-1800 reactor core have been developed. In both designs mixed nitride fuel is supposed to be used:

- UPuN for the first loading,
- UPuN+MA for the next loadings.

At realization of researches the shortage of data on nitrides properties, on specific features of nitride behavior under irradiation is felt.

3

Introduction

Domestic experience on irradiation behavior of nitrides

- BR-10 reactor:
two loadings with UN (660 and 590 fuel pins). All fuel pins are helium-bonded. Maximum burn-up ~9 at%.

- BOR-60 reactor:

- 1) tens pins with UN, max burn-up > 8 at%,
- 2) few pins with UPuN, max burn-up 4at %, 8.95at %. All pins are helium-bonded. At the moment 4 helium-bonded pins with UPuN with increased Pu content (45 % and 60 %) under irradiation within the frame of joint Russian-French experiment BORA-BORA. Planned maximum burn-up – 11at%.

4

Operation conditions and geometry of BR-10 pins with nitride fuel

#	Parameter	IV load	V load
1	Reactor power, MW	8	8
2	Operating period, efpd.	882	970...1130
3	Pellet density, g/cm ³	12...13.4	12...13.4
4	Max linear rating, KW/m	45.0	45.0
5	Max burn-up, at%	8.0	8.8
6	Max neutron flux, n/cm ² ·s	8.6*10 ¹⁴	8.6*10 ¹⁴
7	Inlet coolant temperature, °C	325...350	325...350
8	Max inlet/outlet coolant temperature increase, °C	165	165
9	Diameter*wall thickness of cladding, mm	8.4*0.4	8.4*0.4
10	Fuel pellet diameter, mm	7.4	7.4
11	Core height, mm	400	400
12	Gas plenum height (top), mm	100	100

5

Performance calculation of BR-10 pin

The most probable reason of fuel failure is fuel-cladding mechanical interaction (FCMI)

The calculations of temperature and stress-strain state of the pin are conducted by the KONDOR code in 9 sections through the pin height. Maximum fuel temperature at BOL - 1025° C, at EOL - 807° C (N=8MW). In real conditions the reactor power was equal to 8MW in different cycles, at the best, only 60 % of the total time, therefore fuel temperature for a long operation time was even lower than the obtained values.

7

Results of UN irradiation in BR-10.

IV core loading	V core loading
1983-1989 for 882 efpd, max burn-up 8 at% (design value 8at%)	1990-2002 for 1481 efpd, max burn-up 8.8 at% (design 8 at%).
Number of failures under operation (DND signal) - 2 (0)	Number of failures under operation (DND signal) - 24 (1)
1) 33 spent FAs with max burn-up 1.2at%-6.23at% are checked	1) 63 spent FAs with max burn-up 6.95at% (1), 7.62at%(1), other 8.25-8.79at%
2) 5 FAs (5.68at%-6.23at%) - gas leakage pins, 2 FAs(5.68 at%, 5.84 at%) - DND signal	2) 20 FAs with gas leakage pins: 1- 6.95at%, other 8.25-8.78at%

6

Performance calculation of BR-10 pin

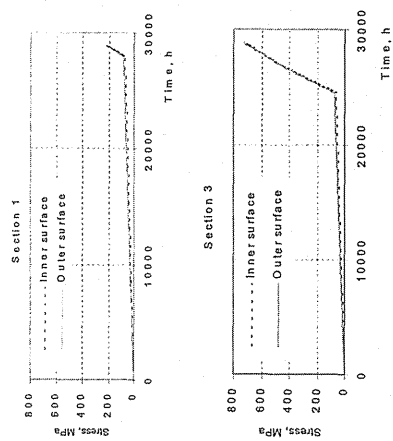
Two options of nitride swelling laws were used:

- 1) swelling rate $S=1.7\%$ per 1at%.
- 2) $S = S_{gas} + S_{solid} = f(T, P_{cont}, p, b)$ (Zimmerman).

For the first option the calculation showed, that at 1200efpd the FCMI takes place in all sections, except for two upper. First of all the contact begins in central section (#5). For the second option no contact in all sections up to the end of operating period, i.e. no FCMI up to burn-up values more than 9 at%. In this case fuel pin failures in BR-10 could not be explained by FCMI.

8

Cladding hoop stresses in BR-10 fuel pin



9

PIE of BR-10 nitride (IV loading)

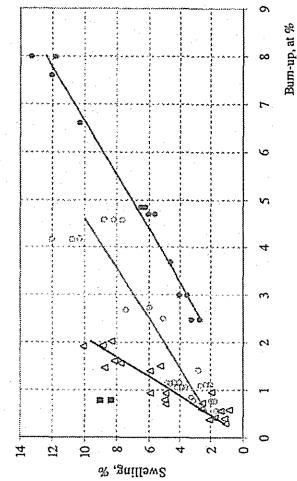
The PIE of 6 fuel assemblies of IV reactor loading have been carried out.

The results of the investigations of swelling and gas-release from nitrides after irradiation of fuel pins in the BR-10 reactor, in comparing the American data, are given in Fig. 1, 2. There are no representative experimental data on swelling and gas release of nitride or carbide fuel with different type and value of the porosity today.

10

Swelling of nitride fuel

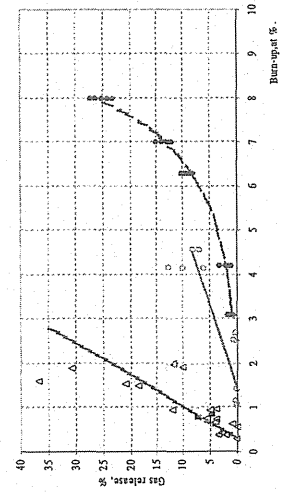
Δ UN, max fuel temperature 1675 K, density 93% USA,
 \circ UN, max fuel temperature 1460 K, density 95% USA,
 \bullet UN, max fuel temperature 1173 K, density 85 - 94% BR-10
 \blacksquare UN, max fuel temperature 1953 K, density 87% USA



11

Gas release from nitride fuel

Δ UN, max fuel temperature 1675 K, density 93% USA,
 \circ UN, max fuel temperature 1460 K, density 95% USA,
 \bullet UN, max fuel temperature 1173 K, density 85 - 94% BR-10
 \blacksquare UN, max fuel temperature 1953 K, density 87% USA



12

PIE of BR-10 nitride (V loading)

In 2002 r FA selection was conducted from among suspected on a leakage for PIE.

FA AB811 №. 60 was discharged from the reactor on April 24, 1999 at 8.4 at% together with other FAs with high burn-ups due to coolant activity increase caused by pins failures.

At the PIE of A B811 №. 60 basic attentions planned to be given to the searching of leaked pins and location of an imperfection. Besides the dependence of fuel swelling on temperature and density should be studied. Currently the PIE is delayed due to lack of funding.

13

$UPu_{0.45}N$ and $UPu_{0.6}N$ powder has been made of initial metals U and Pu (VNIINM, Moscow)

Parameter	$UPu_{0.45}N$	$UPu_{0.6}N$
Density, g/cm ³	12.15 to 12.17	12.1 to 12.16
Content of Pu, wt%	45.0±2	60.0±2
Content of N, O, C, wt%	N 5.3, O < 0.15, C < 0.1	N 5.3 to 5.4, O < 0.15, C < 0.1
Diameter, mm	5.8 to 5.9	5.8 to 5.9
Height, mm	8.85 to 10.2	8.85 to 10.4
Non-uniformity of Pu distribution, %	±3.	±3.

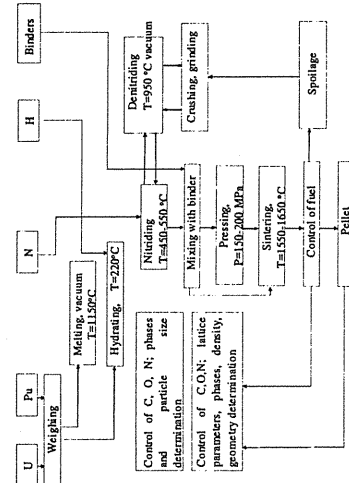
15

BORA-BORA experiment: fabrication, irradiation in BOR-60 and PIE of high Pu content fuels

Experiment has been under way since 1996.

- 4 fuel pins with $UPu_{0.45}O_2$ pellets
- 4 fuel pins with $UPu_{0.45}O_2$ vibropac fuel
- 2 fuel pins with $UPu_{0.45}N$ pellets
- 2 fuel pins with $UPu_{0.6}N$ pellets
- 2 fuel pins with PuN + ZrN pellet fuel
- 2 fuel pins with $PuO_2 + MgO$ pellet fuel

14



Nitride fabrication from metals.

16

Fabrication of PuN+ZrN fuel

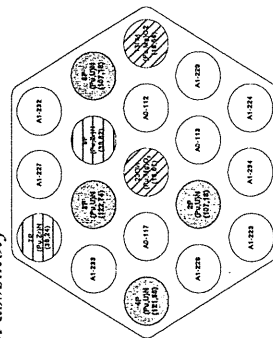
PuN+ZrN fuel was fabricated in VNIINM, Moscow, from following initial materials:

- Zr nitride obtained from high temperature nitriding (with nitrogen gas) of electrolytic powder of Zr,
- Pu nitride obtained by hydrogenating of initial Pu metal and then nitriding;
- 40wt%PuN+ 60wt%ZrN obtained by mixing of initial individual powders of Pu and Zr.

Not pure solid solution composed of two phases enriched by Pu and Zr. Homogeneous solid solution expected to be formed under irradiation.

17

BORA-BORA: fuel assembly



- FA-263E
- pellet fuel pins (UN-PuN)
 - pellet fuel pins (PuO₂, MgO)
 - pellet fuel pins (PuN - ZrN)
 - regular pins of disassembly FA

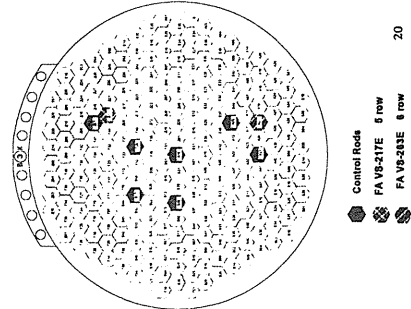
19

Fabrication of PuN+ZrN fuel

Parameter	Value
Density, g/cm ³	74 to 7.5
Content of Pu, wt%	37.5
Content of N, O, C, wt %	N 9.85 to 9.9, O 0.2, C 0.2
Pellet diameter, mm	5.8 to 5.9
Pellet height, mm	8.85 to 10.1
Non-uniformity of distribution	Pu ±4 %

18

Irradiation in BOR-60 reactor for 514 efpd (1 stage)



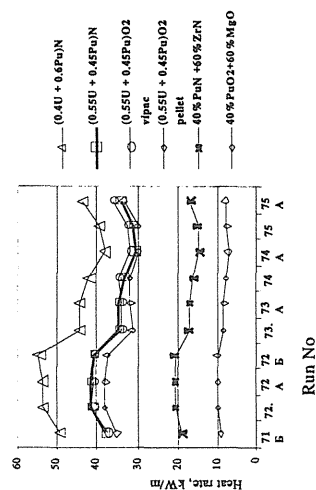
- Control Rods
- FA VS-217E 5 row
 - FA VS-263E 6 row

20

- August 2000 – loading of two dismantable FAs in BOR-60:
FA VS-217E - 5th row (MOX)
FA VS-263E - 6th row (nitrides, inert matrices)
- November, 2002 - discharge for intermediate PIE at burn-ups 5.4 - 11.3 at%.



Maximum linear rating of BORA-BORA fuels under irradiation (I stage)



21

Post-irradiation examinations of BORA-BORA fuels

- Post-irradiation examinations are carried out by RIAR. The first phase of intermediate PIE (NDE methods) of the fuel pins has been accomplished – all fuel pins had visual inspection and leak testing by ^{85}Kr . More detailed NDE examinations were performed for six fuel pins with oxides and nitrides (each fuel composition was represented by one fuel pin) – diameter measurement, eddy-current flaw detection, gamma-scanning, analysis of the under-cladding gas.

23



BORA-BORA irradiation parameters

Maximum fuel burn-up, at% :

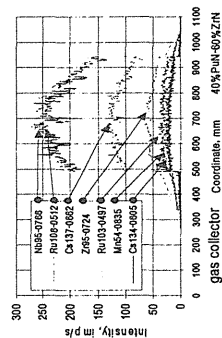
40%PuN + 60%ZrN
11.3at% ${}^{241}\text{Pu}$ UPu_{0.6}N_{0.4} 7.0at%Maximum damage dose
23 dpaMaximum cladding temperature
590 °C

22



Post-irradiation examinations of PuN-ZrN

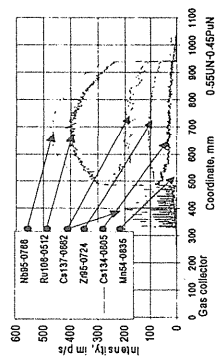
Distributions of migrating Cs and poor-migrating Zr and Ru fission products (FPs) in the fuel pins with ZrN fuel correspond to neutron flux distribution under irradiation and show no axial migrations both of fuel and volatile FPs.



24

Post-irradiation examinations of UPu_{0.45}N

In pins with UPu_{0.45}N periodic activity decrease both of migrating and poor-migrating FPs is observed along the whole core, its causes will be identified in destructive examinations.

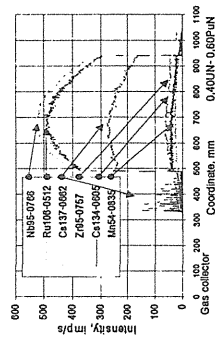


25

Post-irradiation examinations of UPu_{0.6}N

Pins with UPu_{0.45}N and UPu_{0.6}N are characterized by release of volatile FPs (Cs) in the lower blanket.

Cs deposits on the pellets surface and in inter-pellets gaps. Periodic peaks of activity correspond with the height of individual pellets in blanket.



26

Post-irradiation examinations of BORA-BORA fuel (cont.)

Gas composition was identified for each fuel pin by mass-spectrometric method. Taking into consideration measurement error, in the pin with PuN+ZrN no gas release is observed. In the fuel pins with UPu_{0.45}N and UPu_{0.6}N a release of gaseous FPs (Kr, Xe) is registered.

Non-destructive examinations have shown:

- all fuel pins are found to be leak-tight after the first irradiation stage;
- in the PuN+ZrN fuel pins no axial migrations of fuel, volatile FP and gaseous FPs are registered.

27

Post-irradiation examinations of BORA-BORA fuel (cont.)

The destructive examinations of fuel pins with all fuel types are under way: ceramography, electron probe microanalysis (EPMA), analysis of the residual gases, fuel density, burn-up (Nd analysis by EPMA), X-ray structure analysis (OM, lattice parameters, phases).

After leak-testing by ⁹⁵Kr and visual inspection ten fuel pins have been reassembled in VS-263 and reloaded in the BOR-60 core for the second irradiation stage in November, 2003. The plan is to continue irradiation up to burn-up >11at% for mixed nitrides and up to a burn-up of about 20at% for PuN+ZrN.

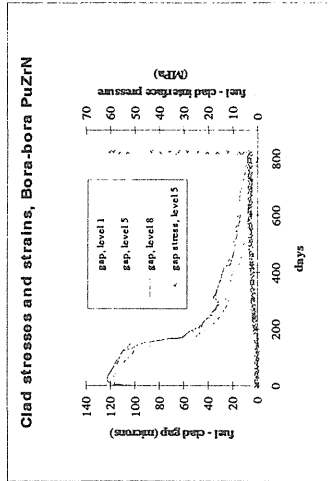
28

BORA-BORA calculation researches

- Before fuel loading the comparative calculations on fuel performance were done by KONDOR and NITRAF codes for nitrides. According to calculation fuel should be safe before irradiation completion. Satisfactory agreement of calculation results. Due to shortage on nitrides data (swelling, creep, thermal conductivity, gap conductance model) some difference between results.
- Additional data on some properties after PIE. Validation of codes for nitrides and inert-matrices fuels.

29

Example of NITRAF code calculation



30

Transmutation of MA

Uranium free nitride fuels (IMF) have been proposed for Am and Cm transmutation in ADS with fast neutron spectrum in Europe. The fuel allows to avoid any additional actinides production; it is compatible with PUREX process. Good matrix choose may improve poor properties of MA.

Presently several IMF types are investigated in Japanese, EU and US research programs. The programs cover study of different fabrication techniques, out-of-pile properties, modeling, irradiation tests and post-irradiation examinations. Today there are few data on properties and irradiation behavior of uranium free nitride fuel even w/o MA. MA bring additional problems (poor thermal properties, high volatility, helium production, chemical interaction, actinide migration).


31

MATINE: objective

Beginning on May, 1 2004 the ISTC Project "MATINE: Study of Minor Actinide Transmutation in Nitrides: modelling and measurements of out-of-pile properties" - ISTC Project has started. The objective of the Project is to carry out comprehensive performance modeling of (Pu,Am,Cm,Zr)N (with ZrN=60%, Pu/Am/Cm=40/50/10) fuel under irradiation in fast neutron spectrum of ADS, currently under development in Europe, up to high burn-up in order to compare relative performance of helium, sodium and lead-bismuth bonded pins.

The main result of the project is identification of uranium-free nitride fuel types that would perform well under irradiation to high burn-up in a fast neutron spectrum.

32




MATINE - Scope of activity (Task 1)

The Project consists of four tasks.

First task - compilation of literature data from existing nitride investigations in – and outside of Russia (UN, UPuN, ZrN, PuN+ZrN, UN+ZrN) in addition with compilation of data on all types of MA fuels irradiation behavior. The objective of this task is to perform input data for KONDOR and VIKOND codes (properties of (Pu,Am,Cm,Zr)N (Pu/A m/Cm=40/50/10 with ZrN=60%) . KTH (Sweden) will prepare the input data on irradiation conditions and geometry of ADS core element.

33




MATINE - Scope of activity (Task 2)

Second task Preparation of technological equipment for fabrication of (Pu,Zr)N; refinement of technological process of fuel fabrication; pellets fabrication and monitoring of fuel quality. Installations upgrade, techniques refinement. Experimental study of basic out-of-pile properties

- high temperature stability
- thermal conductivity
- high temperature creep

34



MATINE - Scope of activity (Task 3)

Third task: Codes up-dating. Modeling of (Pu,Am,Cm,Zr)N performance


- pellet fuel for helium, sodium and lead-bismuth bonded fuel pin
- vibropack fuel for helium-bonded pins only.

Parameters to be investigated and determined:

- optimum range of power density;
- optimum value of fuel porosity;
- allowable burn-up value;
- allowable Am content (impact of Pu/Am ratio on fuel performance).

Corrections of calculations in accordance with new experimental data.

35



MATINE - Scope of activity (Task 4)

Fourth task: technical – economical assessments of the feasibility to fabricate nitride fuels with atomic fraction of ZrN inert matrix up to 60 ± 10 %, containing up to 10 atomic percent curium, at RIAR site.

36



MATINE is well in line with following current Programs

BORA-BORA Program (CEA-MINATOM collaboration)

Fabrication, irradiation in BOR-60 of 2 fuel pins with 40%PuN+60%ZrN up to 22at%.

AMBOINE Program (CEA-MINATOM collaboration)

Fabrication of Am-containing oxide fuel (Pu,Am)O₂+UO₂, (Pu, Am)O₂+MgO (VIPAC technique). Pyrochemistry in molten salts. Possible irradiation in BOR-60.

CONFIRM program

Modeling, fabrication, characterization of (Pu,Zr)N, (Pu, Am,Zr)N. Irradiation of (Pu,Zr)N pins up to 12at% in Studsvik reactor.

37



Conclusion (UPuN data)

I. Additional experimental researches required for correct prediction of fuel elements performance of advanced fast reactors.

- Technological study of UPuN pellets fabrication of necessary purity, porosity type, chemical content.
- Out-of-pile study of UPuN properties:
 - creep rate as function of density, temperature, stress, chemical composition, fabrication technology;
 - high temperature behavior.
- PIE of already irradiated or currently irradiated fuel pins in order to define reasons of pins failures, and also fuel swelling data and gas release in dependence on fuel chemical composition, value and type of porosity, FCCI.

38



Conclusion (BORA-BORA)

II. Nitrides for actinides transmutation is under consideration in many countries. Most attractive innovative fuel is uranium free fuel that avoids any additional actinides production.

First stages of irradiation and PIE of nitrides (with and w/o U) with ~ 40% Pu are completed. The fuels were irradiated in BOR-60 reactor (BORA-BORA experiment).

PIE results have shown: small claddings deformations, fuel column integrity, no axial fuel migration, under-cladding gas volume and composition within anticipated limits. The PIE have shown that fuel irradiation could be prolonged.

39



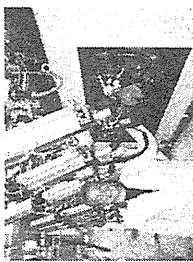
Conclusion (MATINE)

III. In addition to BORA-BORA irradiation behaviour of (Pu,Zr)N, MATINE program will give some thermo-physical properties of (Pu,Zr)N required for fuel performance calculation.

Besides comparative modelling data of both pellet and vibropacked (Pu,Am,Cm,Zr)N fuel pins with different sub-layers will help to define best solution for fuel pin design of fast neutron ADS. KTH (Sweden) prepared input data on irradiation conditions and geometry of ADS core elements, necessary for fuel performance modelling.

40

R&D on nitride fuel cycle technology in Europe



Janne Wallenius

Department of Nuclear & Reactor Physics, Royal Institute of Technology

Background and motivation



- In the European Union, R&D on minor actinide burning in ADS is performed as part of Framework Program 5 & 6.
- Composite oxide fuels (CERMET or CERCER) are the main candidates for ADS.
- Nitride fuel is considered as backup solution, due to better solubility in nitric acid (PUREX compatible).
- Nitride fuels also considered for gas cooled fast reactors (GEN-IV).

Outline



- Background
- Development of fabrication processes
- Measurement of thermo-physical properties
- High temperature stability
- Performance and safety modelling
- Irradiation test
- Future activities and international collaborations
- Summary

Development of fabrication processes

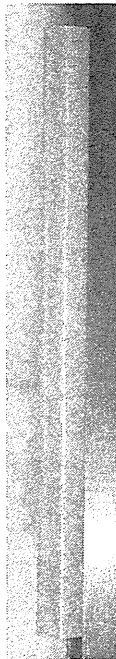


- Dust free fabrication processes preferred for Am & Cm fuel fabrication.
- Sol-Gel production of porous microspheres containing inert matrix and plutonium.
- Infiltration of americium and curium (in solution)
- Coagulation casting of microsphere suspension into pellets, or
- Vibro-packing (VIPAC) of microspheres in fuel pin

Powder pressing route for (Pu,Zr)N



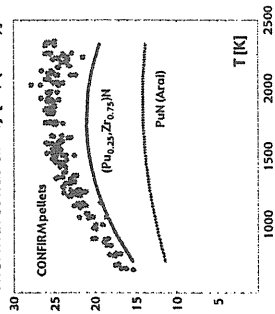
- Development of wet processes not ready in time for CONFIRM irradiation test in Studsvik.
- Carbo-thermic nitridation of PuO_2 and ZrO_2 powders used for fabrication of (Pu,Zr)N
- First samples made using Ar-H_2 for decarburisation contained high C & O impurity levels
- Modelling indicated use of $\text{N}_2\text{-H}_2$ for decarburisation could improve results.
- Thermo-chemical simulation described in J. Nucl. Sci. Tech. 41 (2004) 457.
- Oxygen levels < 0.2 weight % was achieved with this method. Pellet density $\pm 82\%$ TD.



Thermal conductivity of (Pu,Zr)N



Thermal conductivity [W/(m·K)]



- The thermal diffusivity and heat capacity of (Pu_{0.32}Zr_{0.72})N pellets were measured by CEA at Cadarache.
- The derived thermal conductivity is slightly larger than prior assessment of AEA-T, in spite of oxide impurities!
- Pellets remained stable at T = 2340 K, under 1 bar of nitrogen.

Sol-Gel route for (Am,Zr)N



- Mixing oxide microspheres with carbon did not yield good quality pellets.
- Adding carbon to the feed solution (Carbon Integration Method), zirconium oxide beads with homogeneous carbon distribution are obtained.
- Actinide nitrate is then infiltrated into the porous beads.
- Calcination converts hydroxides to oxides.
- Carbo-thermic nitridation yields nitrides with low oxygen impurity.



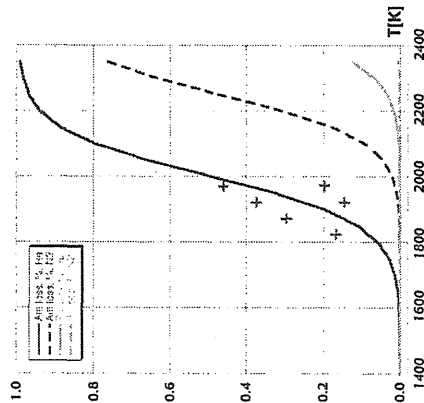
(U,Zr)N pellets

High temperature stability: experiment



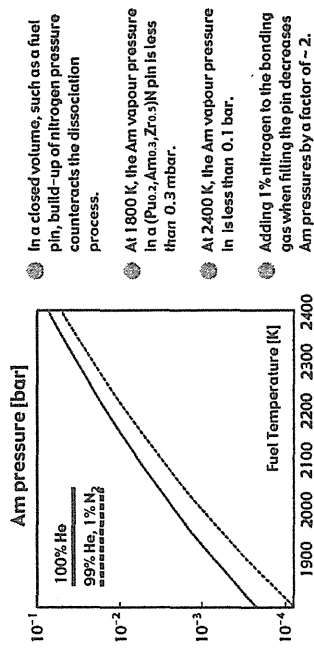
- High temperature, high pressure tests of UN & (U,Zr)N stability were performed.
- In the UN samples, formation of metallic uranium occurred at T = 2410 °C. Liquid uranium had reacted with the tungsten capsule.
- In the (U_{0.2}Zr_{0.8})N samples, no reaction with the tungsten capsule was observed.
- Solidus and liquidus temperatures of (U_{0.2}Zr_{0.8})N were found to be T_{sol} = 2610 °C & T_{liq} = 2760 °C
- Results published in J. Nucl. Mat. 320 (2003) 44.

High temperature stability: modelling



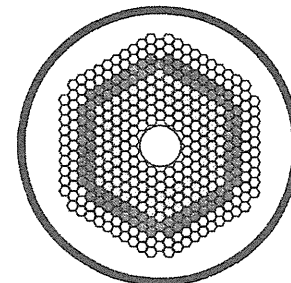
- Thermo-Calc used for thermo-chemical modelling of ZrN , PuN and AmN stability in Helium and Nitrogen atmospheres.
- Gibbs energy for AmN taken from Ogasawara et al.
- Vaporisation of AmN in 1 bar inert atmosphere is significant above 1600 K. Predicted losses consistent with Los Alamos experiment.
- JAERI observed 2% losses of Am when sintering (Am , ZrN) during 10 hours at 1800 K in nitrogen atmosphere.

Stability under irradiation conditions



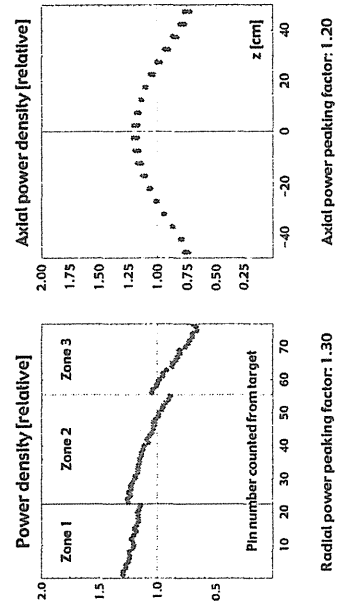
- In a closed volume, such as a fuel pin, build-up of nitrogen pressure counteracts the dissociation process.
- At 1800 K, the Am vapour pressure in α ($Pu_{0.2}Am_{0.3}Zr_{0.5}N$) pin is less than 0.3 mbar.
- At 2400 K, the Am vapour pressure in is less than 0.1 bar.
- Adding 1% nitrogen to the bonding gas when filling the pin decreases Am pressures by a factor of ~ 2 .

Nitride fuel performance in ADS



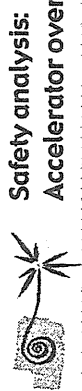
- Core power: 800 MWth
- Pin power: 36 kW/m
- Fuel column height: 1.0 m
- Clad inner/outer diameter: 5.0/5.7 mm
- Pin P/D: 1.75
- $Pu/Am/Cm \approx 40/50/10$
- Matrix fractions: $0.60/0.50$
- k -eigenvalue @ BOL: 0.97

Power density profiles

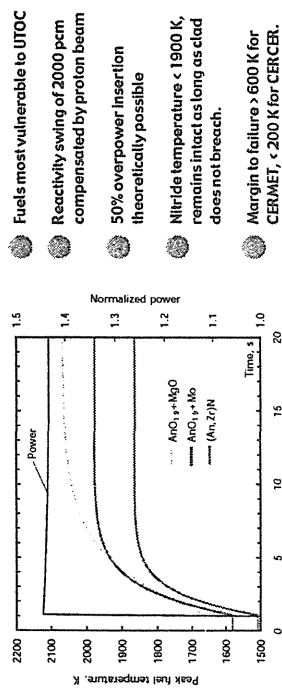


Axial power peaking factor: 1.20

Radial power peaking factor: 1.30



Safety analysis: Accelerator over-current



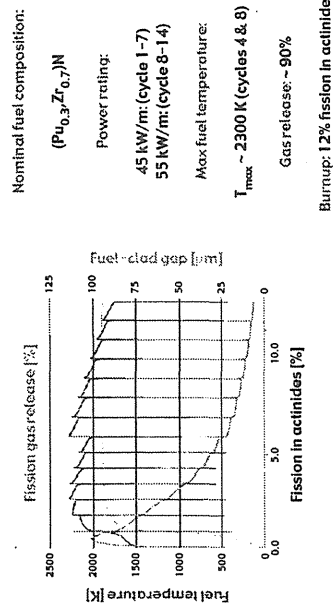
Irradiation test in Studsvik



- 4 (Pu, Zr)N pins were fabricated by PSI & delivered to Studsvik.
- 2 pins with 30 molar % Pu, 2 pins with 20 molar % Pu.
- Hafnium shielded rig used for irradiation during 1.4 cycles
- NaK capsule used for heat conduction.
- Issue about fission gas leakage identified by safety committee.
- Rig redesigned to pressurise the NaK capsule.
- Better seismic analysis required by authority.
- Start of irradiation delayed until 2005.



Thermo-mechanical modelling of (Pu, Zr)N irradiation in R2



Future activities & international collaborations

- PIE of irradiated CONFIRM pins included in EUROTRANS project.
- Aqueous dissolution and separation of unirradiated (Pu, Zr)N to be made by Chalmers University of Technology in Göteborg.
- Irradiation of sodium bonded (Pu, Am, Zr)N pins to start in Phenix in 2006. Pellets provided by Los Alamos (FUTURIX collaboration).
- High temperature stability test of (Pu, Zr)N will be made by Bochkov Institute in Moscow (MATINE project).
- Thermo-mechanical modelling of (Pu, Am, Zr)N irradiation in He, Na and Pb-Bi bonded pins to be made by IPPE in Obninsk (MATINE project).



Summary

- ☑ Methods for fabrication of transuranium nitrides have been developed.
- ☑ Thermal conductivity of (Pu,Zr)N has been measured
- ☑ 4 (Pu,Zr)N pins have been fabricated, irradiation to start in Studsvik in 2005.
- ☑ Irradiation at ~ 50 kW/m was calculated to be feasible.
- ☑ A design and safety assessment of an 800 MWe ADS with nitride fuel was made.
- ☑ PIE of CONFIRM pins planned within the EUROTRANS project.
- ☑ Irradiation of sodium bonded (Pu,Am,Zr)N to start in Phenix 2006 (FUTURIX).
- ☑ MATINE project: high T stability test of (Pu,Zr)N and modelling of (Pu,Am,Zr)N

This is a blank page.

国際単位系 (SI) と換算表

表 1 SI 基本単位および補助単位

量	名 称	記 号
長 さ	メ ー ト ル	m
質 量	キ ロ グ ラ ム	kg
時 間	秒	s
電 流	ア ン ペ ア	A
熱力学温度	ケ ル ビ ン	K
物 質 量	モ ル	mol
光 度	カ ン デ ラ	cd
平 面 角	ラ ジ ア ン	rad
立 体 角	ステラジアン	sr

表 3 固有の名称をもつ SI 組立単位

量	名 称	記号	他の SI 単位 による表現
周 波 数	ヘ ル ツ	Hz	s ⁻¹
力	ニ ュ ー ト ン	N	m·kg/s ²
圧 力 , 応 力	パ ス カ ル	Pa	N/m ²
エネルギー, 仕事, 熱量	ジュ ー ル	J	N·m
工 率 , 放 射 能	ワ ッ ト	W	J/s
電 気 量 , 電 荷	ク ー ロ ン	C	A·s
電位, 電圧, 起電力	ボ ル ト	V	W/A
静 電 容 量	ファラド	F	C/V
電 気 抵 抗	オ ー ム	Ω	V/A
コンダクタンス	ジーメンス	S	A/V
磁 束	ウェーバ	Wb	V·s
磁 束 密 度	テ ス ラ	T	Wb/m ²
インダクタンス	ヘ ン リ ー	H	Wb/A
セルシウス温度	セルシウス度	°C	
光 束	ル ー メ ン	lm	cd·sr
照 度	ル ク ス	lx	lm/m ²
放 射 能	ベ ク レ ル	Bq	s ⁻¹
吸 収 線 量	グ レ イ	Gy	J/kg
線 量 当 量	シーベルト	Sv	J/kg

表 2 SI と併用される単位

名 称	記 号
分, 時, 日	min, h, d
度, 分, 秒	°, ', "
リットル	l, L
トン	t
電子ボルト	eV
原子質量単位	u

$$1 \text{ eV} = 1.60218 \times 10^{-19} \text{ J}$$

$$1 \text{ u} = 1.66054 \times 10^{-27} \text{ kg}$$

表 4 SI と共に暫定的に維持される単位

名 称	記 号
オングストローム	Å
バ ー ン	b
バ ー ル	bar
ガ リ ー	Gal
キ ュ リ ー	Ci
レン ト ゲ ン	R
ラ ド	rad
レ ム	rem

$$1 \text{ Å} = 0.1 \text{ nm} = 10^{-10} \text{ m}$$

$$1 \text{ b} = 100 \text{ fm} = 10^{-28} \text{ m}^2$$

$$1 \text{ bar} = 0.1 \text{ MPa} = 10^5 \text{ Pa}$$

$$1 \text{ Gal} = 1 \text{ cm/s}^2 = 10^{-2} \text{ m/s}^2$$

$$1 \text{ Ci} = 3.7 \times 10^{10} \text{ Bq}$$

$$1 \text{ R} = 2.58 \times 10^{-4} \text{ C/kg}$$

$$1 \text{ rad} = 1 \text{ cGy} = 10^{-2} \text{ Gy}$$

$$1 \text{ rem} = 1 \text{ cSv} = 10^{-2} \text{ Sv}$$

表 5 SI 接頭語

倍数	接頭語	記 号
10 ¹⁸	エクサ	E
10 ¹⁵	ペタ	P
10 ¹²	テラ	T
10 ⁹	ギガ	G
10 ⁶	メガ	M
10 ³	キロ	k
10 ²	ヘクト	h
10 ¹	デカ	da
10 ⁻¹	デシ	d
10 ⁻²	センチ	c
10 ⁻³	ミリ	m
10 ⁻⁶	マイクロ	μ
10 ⁻⁹	ナノ	n
10 ⁻¹²	ピコ	p
10 ⁻¹⁵	フェムト	f
10 ⁻¹⁸	アト	a

(注)

- 表 1—5 は「国際単位系」第 5 版, 国際度量衡局 1985 年刊行による。ただし, 1 eV および 1 u の値は CODATA の 1986 年推奨値によった。
- 表 4 には海里, ノット, アール, ヘクタールも含まれているが日常の単位なのでここでは省略した。
- bar は, JIS では流体の圧力を表わす場合に限り表 2 のカテゴリーに分類されている。
- EC 閣僚理事会指令では bar, barn および「血圧の単位」mmHg を表 2 のカテゴリーに入れている。

換 算 表

力	N (=10 ⁵ dyn)	kgf	lbf
	1	0.101972	0.224809
	9.80665	1	2.20462
	4.44822	0.453592	1

$$\text{粘 度 } 1 \text{ Pa} \cdot \text{s} (= \text{N} \cdot \text{s} / \text{m}^2) = 10 \text{ P (ポアズ)} (\text{g} / (\text{cm} \cdot \text{s}))$$

$$\text{動粘度 } 1 \text{ m}^2 / \text{s} = 10^4 \text{ St (ストークス)} (\text{cm}^2 / \text{s})$$

圧	MPa (=10 bar)	kgf/cm ²	atm	mmHg (Torr)	lbf/in ² (psi)
	1	10.1972	9.86923	7.50062 × 10 ³	145.038
力	0.0980665	1	0.967841	735.559	14.2233
	0.101325	1.03323	1	760	14.6959
	1.33322 × 10 ⁻⁴	1.35951 × 10 ⁻³	1.31579 × 10 ⁻³	1	1.93368 × 10 ⁻²
	6.89476 × 10 ⁻³	7.03070 × 10 ⁻²	6.80460 × 10 ⁻²	51.7149	1

エネルギー・仕事・熱量	J (=10 ⁷ erg)	kgf·m	kW·h	cal (計量法)	Btu	ft·lbf	eV
	1	0.101972	2.77778 × 10 ⁻⁷	0.238889	9.47813 × 10 ⁻⁴	0.737562	6.24150 × 10 ¹⁸
	9.80665	1	2.72407 × 10 ⁻⁶	2.34270	9.29487 × 10 ⁻³	7.23301	6.12082 × 10 ¹⁹
	3.6 × 10 ⁶	3.67098 × 10 ⁵	1	8.59999 × 10 ⁵	3412.13	2.65522 × 10 ⁶	2.24694 × 10 ²⁵
	4.18605	0.426858	1.16279 × 10 ⁻⁶	1	3.96759 × 10 ⁻³	3.08747	2.61272 × 10 ¹⁹
	1055.06	107.586	2.93072 × 10 ⁻⁴	252.042	1	778.172	6.58515 × 10 ²¹
	1.35582	0.138255	3.76616 × 10 ⁻⁷	0.323890	1.28506 × 10 ⁻³	1	8.46233 × 10 ¹⁸
	1.60218 × 10 ⁻¹⁹	1.63377 × 10 ⁻²⁰	4.45050 × 10 ⁻²⁶	3.82743 × 10 ⁻²⁰	1.51857 × 10 ⁻²²	1.18171 × 10 ⁻¹⁹	1

$$1 \text{ cal} = 4.18605 \text{ J (計量法)}$$

$$= 4.184 \text{ J (熱化学)}$$

$$= 4.1855 \text{ J (15 °C)}$$

$$= 4.1868 \text{ J (国際蒸気表)}$$

$$\text{仕事率 } 1 \text{ PS (仏馬力)}$$

$$= 75 \text{ kgf} \cdot \text{m/s}$$

$$= 735.499 \text{ W}$$

放射能	Bq	Ci
	1	2.70270 × 10 ⁻¹¹
	3.7 × 10 ¹⁰	1

吸収線量	Gy	rad
	1	100
	0.01	1

照射線量	C/kg	R
	1	3876
	2.58 × 10 ⁻⁴	1

線量当量	Sv	rem
	1	100
	0.01	1

(86 年 12 月 26 日現在)



古紙配合率100%
白色度70%再生紙を使用しています